UCRL - 3471
cy 2

UNIVERSITY OF CALIFORNIA

Radiation Laboratory

TWO-WEEK LOAN COPY
This is a Library Circulating Copy
which may be borrowed for two weeks.
For a personal retention copy, call
Tech. Info. Division, Ext. 5545

BERKELEY, CALIFORNIA

UCRL-3471
c.2

DISCLAIMER

This document was prepared as an account of work sponsored by the United States Government. While this document is believed to contain correct information, neither the United States Government nor any agency thereof, nor the Regents of the University of California, nor any of their employees, makes any warranty, express or implied, or assumes any legal responsibility for the accuracy, completeness, or usefulness of any information, apparatus, product, or process disclosed, or represents that its use would not infringe privately owned rights. Reference herein to any specific commercial product, process, or service by its trade name, trademark, manufacturer, or otherwise, does not necessarily constitute or imply its endorsement, recommendation, or favoring by the United States Government or any agency thereof, or the Regents of the University of California. The views and opinions of authors expressed herein do not necessarily state or reflect those of the United States Government or any agency thereof or the Regents of the University of California.

UCRL-3471

UNIVERSITY OF CALIFORNIA
Radiation Laboratory
Berkeley, California

Contract No. W-7405-eng-48

NUCLEAR PROPERTIES OF SOME NEUTRON-DEFICIENT ISOTOPES OF EMANATION, POLONIUM AND ASTATINE

Allan W. Stoner

(Thesis)

June 27, 1956

Printed for the U. S. Atomic Energy Commission

NUCLEAR PROPERTIES OF SOME NEUTRON-DEFICIENT ISOTOPES OF EMANATION, POLONIUM, AND ASTATINE

Contents

Part I

Abstract 3

I. Introduction 4

II. Experimental Methods 7

A. Production and Purification of Isotopes 7

B. Instruments 12

III. Decay Schemes 16

A. Polonium-207 16

B. Polonium-206 42

C. Astatine-209 57

D. Astatine-208 70

E. Emanation-211 78

Part II

IV. Instroduction 94

V. Experimental 95

VI. Results 98

VII. Discussion 107

Acknowledgment 108

References 109

NUCLEAR PROPERTIES OF SOME NEUTRON-DEFICIENT ISOTOPES OF EMANATION, POLONIUM AND ASTATINE

Allan W. Stoner

Radiation Laboratory
and
Department of Chemistry and Chemical Engineering
University of California Berkeley, California

June 27, 1956

ABSTRACT

A study of electron-capture and alpha-decay characteristics has been carried out for several nuclides in the neutron-deficient and proton-excess region near the double closed shell, Pb^{208}. Complete decay schemes are presented for At^{209} and Po^{207}. Tentative decay schemes are given for Em^{211}, At^{208}, and Po^{206}. The studies were carried out with variable and permanent-field beta spectrometers, scintillation detectors, coincidence techniques, and a magnetic alpha-particle spectrograph. A comparison of the experimentally determined levels with the levels expected from various extensions of the single-particle model has been discussed.

In the second part, a study of several new emanation isotopes prepared by the bombardment of gold with 140-Mev nitrogen ions has been carried out. Em^{208}, Em^{207}, Em^{206}, and Em^{204} were produced and studied in the alpha pulse-height analyzer. The mass assignments of the activities were made by observing the growth and decay of the alpha-emitting daughters, At^{207} and Po^{202}. Alpha and electron-capture decay branching was measured for Em^{207}, Em^{206}, and Po^{202}. These new isotopes have been correlated with alpha systematics.

I. INTRODUCTION

This thesis describes an experimental program to study the methods of preparation of a large number of radioactive isotopes in the neutron-deficient and proton-excess region near the double closed shell, Pb^{208}, and to study in detail the alpha, beta, and gamma radiations of these isotopes. The experimental data were used to determine as completely as possible an energy-level scheme for the isotopes in the region. Such a scheme is of considerable interest for this particular group of isotopes because of correlations with the single-particle model and the modified-particle model by Pryce.

One of the tests that can be applied to any of the various models of the nucleus that have been proposed is its ability to predict ground-state spin and parity and the spin, parity, and energy of excited states. In certain regions the nuclear model may be highly successful, whereas in another region it may appear to fail. In the mass region near Pb^{208} the shell model by Mayer[1] or by Haxel, Jensen, and Suess[2] is firmly established by many lines of physical evidence related to nucleon stability or the various properties of the ground-state configurations. Pb^{208} itself is a "doubly magic" nucleus because it contains a filled shell of 82 protons and a filled shell of 126 neutrons. A brief outline of the single-particle model and its implications in the region near the doubly magic closed shell is given in the following.

According to the single-particle model, the ground and excited states of an even-odd or odd-even nuclide depend essentially upon the odd particle. The ground state of a nucleus should be represented by this particle in its lowest energy state and the excited states by the promotion of this particle to higher energy states which are predicted by the order of filling of single-particle orbitals. This theory should have its most favorable application in a region near a closed shell since the number of coupled neutrons and coupled protons in addition to the odd particle will be at a minimum. Then the excited levels observed should closely follow those expected from single-particle excitations. The excited states of one isotope, Pb^{207}, have been completely worked out.[3] This nuclide differs from Pb^{208}, the double closed shell, by one hole in

the neutron shell. A single hole is equivalent theoretically to a single particle outside a closed shell. Then the ground state of Pb^{207} should be represented by a neutron in the lowest energy state available for the 125th neutron. This is a $p-^{1/2}$ state, and the higher-energy orbitals that should form the excited states are $f-^{5/2}$, $p-^{3/2}$, $i-^{13/2}$, and $f-^{7/2}$, in order of increasing energy. The detailed level structure arrived at by coincidence measurements, angular correlation measurements, and multipole order assignment of the transitions agrees with the single-particle levels expected. All the predicted states are observed, and no additional transitions or levels have been reported.

This excellent correlation between the single-particle model and the experimental data was one of the reasons for this study of several neighboring isotopes in order to further investigate the applications of the single-particle model of the nucleus. The excited states of Po^{209}, Bi^{207}, and At^{211} were studied for this purpose. Po^{209} differs from Pb^{207} only in that it has two additional protons, which are coupled to give zero angular momentum in the ground state. In both Po^{209} and Po^{207} the ground states arise from the same $p-^{1/2}$ neutron orbital. The excited levels of Po^{209} are of great interest both for investigating the extension of the single particle model and for determining the effect of coupled particles outside the shell; i.e., determining whether low-lying excited states arise by excitation of the pair of particles outside the shells. This study of Po^{209} levels was carried out by observing the levels that arise in the electron-capture decay of At^{209}. Bi^{207} and At^{211} are both isotopes whose excited states may be correlated with single-particle excitation, but they differ from the previous case because the odd particle in both cases is a proton. Bi^{207} is two neutrons and one proton removed from the double closed shell. At^{211} also is three particles removed from the double closed shell, but all three particles are protons in this case. The excited levels of Bi^{207} were observed by studying the Po^{207} electron-capture decay, and the At^{211} levels by Em^{211} electron-capture decay.

In this same mass region the modified particle model by Pryce may also be investigated. This model is useful for even-even and odd-odd isotopes near a double closed shell. The most successful application

of this model so far has been in the study of the Pb^{206} level scheme. Pryce and Alburger did a detailed experimental investigation[5] and correlated the data with a theoretical study of the isotope by Pryce.[4] The theoretical work was based on the experimental excited (neutron) levels observed in Pb^{207}. He predicted the energy of the Pb^{206} configurations by summing together the energy of the two neutron levels in Pb^{207}. Each configuration may have several possible spin values according to the rules of spin vector coupling. In zero-order approximation the levels are degenerate, but they are split when the interaction between the two paired particles is considered. By a detailed analysis of all the possible configurations, including the numerous nondegenerate states from the neutron levels, and by estimating an energy for each level, he was able to establish a set of theoretical levels for Pb^{206}. Only two of the 17 experimental levels failed to fit the theoretical level diagram. The excellent agreement between this model and the experimental data for Pb^{206} made it desitable to obtain additional experimental information that might be used to further investigate the model.

The extension of this model to more neutron-deficient lead isotopes is being carried out by several groups. A detailed theoretical study of Pb^{204} has been made by W. True[6] and an experimental study of Pb^{207}, Pb^{204}, and Pb^{205} by A. Fritsch and J. Hollander.[7] The application of this model to isotopes with protons beyond the closed shell has not been carried out. A short analysis by a group here of the levels of Po^{210} found by At^{210} electron-capture decay has shown that the model applies for the two-proton case (At^{210}).[43] The Pryce model has not yet been applied to nuclei where the particles are different and a large number of levels are to be expected. The ideal case would be Bi^{208}, in which the excited states would arise from a neutron-proton coupling. Unfortunately, the electron-capture decay of Po^{208} is highly forbidden, owing to a large spin change, so very little is known or probably will be learned concerning the Bi^{208} excited states. The next odd-odd isotope to which the Pryce model may be applied is Bi^{206}. It is three neutron holes and one proton removed from the double closed shell. The excited states of this isotope were studied in this work by investigating the electron-capture decay of Po^{206}.

To complete the study of the excited states in this mass region, the electron-capture decay of At^{208}, giving the levels in Po^{208}, has been investigated. This isotope is compared with respect to even-even nuclei systematics.

Next in this thesis the cyclotron bombardment methods, the radiochemical purification methods, and the instrumental methods used in this research are described. The experimental data on the radiations of the individual isotopes are then described. New information was obtained on the decays of Po^{207}, Po^{206}, At^{209}, At^{208}, and Em^{211}. Level schemes are discussed as far as the data permit. The most complete level schemes are found for the isotopes Po^{207} and At^{209}.

II. EXPERIMENTAL METHODS

A. Production and Purification of Isotopes

Preparation of Emanation-211

Em^{211} was prepared by the spallation of thorium metal with 340-Mev protons in the internal beam of the 184-in. cyclotron by means of the methods described by Momyer and Hyde.[8] The thorium was dissolved in hot, concentrated hydrochloric acid with sodium fluosilicate used to catalyze the reaction. The gases evolved were trapped in a U-tube in a vacuum system at liquid nitrogen temperatures. Emanation was fractionated from the other gases in the vacuum system and samples were prepared from the purified emanation by the glow-discharge technique.

The emanation is held interstitially in a metal lattice of a 10-mil wire with sufficient force so that it cannot be removed in ordinary working vacuums (10^{-5} to 10^{-6} mm Hg) at room temperature, but can be removed by raising the temperature several hundred degrees. Ten-mil wire samples prepared in this manner were used as sources in the permanent-magnet electron spectrographs and the alpha-particle spectrograph. The energy resolution of the peaks observed in the various instruments corresponds to that expected of a mass-free "thin" sample.

Samples were not prepared until approximately 16 hr after bombardment, so that shorter-lived emanation isotopes such as Em^{209}, Em^{210}, and Em^{212} could decay out. After this time, the only emanation isotopes present were Em^{211} and Em^{222}. Since the latter has a 3.8-day half life

and is produced with a smaller cross section, it contributes only a few tenths of a percent to the total activity. The amount of fission gases, krypton and xenon, was so small that they could not be detected; this is due to their removal during transfer operations in the vacuum system and to the short half lives of the isotopes formed in fission. The purity of the Em^{211} was checked by following the alpha decay of the samples and they gave a 16±1-hr half life over several half lives after an initial growth due to At^{211} and Po^{211} activity. The samples prepared were approximately 5×10^7 disintegrations per min. This represented an approximate 10% yield for the glow discharge method.

Preparation of Astatine Isotopes

Astatine isotopes were produced by several methods, so that the ratio of isotopes could be varied greatly in order to facilitate correct assignments of gamma-ray transitions. Large quantities of At^{209} were prepared by bombardment of bismuth metal that had been alloyed onto a 10-mil aluminum plate in a layer approximately 20 mils thick. These targets were clamped into a water-cooled target holder and mounted so as to intercept the deflected helium-ion beam of the 60-in. Crocker Radiation Laboratory cyclotron. In this type of bombardment At^{211}, At^{210}, and At^{209} are all prepared, but by varying the energy of the helium-ion beam, one can vary the amount of At^{209} relative to At^{210} from zero to approximately one-half of the total activity. The beam was limited to 15 microampere/hr to prevent the loss of astatine by volatilization or the melting of the bismuth target material.

The astatine was separated and purified by a volatilization method following previously developed techniques.[49] The bismuth target material was melted in a quartz tube in a vacuum system. A stream of nitrogen (1 to 2 mm pressure) introduced just above the molten bismuth carried the astatine along in the system and prevented it from condensing on the glass surfaces. The astatine was collected on a cold finger at liquid nitrogen temperature. The finger had been previously coated with a thin layer of ice. The layer of ice was then melted into a test tube and a 10-mil silver wire approximately 1-1/16 in. long was immersed in the solution. After 2 hr of stirring, 50% of the astatine had plated out on the wire. The wires, when mounted, were excellent line sources for the

beta spectrometers and the alpha-particle spectrograph.

At^{209} was prepared isotopically pure, but in much smaller quantities, by an indirect process involving its isolation from Ra^{213}. The decay sequence involved is $Ra^{213} \xrightarrow[2\ min]{\alpha} Em^{209} \xrightarrow[31\ min]{EC\ 85\%} At^{209}$. The 2-min Ra^{213} was produced by the spallation of thorium metal with 340-Mev protons in the 184-in. cyclotron.[8] After a short bombardment in the cyclotron the thorium target was immediately dissolved and the radium was removed from solution by coprecipitation on $BaCl_2$ from concentrated hydrochloric acid. The precipitate was immediately dissolved in water and reprecipitated by passing hydrogen chloride gas through the solution in order to obtain a higher degree of purity. The precipitate was then introduced into a vacuum system and dissolved in water. The sample was then allowed to remain for 15 min so that most of the 2-min Ra^{213} could decay. By activity, Ra^{213} is the main isotope present in the radium fraction so isolated. Its decay product, Em^{209}, which has a 31-min half life, is collected in a U-tube at liquid nitrogen temperatures. This is the only emanation isotope present, as the other two isotopes with half lives long enough to be collected (Em^{221} and Em^{222}) are the daughters of long-lived radiums. The Em^{209} was then moved to a clean tube on the vacuum system where its decay products, Po^{205} (from 15% alpha branching) and At^{209}, are collected. The sample was then allowed to decay from 4 to 6 hr so that the 1.5-hr Po^{205} could decay out. After 6 hr only pure At^{209} remained. Samples of approximately 3000 disintegrations/min of At^{209} could be prepared by this procedure; this amount was enough for gamma-gamma coincidence and gamma-ray intensity measurements.

At^{208} was produced by helium-ion bombardment of bismuth metal in the 184-in. cyclotron. It was necessary to use the larger cyclotron as the energy of the helium-ion beam of the 60-in. cyclotron, is not high enough to produce (α,5n) reaction on bismuth in high yields. The astatine was purified by dissolving the bismuth in concentrated nitric acid and then evaporating it to dryness in the presence of excess hydrochloric acid. The resulting hydrochloric acid solution was diluted to 6N and the astatine extracted into diisopropyl ether. The organic layer was washed several times with 3M hydrochloric acid with ferrous ion added. The ether was then slowly evaporated off over a water solution so that

the purified astatine was in a water solution. Samples prepared by this method contained all the astatine isotopes of mass numbers 206 through 211, so that the resulting gamma spectrum was too complex to be analyzed. However, these samples were used for "milking" experiments to determine the half life of At^{208}.

Isotopically pure At^{208} was obtained as the decay product of Fr^{212}.[10] The Fr^{212} was produced by the spallation of thorium with 340-Mev protons in the internal beam of the 184-in. cyclotron. It was separated from both fission and spallation products by a silicotungstic acid precipitation method as developed by Hyde.[11] The alpha branching of Fr^{212} yields the 1.7-hr At^{208} and the electron-capture branching gives Em^{208}, which subsequently forms Po^{208} and Bi^{208}. These two isotopes have long half lives and very little gamma radiation; therefore, all the gamma radiation observed after the Fr^{212} has decayed out belongs to At^{208}. A maximum of 10^6 disintegrations/min of At^{208} was prepared in this manner.

Preparation of Polonium

Po^{207} was prepared by helium-ion bombardment of lead chloride in the Crocker Radiation Laboratory 60-in. cyclotron. The lead chloride used was enriched in Pb^{206}. The exact isotopic composition is Pb^{206}, 59.7%; Pb^{207}, 25.2%; and Pb^{208}, 15.1%. The amount of Pb^{204} present is negligible. A special target assembly-- a pistol-grip target assembly which has been discussed elsewhere--was used for the irradiation.[44] The beam was attenuated to approximately 40 Mev with a 2-mil platinum foil in order to use the largest cross section possible for an $(\alpha,3n)$ reaction on lead.[30] At this energy no $(\alpha,4n)$ reactions take place; therefore, there is no Po^{206} activity produced. Po^{208} and Po^{209} are produced, but they have long half lives and no appreciable gamma-ray activity. Thus, all gamma and electron radiations of the purified polonium fraction are due to Po^{207}.

The polonium was recovered from the lead chloride target by the use of a radiocolloidal property of polonium which is discussed by Treiman et al.[12] The method depends on the adsorption of the colloidal polonium hydroxide on glass wool as a means of a gross separation from lead and bismuth. The lead chloride target was dissolved in hot, weak hydrochloric acid (pH 4.3) containing glass wool. After dissolution was

complete, the solution and glass wool were heated and agitated for 15 min. The glass wool was then removed and thoroughly washed with hot water. The polonium adheres to the glass wool while lead and bismuth remain in solution. The polonium was removed from the glass wool by leaching with concentrated hydrochloric acid followed by extraction into tributyl phosphate. The organic layer was scrubbed several times with concentrated hydrochloric acid to remove small quantities of lead and bismuth chlorides. Polonium stays in the organic layer when washed first with hydrochloric acid and then pure water. The polonium was next back-extracted with concentrated nitric acid. From this solution the necessary samples could be prepared for the various instruments. The over-all chemical yield for this separation was estimated to be 25%.

When samples in the form of line sources were required, as in the beta spectrometer and the alpha-particle spectrograph studies, the samples were prepared in a different manner. The target was dissolved in hot concentrated hydrochloric acid and a 10-mil silver wire was added to the hot solution. The solution was stirred for several hours and the polonium plated out on the wire with yields up to 50%. The polonium plated out by this manner was free of any foreign activity. However, this type of sample preparation cannot be used when astatine or bismuth (in low concentrations) is present, as they plate out also.

Po^{206} was prepared by the same bombardment method except that the platinum absorber used in front of the target was reduced to 1/4 mil. This allowed bombardment with 48-Mev alpha particles and subsequent formation of Po^{206} by $(\alpha,4n)$ reactions. The platinum foil is required in this case only to hold the powder (lead chloride) in the target assembly. When pure Po^{206} was desired, the targets were set aside for several days to allow Po^{207} to decay. The polonium was then purified by the tributyl phosphate solvent extraction procedure described above.

An alternate method was used in some cases for the production of Po^{206}. This was required because the lead chloride assembly was limited, by heat dissipation difficulties, to approximately 8 microamperes of the helium-ion beam. Therefore, in order to prepare large samples of a 9-day activity, long bombardment times are required. To overcome this, lead metal (25.6% Pb^{206}, 1.5% Pb^{204}, 21% Pb^{207}, and 52% Pb^{208}) was pressed

into grooves 1 by 1/8 by 1/32 in. in a copper block. This assembly can be water-cooled quite efficiently, as copper is an excellent heat conductor, and a beam current of 25 to 30 μamp is possible. Much larger samples of Po^{206} can be formed in this manner because of increased beam current and additional target material, but the one disadvantage is that large quantities of alpha activity (Po^{208}, Po^{209}, and Po^{210}) are formed. The polonium was isolated from these targets by the radiocolloidal absorption method described above.

B. Instruments

A great variety of instruments were used during the course of this work. A short description of each instrument is given when the information is useful in understanding and evaluating the experimental data. References are given to detailed descriptions of the most important spectrometers.

The term "energy resolution" or "resolution" appears many times and in each case the meaning is the same. The resolution of a peak is the full width at half intensity. The resolution, expressed in percent, is the full width at half intensity in units of energy divided by the energy of the peak and multiplied by one hundred.

Alpha-Particle Spectrograph

The alpha-particle spectrograph employed in this work resembles a mass spectrograph in which the normal ion source has been replaced by an alpha-emitting source.[14] It employs a 60° sector magnet, and the normal trajectory has a radius of curvature of 75 cm. The transmission and energy resolution depend on the slit system used, but for normal operation have values around $4 \times 10^{-3}\%$ and 0.2%, respectively. The receiver consists of a photographic plate which, upon development and examination under a microscope, reveals a characteristic black rectangular track for each alpha particle that has impinged upon it. These tracks, when plotted versus position on the plate, describe the alpha-particle energy spectrum of the sample. Intensities and energies can be determined from these graphs. Mass-free line samples are necessary and are prepared by vacuum sublimation or by electroplating. This instrument is referred to as the alpha-particle spectrograph.

Alpha Pulse-Height Analyzer

A 48-channel differential alpha pulse-height analyzer has been extensively used in this work to determine alpha energies and the degree of purity of samples.[15] Briefly, it consists of an argon, filled gridded ionization chamber in which a pulse is produced, by ionization, that is proportional to the alpha energy. This pulse from the ionization chamber was amplified in a preamplifier, then in a linear amplifier, and was then introduced into a 48-channel differential pulse-height analyzer. Gain and bias controls on the analyzer permitted the inspection of any predetermined energy internal with the full 48 channels. A plot of counts per channel versus channel number gives the energy spectrum of the alpha particles. Mass-free samples have approximately 1% resolution and 50% geometry. This instrument is referred to as the alpha-pulse analyzer.

Gamma-Ray Spectrometer

Gamma-ray intensities and energies were determined by use of the 50-channel differential pulse-height analyzer.[16] The gamma rays are detected by use of a sodium iodide crystal mounted on a Dumont 6292 photomultiplier tube. The gamma ray on striking the sodium iodide causes a pulse of light, proportional to the photon energy, which is picked up by the photomultiplier tube. The output pulse from the photomultiplier is amplified and then introduced into a 50-channel differential pulse-height analyzer. By proper adjustment of the gain and bias controls any predetermined energy range may be observed on the full 50 channels. A plot of counts versus channel number gives the photon energy spectrum of the sample. The peaks recorded in this manner have 8 to 10% resolution. A correction for counting efficiency must be made before the intensities of the peaks are determined. This correction has been experimentally determined by Hollander and Kalkstein, and their values were used in all intensity measurements.[17] For absolute abundance measurements of a peak, additional geometry correction must be made. The geometry for the different counting positions was measured by use of the 60-kev gamma ray of Am^{241}. This 50-channel differential pulse-height analyzer is referred to as the "scintillation spectrometer".

Coincidence-Measuring Instrument

Gamma-gamma-ray coincidences were measured by utilizing the scintillation spectrometer and a coincidence circuit coupled with a single-channel analyzer.[18,19] Two sodium iodide crystals mounted on RCA 5819 photomultiplier tubes were placed at 180° to each other with the sample between them. The pulse from one counter is fed into a single-channel analyzer and then introduced into a coincidence unit. The single-channel analyzer may be set so that the pulse from only one gamma ray is passed through it. This pulse is used to gate the pulses from the other sodium iodide counter in the coincidence circuit so that only the gamma rays in coincidence with it are detected and recorded on the scintillation spectrometer. The energy spectrum shows those gamma rays that are in coincidence with the gating photon (the photon selected on the single-channel analyzer). This coincidence unit had a resolving time of 2 to 3×10^{-6} sec. Alpha particle—gamma ray coincidences may be measured by this same setup if a zinc-coated RCA 5819 photomultiplier tube is substituted for the soidum iodide crystal which functions as the gate for the coincidence unit. Then only those gamma rays in coincidence with alpha particles are recorded on the scintillation spectrometer.

Delayed-Coincidence Instrument

Metastable states (half life from 10^{-7} to 10^{-9} sec) were searched for by use of a fast coincidence instrument.[36] The electromagnetic radiations were detected by use of a sodium iodide crystal mounted on an RCA 5819 photomultiplier tube. A Los Alamos type single-channel analyzer was used for the analysis of the pulses from the photomultiplier tube in order to select the "gate" photons. All photons in coincidence with the gate were recorded on the scintillation spectrometer. A delay wasintroduced in the gating circuit before the coincidence circuit so that only gamma rays emitted after a certain delay would be counted. By varying the length of the delay over a wide range and measuring the change in the counting rate, one may measure the half life of the transition. If the transition is too fast for measurement, a limit on the half life may be established. This limit is determined by the resolving time of the instrument, which is 2×10^{-9} sec.

Beta-Ray Spectrometers

1. Variable-field spectrometers

For determining the energies and intensities of the numerous electron lines, several different instruments were used. A double-focusing variable-field spectrometer of 25-cm radius, based on the design of Svartholm and Siegbahn, was used extensively.[20] An adjustable-slit system was used for focusing, and a side-window Geiger counter with a thin vinyl plastic window was used for detection of the electrons. The counting gas used was 90% argon and 10% ethylene. The transmission of this instrument is 0.05% and resolution is 0.3%. Very thin vaporized or electroplated samples were used in order to reduce scattering. Excellent lines were recorded with this instrument.

A second beta spectrometer of the magnetic-lens type was used in several instances when the total disintegration rate of the sample was too low or the conversion coefficient was too low to permit the use of the double-focusing spectrometer.[21] It consists of a cylindrical magnetic field in which electrons are introduced at one end and focused at the other. An anthracene crystal was used to detect the electrons, and this limited the instrument to measurements of electrons with energies greater than 150 kev. This instrument has 3% resolution and 1% transmission. It was used extensively for the study of high-energy transitions where the conversion coefficients are very low.

2. Permanent-magnet field

Permanent-magnet electron spectrographs were used for very accurate energy measurements. Four such instruments are available in this laboratory. The specifications concerning field strength, resolution, and energy range are given for each magnet in Table I. These instruments have been used only for measurement of energies and not for the measurement of intensities. It was found that owing to the lack of good efficiency curves for the detection of electrons by the photographic emulsion, the intensities differed very greatly from those determined on the double-focusing spectrometer. However, in all the tables of conversion electrons observed in the permanent-magnet spectrographs the estimated visual intensity of the lines has been recorded. These intensities may be used for comparison within a small energy range, but

cannot be used for K/L ratios or K line intensity comparisons. L_I, L_{II}, and L_{III} intensity comparisons are valid and were of considerable importance in determining the multipolarity of gamma transitions. The K and L electron conversion edges as compiled by Mihelich, Hill, and Church were used throughout this study for assigning the conversion lines.[45]

Table I

Permanent-magnet spectrograph specifications

	Field (gauss)	Energy (kev)	Energy resolution (%)
PM I	50	0 – 80	0.1
PM II	100	0 – 280	0.2
PM III	240	~80 – 900	0.3
PM IV	350	~200 – 1800	0.3

Samples were prepared by electroplating the activity on 10-mil silver or platinum wire. The design and calibration of cameras, sample-mounting techniques, and details concerning the photographic film have been covered in detail in reports by W. G. Smith[46] and A. Fritsch.[7]

III. DECAY SCHEMES

A. Polonium-207

Po^{207} was first identified by Templeton, et al. in bombardments of lead with 40-Mev helium ions in the 60-in. cyclotron of Crocker Radiation Laboratory.[22] They measured the half life as 5.7 ± 0.1 hr, and determined the alpha-particle energy to be 5.1 Mev, with approximately 0.01% alpha branching and the remainder going by electron capture. By absorption methods, electromagnetic radiation of 1.3 Mev was observed. Later work determined the alpha-particle energy to be 5.10 ± 0.02 Mev.[23]

The electron-capture decay of Po^{207} to levels in Bi^{207} has been studied only briefly before.[24] This work was published in a thesis by P. R. Gray and was done with the aid of this author. The work was then in the form of a perliminary investigation, so that the following discussion, a complete description, includes but greatly extends preliminary work.

In the study presented herein, Po^{207} has been produced by two methods. Isotopically pure Po^{207} was separated as the alpha-decay

product of Em^{211} that had been prepared by high-energy spallation of thorium. This procedure not only verified the mass assignment for the 5.7-hr half life, but also permitted the production of excellent samples for the measurement of gamma-ray intensities. In permanent-magnet and beta-ray spectrometer experiments where much larger quantities of activity were required, the polonium was prepared by bombardment of lead chloride (enriched to 60% Pb^{206}) with 40-Mev helium ions in the 60-in. cyclotron. The chemical separations and the purity of samples prepared in this manner are discussed in the section on experimental methods.

Gamma Spectrometer Measurements of Polonium-207

The gamma and electron spectra have both been investigated in great detail in order to determine intensities and the multipole order of the transitions. The gamma spectrum was studied several times on a scintillation spectrometer, and the spectrum recorded is shown in Fig. 1. The Compton background and the counting efficiency were taken into consideration when the intensities of the photo peaks were calculated. The intensities of the gamma rays relative to the 922-kev peak, which was arbitrarily set equal to 100, are given in Table II. The peak at 511 kev will be shown later to be annihilation radiation due to a small positron branching in the electron-capture decay.

Table II

Po^{207} gamma-ray intensities from scintillation spectrometer studies

Energy (kev)	Intensity (relative)
406	22 ± 5
511	~ 0.6
743	73 ± 14
992	100 ± 20
1149	~ 1

Measurement of Electron Conversion Lines of Polonium-207

The electron spectrum of Po^{207} has been analyzed by several different means. Permanent-magnet spectrographs were used to determine precise energies; the double-focusing spectrometer for high-resolution intensity measurements; and the magnetic-lens spectrometer for determination

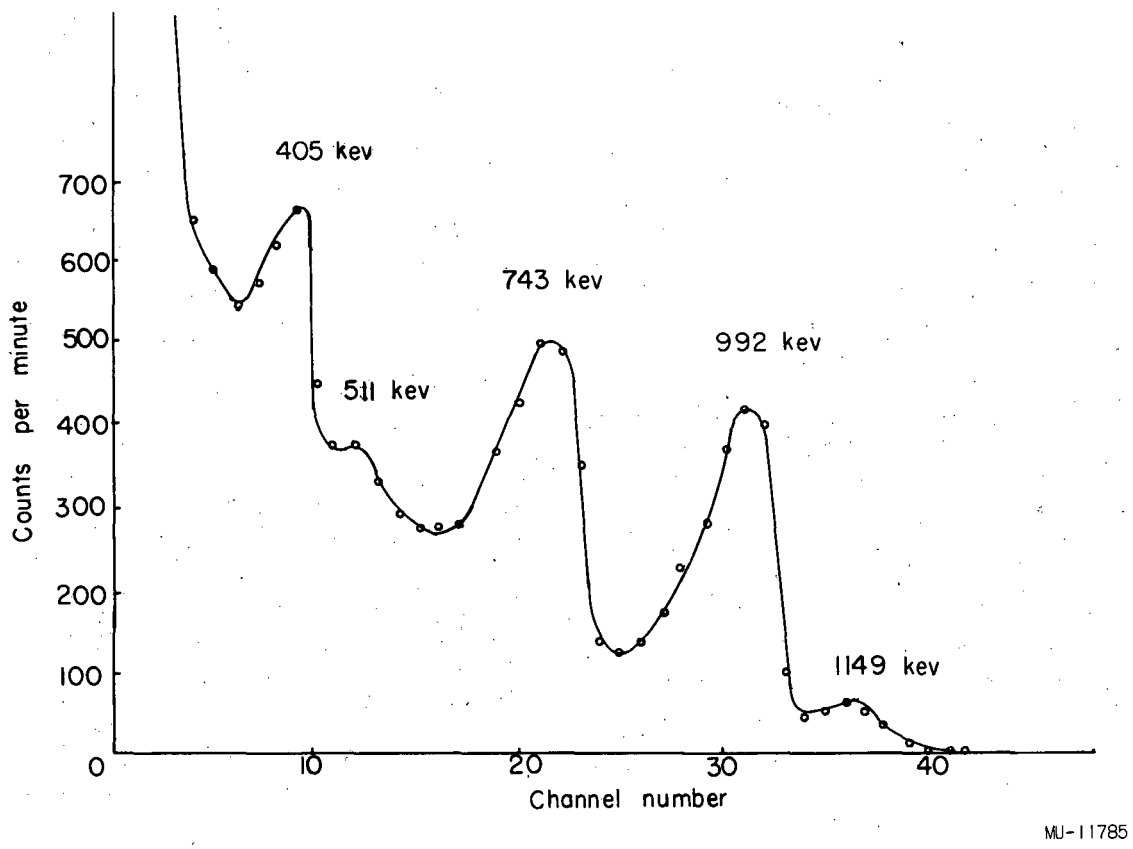

Fig. 1. Gamma-ray spectrum of Po^{207} as observed on the scintillation spectrometer.

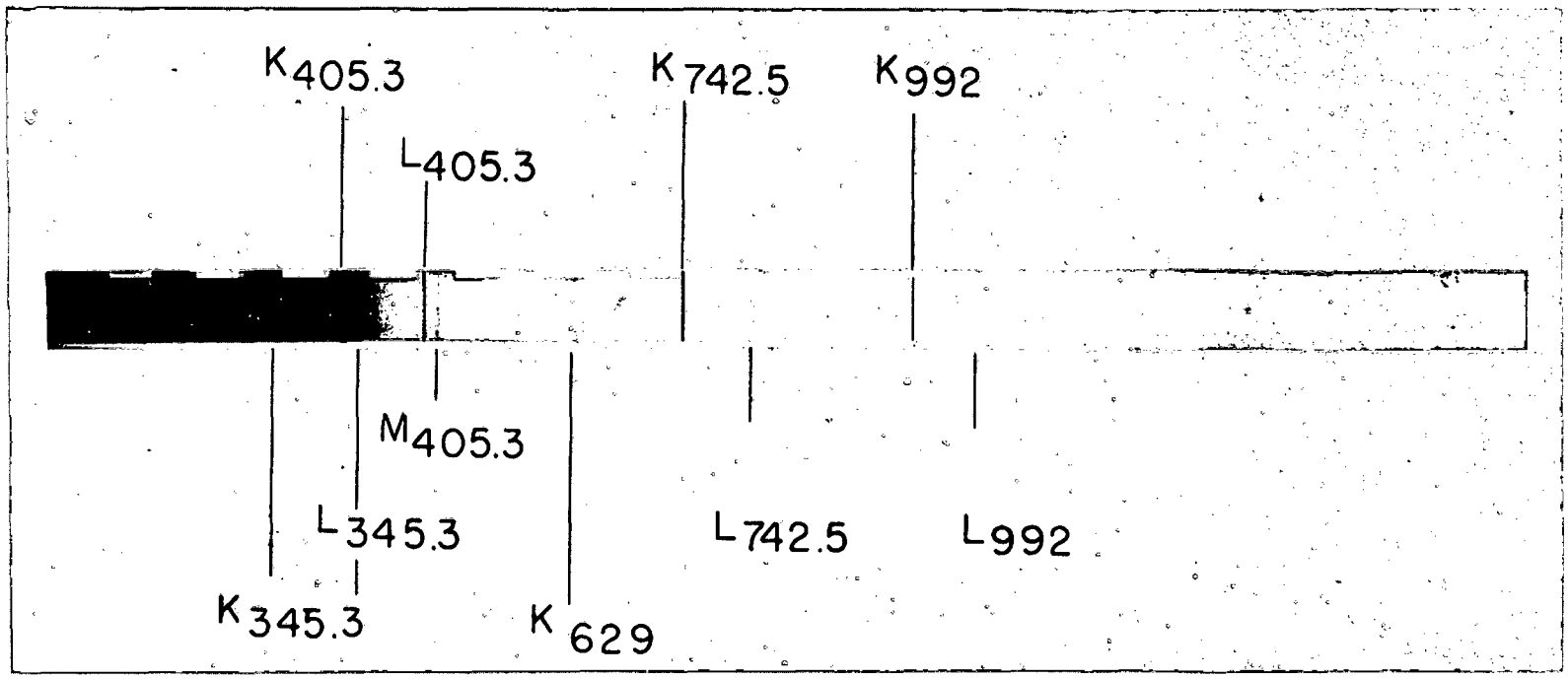

ZN-1525

Fig. 2. Photographic exposure of Po^{207} electron spectrum as observed on the 350-gauss permanent-magnet spectrograph.

of K/L ratios of high-energy transitions and to check the decay of each peak for verification that it belongs to Po^{207}.

Samples mounted on 10-mil silver wires were run in the permanent-magnet spectrographs. Table III gives the results obtained from several exposures on PM IV, which records electron lines up to 1.6 Mev. The lines tabulated are just those which can be most confidently assigned. The column marked "Intensity" is a visually estimated intensity with respect to the most intense line in the exposure. Other lines, which are from weaker transitions, are recorded in the first group of Table IV. The second group of lines in Table IV is definitely assignable to Po^{207}, but only one line has been seen for each transition, which makes assignments to conversion shells ambiguous. The intensities given in Tables III and IV are only approximate, and no correction has been made for the efficiency of detection. A photograph of one exposure on PM IV is given in Fig. 2. No attempt was made to analyze lines below 200 kev in the exposures made on PM IV, since a much better determination could be made by using lower-field permanent-magnet spectrographs. This film shows the quality of the electron lines that were observed in permanent-magnet spectrograph exposures.

Table III

Conversion electrons of Po^{207} observed in 350-gauss permanent-magnet spectrograph

Electron energy (kev)	Conversion edge	Gamma-ray energy (kev)	Gamma-ray energy (kev)	Intensity*
1058	K	1148.5	1148.5 ± 3.5	VW
900.7	K	991.2	-	S
976.0	L	991.7	991.6 ± 3.0	M
989.3	M	992.0	-	VW
652.3	K	742.8	-	S
726.6	L	743.0	742.8 ± 2.2	M
738.6	M	742.6	-	VW
315.0	K	405.7	-	VVS
389.0	L	405.3	405.5 ± 0.7	S
401.0	M	405.3	-	M
254.9	K	345.4	345.4 ± 0.7	VS
328.7	L	345.1	-	M
341.4	M	345.4	-	W

*Visual intensities are tabulated by using the following scale:

VVS= very, very strong	SM= strong moderate	SW= strong weak	W= weak
VS= very strong	M= moderate	W= weak	VW= very weak
S= strong	WM= weak moderate	VW= very weak	VVW= very, very weak

Table IV

Additional conversion electron lines of Po^{207} observed in 350-gauss permanent-magnet spectrograph

Electron energy (kev)	Conversion shell	Gamma-ray energy (kev)	Intensity* (visual)
Group I			
539.4	K	629.9	M
239.6	K	329.1	M
180.3	K	270.8	S
291.1	L	307	WM
217.1	K	307	S
	L	233.0	
233.1	L	249.5	SM
206.6	L	223.0	SM
Group II			
857.3			VVW
821.3			W
574.8			VVW
467.3			W
306.4			VW
261.3			W
247.1			W
198.1			W

*Visual intensities are tabulated by using the following scale:

VVS= very, very strong	SM= strong moderate	SW= strong weak	W= weak
VS= very strong	M= moderate	W= weak	VW= very weak
S= strong	WM= weak moderate	VW= very weak	VVW= very, very weak

Exposure of samples of Po^{207} on permanent-magnet spectrograph II, which records electrons in the 10- to 280-kev energy range, yielded many electron lines. Those electron lines which could be matched to K and L edges are given in Table V. The relative intensities given are good only for comparison within this table. From this same exposure all additional lines assignable to Po^{207} are recorded in Table VI. This group contains the K/L Auger lines and the other lines that cannot be fitted to K and L conversion shells which yield a reasonable K/L ratio for some type of transition. All the transitions represented in this table by electron lines are quite weak transitions when compared to the high-energy gamma rays. This makes their placement in the decay scheme practically impossible.

The electron spectrum was extensively investigated in two variable-field spectrometers. Small point sources of mass-free polonium were run on the magnetic-lens spectrometer. The intensity data are summarized in Table VII. The limits of error in energy are much greater than those

which have already been presented from permanent-magnet measurements. These data are useful for relative intensities of K conversion lines and K/L ratios.

Table V

Low-energy conversion electron lines of Po^{207} observed in 90-gauss permanent-magnet spectrographs

Electron energy (kev)	Conversion shell	Photon energy (kev)		Intensity*
33.4	K	123.9		W
107.8	L_I	124.2	124.0±0.3	SM
108.3	L_{II}	124.0		VW
110.3	L_{III}	123.7		S
44.8	L_{II}	60.5	60.5±0.2	M
46.9	L_{III}	60.4		M
159.2	K	249.7		WM
119.1	L_I	135.5		W
119.6	L_{II}	135.5	135.5±0.3	WS
121.6	L_{III}	135.5		W
132.1	K	222.6		W
76.1	K	166.6		SW
150.1	L_I	166.5	166.5±0.3	M
150.8	L_{II}	166.5		VW
152.7	L_{III}(?)	166.1		M
161.5	L_I	177.9		W
162.3	L_{II}	178.0	178.0±0.3	W
164.5	L_{III}	177.9		VW
180.7	K	271.2		WM
217.2	L_{II}	233		VW
254.7	K (L of 271)	345.2		W

*Visual intensities are tabulated by using the following scale:

VVS= very, very strong	SM= strong moderate	SW= strong weak	W= weak
VS= very strong	M= moderate	W= weak	VW= very weak
S= strong	WM= weak moderate	VW= very weak	VVW= very, very weak

Table VI

Unassigned conversion electrons of Po^{207} observed in 90-gauss permanent-magnet spectrograph

Electron energy (kev)	Intensity (visual)	Electron energy (kev)	Intensity (visual)*
22.2	W	62.9	WM
39.2	W	63.5	SW
43.8	M	65.4	SW
49.5	M	67.5	W
50.7	W	73.2	W
53.6	W	73.8	W
53.9	W	74.5	M
56.1	VW	121.6	W
57.2	VW	130.7	VW
58.2	M	131.0	VW
58.7	W	141.0	VW
59.1	W	143.7	VW
61.2	WM		

Table VII

Conversion electron data for Po^{207} from magnetic-lens spectrometer experiments

Electron energy (kev)	Conversion shell	Gamma-ray energy (kev)	Intensity**	K/L ratio
256	K	345 ± 5	29 ± 6	6 ± 1
331	L		5	
316	K	407 ± 5	100 ± 20	6.2 ± 1
393	L		16 ± 3	
538	K	629 ± 7		
655	K		54 ± 10	5.7 ± 1
732	L	746 ± 10	9.5	
833	K	924 ± 12	2.2	
904	K	995 ± 12	41 ± 8	4.7 ± 1
981	L		8.7	
1062	K	1153 ± 15	1.2	~4 ± 1
1134	L		0.3	

*Visual intensities are tabulated by using the following scale:

VVS= very, very strong	SM= strongly moderate	SW= strong weak	W= weak
VS= very strong	M= moderate	W= weak	VW= very weak
S= strong	WM= weak moderate	VW= very weak	VVW= very, very weak

Limits of error on the intensities are ± 20% or less. The complete electron spectrum that was observed is shown in Figs. 3a, 3b, and 3c. The spectrum was followed over a 15-hr period and all peaks shown except those marked as "not in Po^{207}" decayed with the correct half life.

** Intensities relative to 407-kev K-conversion line arbitrarily taken as 100.

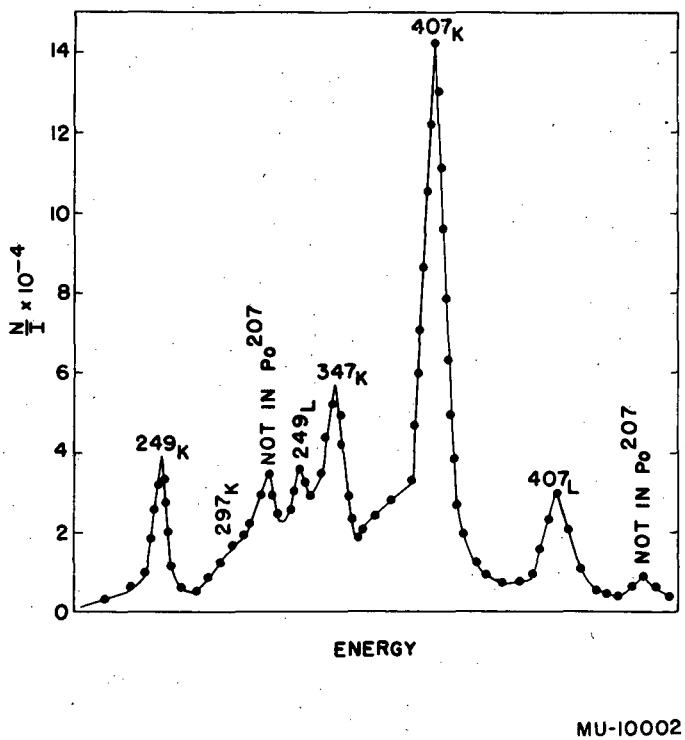

Fig. 3a. Electron spectrum of Po^{207} as observed on the magnetic-lens spectrometer -- 150- to 350-kev region.

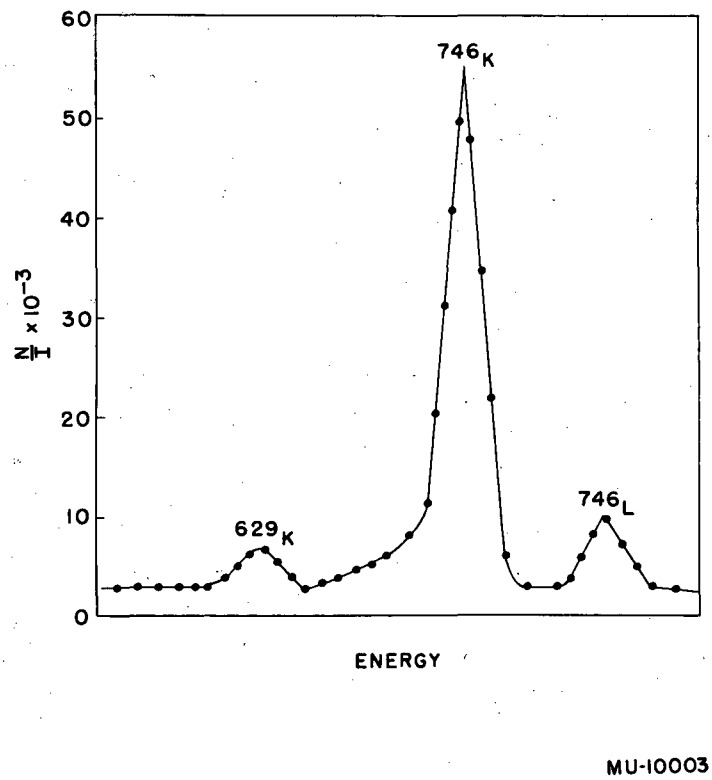

Fig. 3b. Electron spectrum of Po^{207} as observed on the magnetic-lens spectrometer -- 350- to 700-kev region.

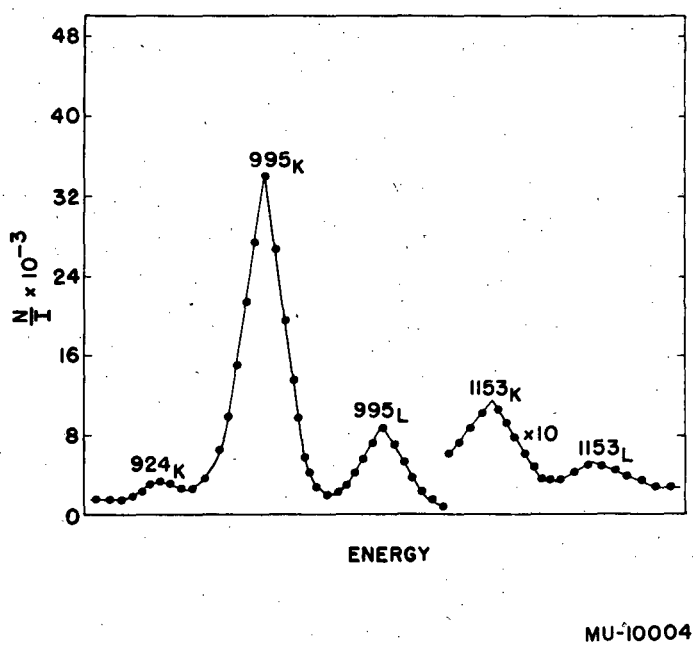

Fig. 3c. Electron spectrum of Po^{207} as observed on the magnetic-lens spectrometer -- 700- to 1100-kev region.

The resolution obtained in these runs was quite low (4%) and consequently the L-shell conversion electrons of the 629- and 924-kev transitions, which would be expected in very low intensity, were not resolvable from the low-energy tailing of the K-conversion electrons of the 743- and 992-kev gamma rays. Also, since no observable electron peak is evident in the 400 to 420 kev region, the gamma-ray at 510 kev is most likely due to annihilation radiation. The remainder of the transitions derived from these data are those which were previously observed.

A third analysis of the electron spectrum was made on the double-focusing variable-field spectrometer. A resolution of 0.15% is obtainable under ideal conditions, but on Po^{207} runs the best resolution obtained was 0.3%. The conversion electron spectrum observed was quite complex up to approximately 350 kev. It was impossible to determine intensities for the weaker lines, so they were omitted in the summary. The prominent electron lines below 350 kev are recorded in Table VIII. The shell assignments are tentative for most of the electron lines. The energies of the observed electron lines agree with the electron lines on permanent magnet studies. The intensities are all relative to the K shell conversion electrons of the 405.5-kev transition, which was taken as 100 units.

Table VIII

Conversion electron data for Po^{207} from double-focusing spectrometer

Electron energy (kev)	Conversion shell	Intensity	Photon energy (kev)
44.8	L_{III}	9.5	60.5 ± 0.2
47.0	L_{III}	9	
74.5	K	31	166 ± 0.5
108	L_I	9	
109	L_{II}	5	124 ± 0.4
110	L_{III}	25	
133	K	45	223 ± 0.7
142	K	24	233 ± 0.7
150	L_I or L_{III}	25	
152	L_{III}	45	
156	K	78	250 ± 0.8
181	L_I	7	223 ± 0.7
217	L_I	41	233 ± 0.7
	K_{307}		307 ± 0.9
230	M_I	3	233 ± 0.7
239	K	14	329 ± 1.0
246	M_I	7	250 ± 0.8
255	K	93	345 ± 1.0
290	L_I	9	307 ± 0.9
315	L_{II}	77	405 ± 1.2
327	L_{II}	23	345 ± 1.0
341	M_I	8	345 ± 1.0
87	K	26	178.0 ± 0.5
120	L_{II}	29	135.6 ± 0.4
122	L_{II}	13	135.6 ± 0.4

The high-energy region was also scanned, and conversion lines from only the 992-, 743-, and 405-kev transitions were observed. additional intensity data were, however, obtained both on relative K-line intensities and on K/L ratios. These results are tabulated in Table IX.

Multipolarity Assignments to Transitions

The next thing to consider in further establishing the decay scheme is the intensity data and multipolarity assignments for the transitions. The K/L ratios tabulated in Tables VII and IX are not enough to establish the multipole order of the transitions without additional data, but they can be used to eliminate many of the less likely cases; i.e., they eliminate M2, M3, M4, M5, E3, E4, and E5. For the 405-kev transition the K/L ratio is 6.1 ± 1. Only pure M1, E1, or M1 plus a small admixture of E2 radiation can have such a high K/L ratio. For the 743-kev gamma ray the K/L ratio is 4.6 ± 1, and the same cases as before must be considered here. In both these cases all other types and allowed mixtures of types of transitions would be outside the experimental error. For the 992-kev transition the ratio is 5.4 ± 1, which allows within the experimental error E1, E2, M1, M2, or M1 + E2 mixtures, with some possibility of M3. For these three transitions consideration of experimentally derived conversion coefficients eliminates many of the possible assignments. In order to calculate a derived conversion coefficient when the absolute number of electrons and photons for the transitions is not known, one has to first determine the multipole order assignment for one transition for which there are both gamma and electron intensity data. The correct theoretical conversion coefficient can then be used to relate the gamma and electron intensity data, and all the remaining information on the other transitions can be normalized to this transition's electron and gamma intensity. The other conversion coefficients can be determined from these related experimental results, and they depend only on the one assumption concerning multipolarity. It appears from the data that the 405-kev gamma ray is the easiest and most plausible for the assumed assignment. The K/L ratio indicates that it has the least number of possible assignments. The amount of E2 conversion can be set as very low by two different considerations. First, the high K/L ratio rules out very much admixture of E2, since this type of transition has a very low K/L ratio (~2.2) at this energy. Second, a very low limit can be set, since neither L_{II} nor L_{III} conversion lines were visible on permanent-magnet spectrograph exposures when the L_I line was quite intense. The relative intensity of conversion in the various shells and the K/L ratio are not sufficient for distinguishing between E1 and M1. About

the only method that can be used to distinguish between these types is to calculate the experimental conversion coefficients for both and determine which gives the best fit to the data. This was done, and the E1 case did not give suitable results. Therefore, with the 405-kev gamma ray considered as an M1 transition and with 2.78×10^{-1} as the theoretical K-conversion coefficient from Rose's tables,[26] the K conversion of the 992- and 743-kev gamma-rays can be calculated. The results of such a calculation are shown in Table XI. The gamma-ray intensity in Column 3 is the intensity relative to the most intense peak in the spectrum (992 kev). The intensities in Column 5 are normalized to the 405-kev photon intensity, which was calculated by using the electron intensity of the K-conversion line and the theoretical K conversion coefficient. The experimental coefficients were calculated by dividing Column 2 by Column 5. For the 992-kev gamma ray the conversion coefficient comes within the experimental error of an M1. An upper limit of approximately 5% of the photon intensity can be set for the amount of E2 conversion in the 992-kev transition. The 743-kev transition also is predominantly of M1 character, with an upper limit of 10% photon intensity for E2 conversion admixture. The three transitions considered are all predominantly M1 transitions within the limits of experimental error, and reasonably low limits of E2 admixture may be set. In addition to the above multipole order assignments, a number of tentative assignments may be made on some of the less intense transitions. From their characteristic L_I and M_I conversions, the gamma rays of 250, 345, 223, and 307 kev can be assigned as M1 transitions.

Table XI

Derived K conversion coefficients of certain Po^{207} transitions

Gamma-ray energy (kev)	Intensity K Electron	Intensity Gamma	Derived conversion coefficient K shell	Gamma-ray intensity (corrected)	Theoretical conversion coefficient
992	40	100	$2.1 \pm 0.5 \times 10^{-2}$	1870	M1 = 2.6×10^{-2} E2 = 6.3×10^{-3}
743	48	73	$3.5 \pm 0.5 \times 10^{-2}$	1370	M1 = 5.5×10^{-2} E2 = 1.1×10^{-2}
405	113	22		405 (calculated)	M1 = 2.78×10^{-1}

The only other possibility is E1, and it seems rather doubtful because this would make the gamma rays more intense by a factor of at least 10, and if they were that intense they should have been observed in the gamma spectrum. The 60-kev gamma ray can be very definitely assigned as an E2 transition on the basis of the equal conversion in the L_{II} and L_{III} shell. This is very characteristic of a low-energy E2 transition.

As a further check on the multipolarity assignments, a search was made for delayed transitions with half lives in the region of 10^{-7} to 10^{-9} second. This was done by gating a delayed fast-coincidence circuit on the K x-rays and observing the remainder of the Po^{207} gamma spectrum that was in coincidence with the x-rays. Then when artificial delays were introduced into the circuits, the counting rate of the peaks decreased. A plot of this decreasing counting rate versus the delay time gives a delay curve. If the transition does not have a lifetime within the region of measurement, the limiting curve can be used to set a limit on the lifetime of the state. A lifetime limit was set for the 992-kev gamma ray at $<4 \times 10^{-9}$ sec for the 743-kev gamma ray at $<5 \times 10^{-9}$ sec, and for the 405-kev gamma ray at $<5 \times 10^{-9}$ sec. The fact that the transitions are very fast and that their lifetimes are not measurable is expected. Since Po^{207} is so close to a closed shell, the transition is most likely a single-particle transition, and the Weisskopf formula for single-particle transition predicts a very short mean life. This applies only to M1, E1, and E2 transitions, for any higher-multipolarity transition might have measurable half lives. The lifetime limits, therefore, eliminate these higher-multipolarity types from consideration as possibilities for the 992-, 743-, and 405-kev transitions.

Identification of Positron Decay in Polonium-207

A special experiment was carried out to determine whether the 510-kev gamma radiation observed in the gamma spectrum could be identified as annihilation radiation, and -- if so -- to determine the amount of positron branching. This was done by taking advantage of the fact that the two annihilation radiations (511-kev photons) are emitted at 180° to each other. Coincidence measurements were made on annihilation radiations at 180°, with approximately 20% geometry in the detectors, and then changing the angle to 90° with the same geometry; a sharp change in coincidence counting rate should indicate that annihilation

radiation is present. This was done, and the counting rate dropped from a counting rate of approximately 50 counts/min for the 180° arrangement to approximately zero at 90°. To measure the amount of positron branching, coincidence measurements were made on a purified sample of Po^{207} at approximately 50% geometry for each crystal detector. A very narrow gate had been set by calibrating the instrument on the 511-kev gamma ray (annihilation radiation) of Na^{22}. The actual coincidences measured give the amount of contribution from annihilation radiation of Po^{207} to that small portion (~500 kev to 520 kev) of the total gamma spectrum. This amount, when corrected for counting efficiency and compared to the intensity of the 992-kev gamma ray -- which is present in 100% abundance -- gives the amount of positron branching. On this basis, the positron branching is calculated to be 0.2%, with a possible error in determination of 50%.

The observation of positrons in polonium is of great interest, since they have not been previously reported above mercury except for a very small positron branching in Np^{234}.[26] The electron-capture process becomes dominant over the positron process as the atomic number of the nuclide increases. The positron decay process follows the same selection rules as beta decay except that a minimum of 1.02 Mev energy is required. In Po^{207}, as is shown in the next section, the decay energy available is about 3 Mev. The decay of Po^{207} to the first excited state of Bi^{207} would be an "allowed" process, and approximately 2 Mev would be available for the decay. A further study aimed at direct observation of the positron spectrum will be necessary before their existance in Po^{207} decay can be confirmed.

Electron-Capture Decay Energy

The decay scheme presented for Po^{207} requires an electron-capture decay energy of at least 2.8 Mev. This decay energy can be calculated by using a method of closed-energy cycles. This method is based on the principle that the energy difference between two isotopes is the same by any path between them. Two paths form a closed decayenergy cycle between the two isotopes. There are several different types of closed energy cycles. For Po^{207} the best estimate of the electron-capture decay energy can be made by using the neutron and proton binding energies

in a closed cycle. The general case using this method, and the cycle specifically for Po^{207} are shown in Fig. 5. There are two paths through which the electron-capture decay energy can be estimated by use of this cycle. If the neutron and proton binding energies of Z^A are known or can be estimated, the electron-capture decay energy for Z^{A-1} is given by

$$E_{EC}\,(Z^{A-1}) = E_n\,(Z^A) - E_p\,(Z^A) - (n-p)$$

A similar path giving the same decay energy requires a knowledge of the neutron and proton binding energies of $(Z-1)^{A-1}$ and Z^{A-1}, respectively. Again,

$$E_{EC}\,(Z^{A-1}) = E_n\,[(Z-1)^{A-1}] - E_p\,(Z^{A-1}) - (n-p)\,.$$

If the neutron and proton binding energies have been calculated or estimated correctly, the electron-capture decay energy will be the same for both paths. The mass difference between the neutron and the proton (n-p) is equal to 0.78 Mev. The cycles involving the electron capture of Po^{207} and Bi^{207} require a knowledge of the binding energies of the last neutron and proton of Po^{208}, the last neutron in Po^{207}, and the last proton in Bi^{207}. The neutron and proton binding energies of Po^{208} and Bi^{207}, respectively, have been calculated through their use in other cycles. The neutron binding energy of Po^{208} and the proton binding energy of Po^{207} must be estimated by extrapolation of the data of Glass et al.[27] The values used for the calculation are:

Neutron binding energies:

$Bi^{206-207}$ = 8.07 Mev (calculated)

$Po^{207-208}$ = 8.5 ± 0.3 Mev (estimated);

Proton binding energies:

$Bi^{207-208}$ = 5.03 Mev (calculated)

$Bi^{206-207}$ = 4.45 ± 0.5 Mev (estimated).

The neutron binding energy cycle used for estimation of the electron-capture decay energy is shown in Fig. 5. The value of the electron decay energy is calculated as 2.80 ± 0.45 Mev; this is close to or greater than the decay energy required by the decay scheme. Many gamma transitions are, however, unassignable in the scheme; so thedecay energy is probably somewhat higher than is proposed.

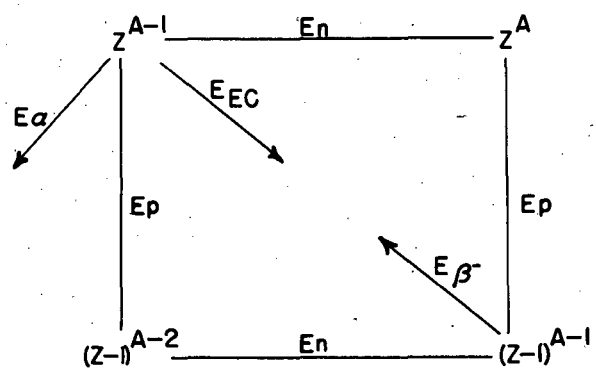

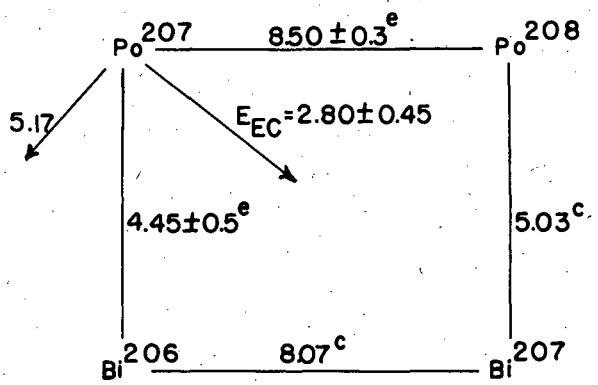

MU-10008

Fig. 5. (Above) Neutron-binding energy cycle, general.
(Below) Neutron-binding energy cycle of Po^{207}.

Decay Scheme and Discussion

The decay scheme can now be further considered with respect to population of excited states by electron capture. Using the multipolarity assignments and intensity data, we can find the total intensity of each transition by summing the gamma and electron intensities for each transition. Analysis of this information gives a reasonable estimate of the amount of electron capture proceeding to each excited state. Fig. 6 shows the results for the more intense transitions. A few percent of the Po^{207} electron-capture decay goes to some additional levels that must be present to explain the unassigned transitions. The largest part of the decay must proceed as shown.

This figure also shows the population to each of the excited states and the corresponding log (ft) values for each transition. Log ft values of around 6 are usually termed as "allowed" and are those expected for a short half life. The data given above all correlate quite satisfactorily for the main paths of electron-capture decay of Po^{207}. There are many more transitions and levels that should be placed in a complete decay scheme but have been omitted here.

In discussing the consistency of the data and the spin assignments, we must first estimate the ground-state spin and parity of the two nuclei, Po^{207} and the daughter nucleus Bi^{207}. A reasonable estimate as to the ground-state spin of Po^{207} can be made from consideration of its odd particle. Po^{207} is three neutrons and two protons removed from the double closed shell. The two protons and two of the neutrons each pair off, with a resultant angular momentum of zero. Therefore the spin of the isotope is the spin of the remaining odd neutron. This odd neutron is the same one as is in the ground state of Pb^{205}, and it is a $f_{5/2}$ level, which would give Po^{207} a 5/2 spin and odd parity. Bi^{207} in ground state is composed of an odd proton and two neutrons beyond the closed shells. The spin here also is the spin of the odd particle. The odd proton in Bi^{207} is in the same level as the odd proton in Bi^{209}, and it has been determined to be an $h_{9/2}$ level in Bi^{209}.[47] So Bi^{207} should have a 9/2 spin and odd parity. With 5/2- and 9/2- as the spins and parities of the two ground states, an electron-capture decay between these two states would have a [$\Delta I = 2$, No] beta decay.

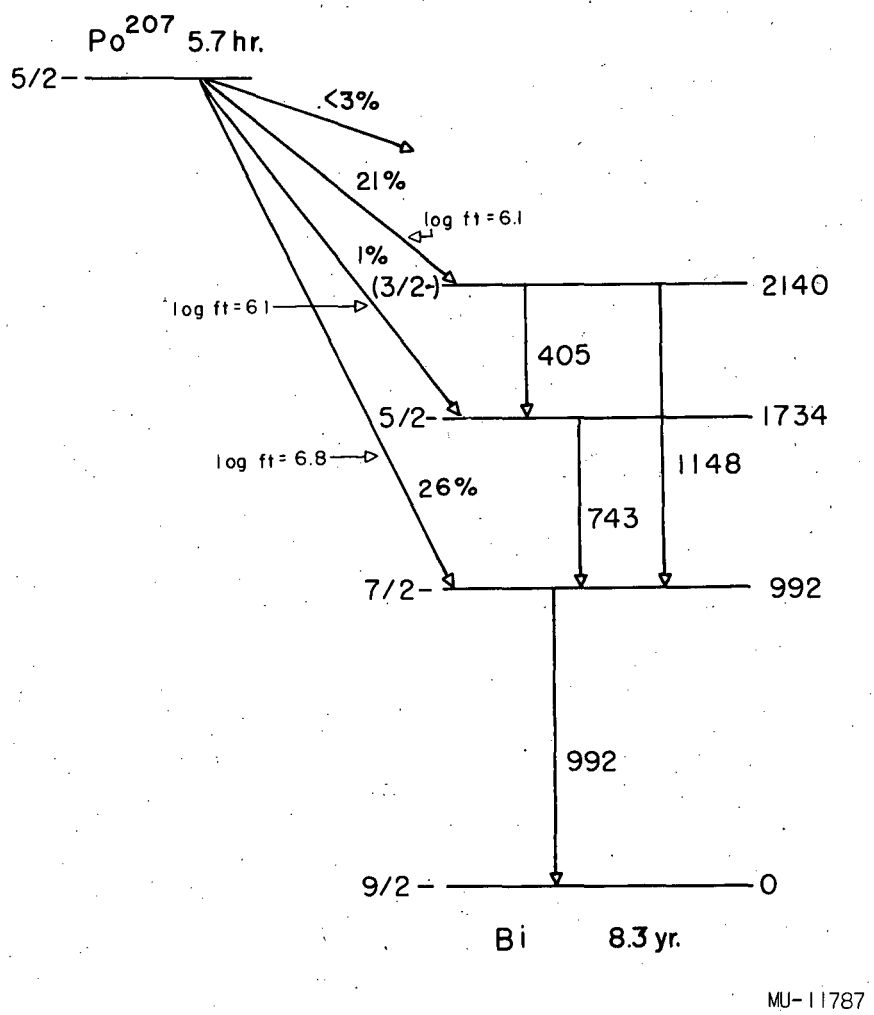

Fig. 6. Suggested electron-capture decay scheme for Po^{207}.

This is a second forbidden case and would have a half life that is too long for a 5.7-hr decay. Therefore, there would be no electron capture directly to the ground state of Bi^{207}.

The spin of the first excited state should correspond to the first level available by promotion of the odd proton. Not too much is known concerning the order of the odd proton levels above the 82-proton closed shell. Inelastic neutron-scattering experiments, however, have shown that the first excited state in Bi^{209} is a 7/2- state, and it appears at 895 ± 25 kev.[28] This level agrees qualitatively with an assignment of 7/2- for the 991-kev first excited state of Po^{207}. This spin assignment and a multipolarity assignment of M1 for the 991-kev transition are also in agreement. This makes electron capture to this level a [$\Delta I = \pm 1$, No] process, which is "allowed" in terms of beta systematics.[29] Such a process is fast and agrees with the short measured half life of Po^{207}, therefore direct capture to this level must take place.

The second excited state is at 1735 kev, and decays only to the first excited state. The inelastic neutron-scattering data on Bi^{209} show a level at 1560 ± 35 kev; but it depopulates directly to the ground state, so that it must not be the same level.[31] With no other information available concerning the excited levels of an $h_{9/2}$ proton, the spin for the second state is rather difficult to assign. A spin of 5/2- agrees the best with the experimental information. A state of this spin should depopulate only to the 7/2-level and should receive a large proportion of the direct electron capture. Reference to Fig. 7 shows that the state does both of these, so 5/2- may be taken as a tentative spin and parity assignment for the second excited state. Such a state is probably the second level of promotion of the odd proton.

It is very difficult to say much more about the remaining excited states. The fact that there are so many excited states in the 1.8-to-2.8-Mev region indicated that they must not be due to only the odd-proton promotion. They may arise from the promotion of the neutron pair to a higher energy state, or the promotion of one of the neutrons out of the pair. Either of these cases would then give rise to numerous additional levels.

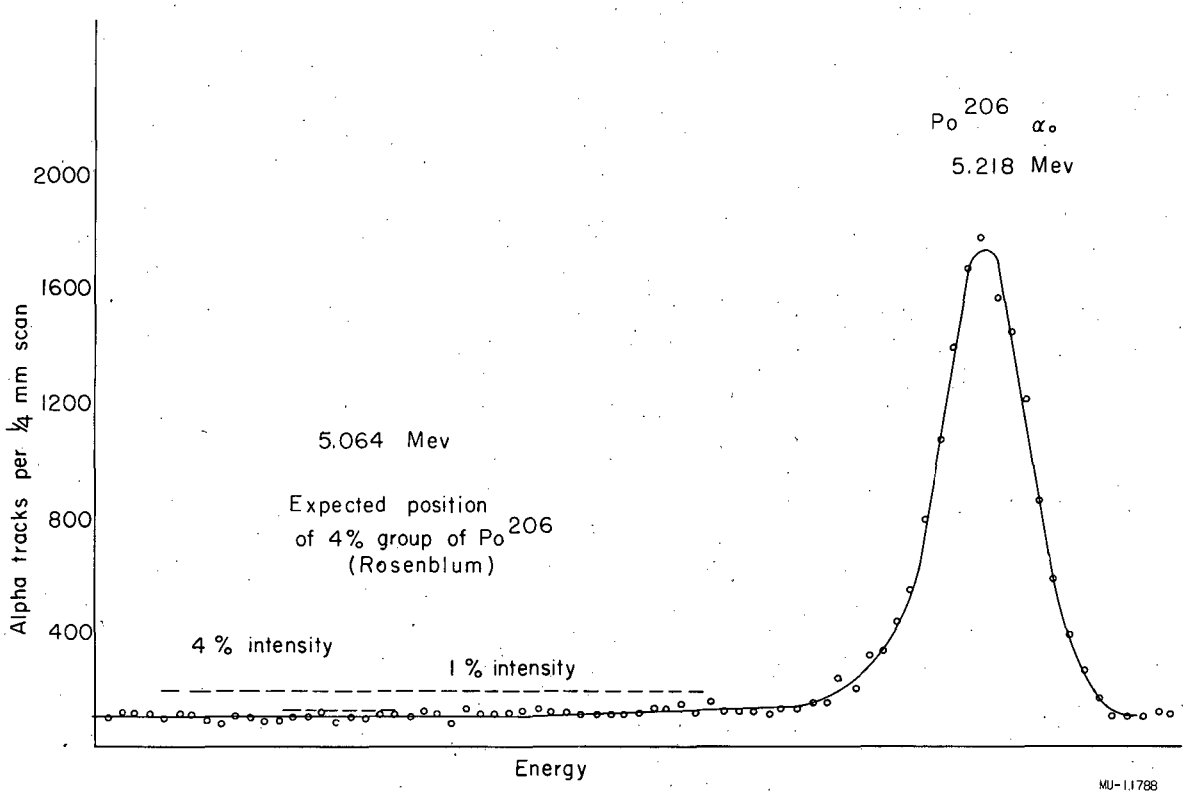

Fig. 7. Alpha spectrum of Po^{206} as observed on alpha-particle spectrograph.

The explanation of the complex level structure above 1.7 Mev, which cannot be explained by the single-particle model, may be qualitatively explained by the work of Pryce.[4] Pryce considered in detail the isotope that is two neutron holes in the 126-neutron shell. This isotope has the same neutron configuration as Bi^{207}, the product nucleus of Po^{207} electron-capture decay. He predicted a $(p_{1/2})^{-2}$ $J = 0$ configuration for the ground state of Pb^{206}. The configuration with the next lowest energy was a $(p_{1/2}\ f_{5/2})^{-2}$ $J = 2$ state with a $(p_{1/2}\ f_{5/2})^{-2}$ $J = 3$ state the next higher in energy. The energy separation between the $J = 0$ and $J = 2$ states was 808 kev. If one assumes that there is no interaction between the proton and a single neutron and that all the interaction takes place between the proton and the neutron pair, it would then follow that these same neutron configurations should influence the levels in Bi^{207}.

On the basis of this assumption concerning interaction between particles, the levels expected in Bi^{207} can be qualitatively outlined. The ground state for Bi^{207} would be a $(p_{1/2})^{-2}$ $J = 0$ and a $(h_{9/2})^{1}$ $J = 9/2$ configuration coupled together. These two states can be coupled only to give a resultant 9/2 spin for the ground state. The first excited state from energy considerations is most likely a $(p_{1/2})^{-2}$ $J = 0$ and an $(h_{9/2})^{1}$ $J = 7/2$ configuration with a resultant 7/2 spin. The next levels probably arise from a $(p_{1/2}f_{5/2})^{-2}$ $J = 2$ and an $(h_{9/2})^{1}$ $J = 7/2$ configuration. This configuration would give rise to 11/2, 9/2, 7/2, 5/2, and 3/2 states, which would be separated in energy owing to interaction between particles. The next group of states would be from the $(p_{1/2}\ f_{5/2})^{-2}$ $J = 3$ and either an $(h_{9/2})^{1}$ $J = 7/2$ or an $(h_{9/2})^{1}$ $J = 5/2$ configuration. These two states would also give rise to many additional levels with half integral spin values between 13/2 and 1/2 and 11/2 and 1/2, respectively. As one continues to higher-energy neutron configurations, the number of levels available becomes increasingly greater.

It is not possible to determine where each of the above energy levels would be expected, since the details of the interaction between the neutrons and proton are not known sufficiently for calculation of energies. However, the fact that the model does predict a large number

of levels that probably lie above 1.7 Mev, and also gives a reasonable explanation for the first excited state makes the model quite plausible. The short outline given here does not attempt to answer questions concerning the population and de-excitation of the numerous levels predicted. It does, however, show a possible method of more completely explaining the level structure of Bi^{207} than is available with the strict single-particle model.

B. Polonium-206

Po^{206} was first identified by Templeton et al. in the high-energy bombardment of bismuth metal with protons and by bombarding lead enriched in lower-mass, stable isotopes with helium ions.[22] They reported a 9-day half life with 90% electron capture and 10% alpha decay. The energy of the alpha particle was determined to be 5.2 Mev.[23] An 0.8-Mev gamma ray was observed in the electron-capture decay by adsorption measurements. Further work by Kelly et al. determined the branching as 96% electron capture and 4% alpha decay.[30] Rosenblum investigated the alpha decay with an alpha-particle spectrograph and reported a 5.218-Mev group of 96% intensity going to the ground state and a 4% group of 5.064 Mev going to an excited state.[31] No work has been published concerning the gamma rays or conversion electrons in the electron-capture decay.

Alpha Spectrum of Polonium-206

When a complete study of Po^{206} was started, it appeared that the alpha decay should be re-examined. This was determined from the fact that when one plots the energies of the first excited state versus the mass numbers for even-even nuclides, the first excited states for the lead isotopes ($Pb^{208, 206, 204, 202}$) should be very high because of the 82-proton closed shell. The first excited state for Pb^{204} from experimental work on the isomer shows this state to be at 890 kev. Since the curves of this type are regular and decrease in energy as one moves away from the 126-neutron closed shell, the first excited state for Pb^{202}, which is the daughter of Po^{206} alpha decay, should come between 500 and 700 kev. The 156-kev value determined by Rosenblum seems very unreasonable. For this reason, a detailed examination of the alpha decay of Po^{206} was undertaken.

The Po^{206} for this series of experiments was obtained by "milking" it from Em^{210}, which was produced by high-energy proton spallation of thorium metal in the 184-in. cyclotron. The emanation fraction was isolated by collecting it in a U-tube on a vacuum system at liquid nitrogen temperatures. The sample collected was predominantly Em^{208}, Em^{209}, Em^{210}, Em^{211}, and Em^{212}. Em^{208}, Em^{209}, and Em^{212} all have short half lives, so the mixture was allowed to decay several hours before further purification, and all isotopes except Em^{210} and Em^{211} will have decayed. The Em^{210} and Em^{211} were transferred to a clean U-tube and the decay products collected. Em^{210} decays by 95% alpha emission to 9-day Po^{206} and 5% electron capture to At^{210}. The At^{210} decays almost entirely by electron capture to the 138-day Po^{210}. Em^{211} decays by 75% electron capture to At^{211}, which decays to Po^{211} and then to Bi^{207}. The 25% alpha branching of Em^{211} forms the 5.7-hr Po^{207}. Out of these decay products only Po^{206}, Po^{207}, Po^{210} and Bi^{207} remain after several days. Only the two polonium isotopes show alpha decay, and the alpha activity of Po^{206} is 15 times that of Po^{210} when branching ratio and half life are taken into consideration. This Po^{206}-Po^{210} mixture was prepared for analysis on the alpha-particle spectrograph both by plating on a 10-mil silver wire and by vacuum sublimation.

The first sample was plated on a silver wire and contained 7.5×10^5 alpha disintegrations/min of Po^{206}. This sample was exposed for 2 days in the alpha-particle spectrograph. The resolution of the alpha peak was not good, owing to sample thickness, and the tailing on the low-energy side made it difficult to look for low-intensity alpha groups. Only one alpha group was observed, corresponding to the 5.218-Mev ground-state transition as seen by Rosenblum. However, owing to the large amount of tailing, a limit of only 3% could be set on the presence of alpha fine structure.

The vaporized sample contained about 10^6 alpha disintegrations per min. Since the Em^{208} had not completely decayed out before purification, there was a small amount of Po^{208} present in the sample. Po^{208} has an alpha group at 5.108 Mev which, if present to a large extent compared with Po^{206}, might interfere in the search for the previously reported 5.064-Mev group of Po^{206}. The first exposure of this sample for

2 days did show the main Po^{206} peak and a group that was probably Po^{208}. Even though Po^{208} was present, no alpha group was seen at 5.064 Mev in an abundance greater than 1%. A second 9-day exposure with this sample confirmed the assignment of the second group to Po^{208}, and allowed a better limit of 0.5% to be set on the second Po^{206} group at 5.064 Mev. The alpha spectrum observed in the second run is shown in Fig. 7.

Stephens, doing alpha-gamma-ray coincidences on Po^{206}, sets a limit of 1.7×10^{-4} photons per alpha for the presence of gamma radiation in the 100-to-300-kev range below the main alpha group.[36] Thus, it seems probable from the alpha spectrum and alpha-gamma-ray coincidence data just presented that the previously reported 4% group in Po^{206} alpha decay does not exist, and that the first excited state of Pb^{202} is not at 156 kev above the ground state.

The sample containing both Po^{208} and Po^{206} allowed a convenient check of the absolute energy of the Po^{206} alpha group. With the 5.108-Mev group of Po^{208} as a standard, the two runs gave 5.216 and 5.219 Mev for the Po^{206} alpha-particle energy, which is in good agreement with Rosenblum's value of 5.218 Mev.

Gamma Spectrometer Measurements of Polonium-206

A study of the electron capture of Po^{206} to the excited states of Bi^{206} has been carried out. Several gamma rays were observed in the Po^{206} decay on the scintillation spectrometer. The spectrum as observed is shown in Fig. 8. The intensities of the gamma rays were determined from several runs, and they are recorded in Table XII. They are related to the 511-522-kev photopeak, which has been arbitrarily set at 100 units. The intensities after correction for counting efficiency are good to ± 20%.

Table XII

Relative intensities of gamma rays of Po^{206}

Gamma-ray energy (kev)	Intensity (relative)
1031	84 ± 16
807	57 ± 11
511-522	100 ± 20
338	41 ± 8
286	35 ± 7

Conversion Electrons of Polonium-206

The conversion electrons from Po^{206} decay have been investigated by use of the permanent-magnet spectrographs. The numerous electron

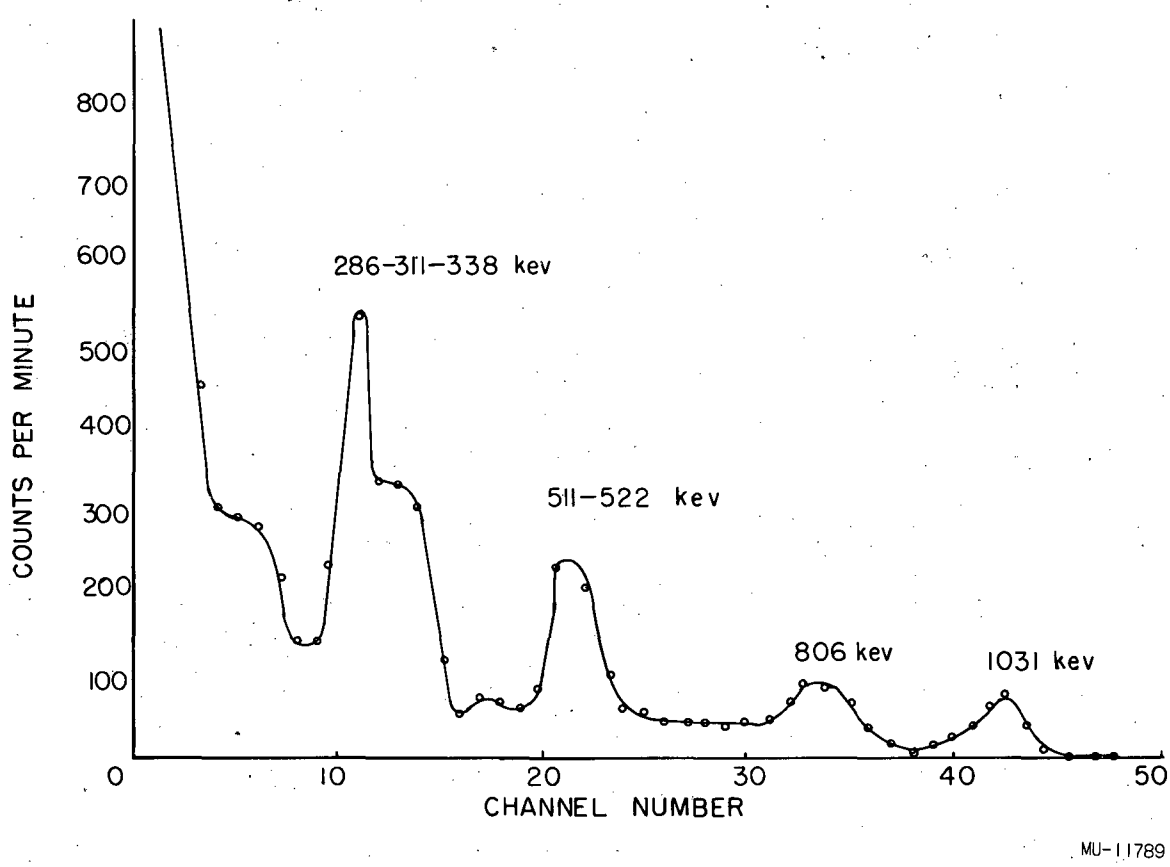

Fig. 8. Gamma-ray spectrum of Po^{206} as observed on the scintillation spectrometer.

lines that were observed, and their assignments, are summarized in Table XIII.

Table XIII

Electron lines and assignments from permanent-magnet spectrograph experiments with Po^{206}

Electron energy (kev)	Conversion shell	Intensity*	Energy (gamma ray)	
1014.7	L	VW	1031	1031 ± 3.0
941.6	K	M	1032	
792	L	VVW	807	807 ± 2.4
716	K	SM	807	
517.5	M	VW	522	
505.7	L	M	522.1	522 ± 1.5
494.5	L	M	511.5	
431.4	K	S	522.1	
421.0	K	VS	511.5	511.5 ± 1.5
334.0	M_I	M	338	
321.5	L_I	S	337.9	
294.7	L_I	M	311.2	338.0 ± 0.3
285.1	N_I	W	286.0	
282.0	M_I	M	286.0	311.0 ± 0.3
269.7	L_I	VS	285.7	
247.8	K	VVS	338.3	
220.3	K	VS	310.8	286.0 ± 0.3
195.2	K	VVS	286.0	
59.3	$N_{II,III}$	M	60.0	
56.8	M_{III}	S	60.0	60.0 ± 0.1
56.2	M_{II}	S	59.9	
46.5	L_{III}	VS	59.9	
44.3	L_{II}	VS	60.0	
372.6	K	WM	463	463 ± 1.4
381.5	K	VW	472	472 ± 1.4
890	K	VW	980	980 ± 3.0

*Visual intensities are tabulated by the following scale:

VVS= very, very strong	SM= strong moderate	SW= strong weak	W= weak
VS= very strong	M= moderate	W= weak	VW= very weak
S= strong	WM= weak moderate	VW= very weak	VVW= very, very weak

The possibility that some of these lines might be due to Bi^{206} daughter activity or Po^{207} contamination in the sample was checked by comparison with plates run with sources of these activities. Those electron lines which were only observed in the high-field permanant-magnet spectrographs PM^{III} and PM^{IV} are limited to 0.3% energy resolution. The lower-energy lines below 300 kev were observed on other permanent-magnet spectrographs where the resolution is 0.1%. The visual intensities given in Column 3 in the table are uncorrected for the efficiency of the film. In Table XIV all the additional electron lines are summarized that are definitely assignable to Po^{206} decay, but which cannot be definitely assigned to a transition that may be placed in the tentative decay scheme.

Table XIV

Unassigned Po^{206} electron lines from permanent-magnet experiments

Electron energy (kev)	Intensity* (visual)	Electron energy (kev)	Intensity* (visual)
80.0	VW	191.0	VW
93.8	WM	193.6	W
107.8	VW	402.6	VW
110.5	W	489	VW
179.7	W	515	VW
180.7	VW		

*Visual intensities are tabulated by the following scale:

VVS= very, very strong SM= strong moderate SW= strong weak W= weak
VS= very strong M= moderate W= weak VW= very weak
S= strong WM= weak moderate VW= very weak VVW= very, very weak

The intensities of the electron lines were determined by analyzing the electron spectrum by use of the double-focusing beta-ray spectrometer. The sample was run at 0.3% resolution, and it is shown in Fig. 9. The intensity data are summarized in Table XV. All the intensities are relative to the K conversion lines of the 286-kev transition. For most of the transitions only K conversion lines were observed, but K/L ratios were determined for those transitions where both lines were seen. These intensities are believed to be accurate to within ± 10%.

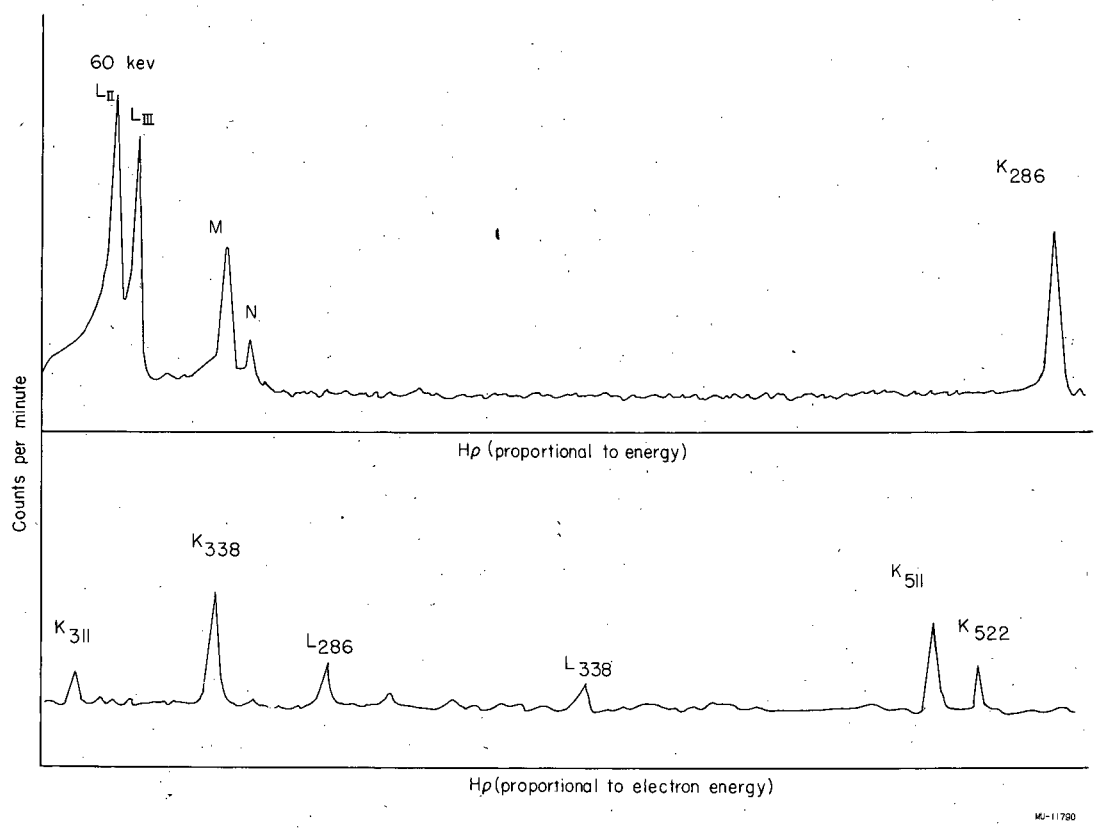

Fig. 9. Electron spectrum of Po^{206} as observed on the double-focusing beta-ray spectrometer.

Table XV

Po^{206} electron lines and intensities from double-focusing beta-ray spectrometer

Electron energy (kev)	Shell assignment	Energy (gamma ray)	Intensity K/L ratio
44.3	L_{II}	60	
46.5	L_{III}	60	
56.4	$M_{II,III}$	60	
59.3	$N_{II,III}$	60	
195	K	286	10 ± 10 5.4 ± 0.5
270	L		18 ± 2
220	K	311	14 ± 1.4 5.0 ± 0.5
248	K		2.8 ± 0.3
321	L	338	49 ± 4.9
421	K	511	19 ± 1.9
431	K	522	10 ± 1
716	K	807	5.7 ± 0.6
941	K	1031	3.2 ± 0.4

Samples of Po^{206} were also run on the magnetic-lens spectrometer in order to determine K/L ratio for the high-energy transitions. This beta-ray spectrometer has only 3% resolution, but can be very useful when the transitions are spaced so that conversion lines do not overlap, since it has quite high transmission (1%). The results found by using this instrument are summarized in Table XVI. K/L ratios have been determined for the 807- and 1031-kev transitions and for the combined 511-522-kev transitions. Also the K conversion line for the 980-kev transition, which was previously indicated in permanent-magnet experiments, was observed. A portion of the electron spectrum is shown in Fig. 10.

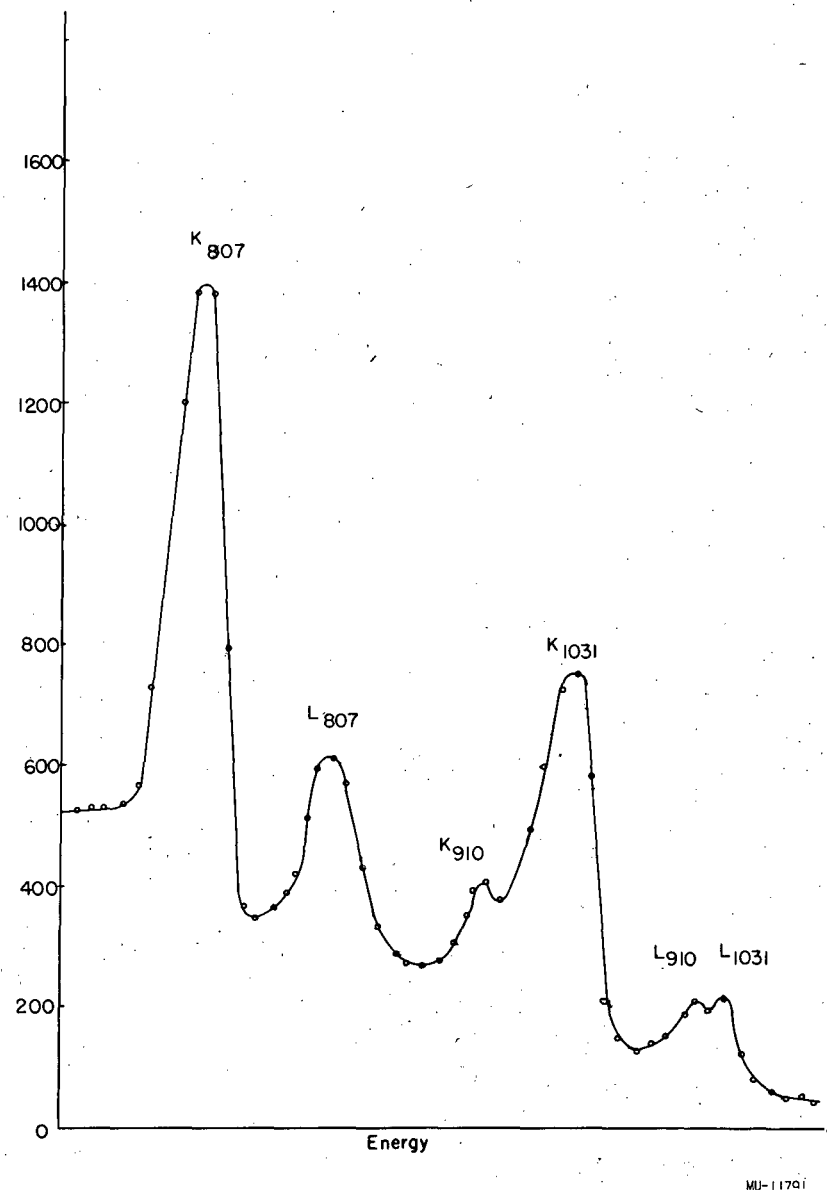

Fig. 10. High-energy electron spectrum of Po^{206} as observed on the magnetic-lens spectrometer -- 700- to 1100-kev region.

Table XVI

Po^{206} intensity data from magnetic-lens spectrometer experiments

Electron energy (kev)	shell assignment	Gamma-ray energy	Intensity	K/L ratio
940	K	1031	100 ± 20	6.5 ± 0.8
1015	L		16 ± 4	
890	K	980	4 ± 1	
715	K		185 ± 37	4.3 ± 0.3
790	L	807	44 ± 9	
416	K	511-522	1000 ± 200	5.0 ± 0.5
500	L		200 ± 40	

Multipole Order Assignments

In any attempt to establish a tentative electron-capture decay scheme for Po^{206}, the multipole orders of the transitions would be very helpful. For many of the transitions the number of possible multipole order assignments may be reduced to only a few by investigating the L-shell conversion pattern and the K/L ratios. The 26-, 311-, and 338-kev transitions show prominent L_I, M_I, and N_I conversion lines, which indicate that these transitions are predominantly M1 or E1. A low limit may be set on the amount of admixture of any other multipole order that has large L_{II} or L_{III} conversion, since neither of these lines was observed in permanent-magnet exposures. For the 511- and 522-kev transitions L conversion electrons were observed, but owing to the resolution (0.3%) they could not be definitely assigned to a specific subshell. The 807 and the 1031 kev transition conversion in the L subshell was observed, but the energy resolution limited any further detailed assignment. K/L ratios for the 286- and 338-kev transitions agree with M1 or E1 assignments and rule out all other possibilities. For the 511- and 522-kev transitions only a combined K/L ratio was obtained, and this was 5.0 ± 0.5. This value favors M1 or E2, but since two K and two L lines are included that may be from entirely different transition types, this ratio is subject to a very large uncertainly in making a multipole order assignment. The K/L ratio of 4.3 for the 807-kev transition makes an E2 the most favorable assignment. The K/L for the 1032-kev transition falls in a region where the K/L ratios converge, so that M1, E1, or M1 + E2 mixture are all plausible assignments.

The K conversion coefficient for these transitions can be used to distinguish between the various multipole orders. A derived K conversion coefficient can be calculated from the relative photon and conversion electron intensities after they have been normalized. The 286-kev transition was assigned as an M1 so that its theoretical conversion coefficient could be used to relate the gamma-ray and electron intensities. The derived K conversion coefficients for the remaining transitions have been calculated and are recorded in Table XVII. The results are quite conclusive for an M1 assignment for the 338-kev transition and an E2 assignment for the 807-kev transition. The K conversion coefficient for the 1031 kev transition agrees with the theoretical value for an E2. For the 511-522-kev transitions the combined K-conversion coefficient falls between that for a pure M1 and a pure E2. So about all that may be concluded concerning the 511- and 522-kev transitions is that each may be anything between a pure E2 and a pure M1 or an M1 + E2 mixture.

Table XVII

Derived K conversion coefficients for Po^{206} transitions

Gamma-ray energy (kev)	Photon intensity (relative)	Electron intensity (relative)	Photon intensity (corrected)	Derived K-conversion coefficient (assumed)	Theoretical K-conversion coefficient
286	35	100	200		5×10^{-1}
338	41	48	235	$2.1 \pm 0.5 \times 10^{-1}$	M1=2.8×10^{-1} E1=1.7×10^{-2}
511 522	100	30	575	$5.2 \pm 0.5 \times 10^{-2}$	M1=9×10^{-2} E2=2.4×10^{-2}
807	57	5.7	328	$1.7 \pm 0.5 \times 10^{-2}$	M1= E2=assumed
1031	84	3.2	480	$6.2 \pm 0.5 \times 10^{-3}$	M1 E2=6×10^{-3} E1=3.3×10^{-3}

Table XVIII summarizes all the transitions observed in the different experiments and their most probable multipole order assignments. All these transitions may be placed in a tentative decay scheme except the 980-kev transition. The proposed decay scheme and tentative spin

assignments to the excited states are given in Fig. 11. The sums of the transitions by any path between levels agree with the experimental error of the energy determination.

Table XVIII

Summary of transitions observed in Po^{206} decay

Energy (kev)	Assignment	Energy (kev)	Assignment
1031	E2	463	--
980	--	338	M1
807	E2	311	M1
511	M1,E2, or (M1+E2)	286	M1
522		60	E2
472	--		

Gamma-Gamma-Ray Coincidence Measurements

Gamma-gamma-ray coincidence measurements were run to check the arrangement of the transitions. When the 1031-kev transition was used as the gating photon, the low-energy gamma rays (286, 311, and 338) were observed to be in coincidence with it. Also a weak coincidence was detected with either the 511- or 522-kev transition. The 807-kev transition as the gating photon showed a very prominent 511-522-kev coincidence peak, with some additional weak coincidences in the 286-, 311- and 338-kev regions. The resolution of the scintillation spectrometr does not allow one to distinguish which of these three gamma rays is in coincidence, so the results cannot be considered conclusive as to gamma-ray placement in the decay scheme. However, the over-all results agree with the proposed decay scheme except that the intensity of the coincidence between the 1031- and 522-kev transitions is weak. All these measurements were made with a 2×10^{-6} sec. resolving time. Additional coincidence measurements were run with a much faster resolving time. By gating on the K x-rays a limit of less than 2×10^{-9} sec for the half life of the transition could be set for the 1031-, 807-, 511-, 338-, 311-, and 286-kev transitions.

Discussion of Spin Assignments

The spin assignments to the various excited states are very tentative and were assigned by intensity considerations.

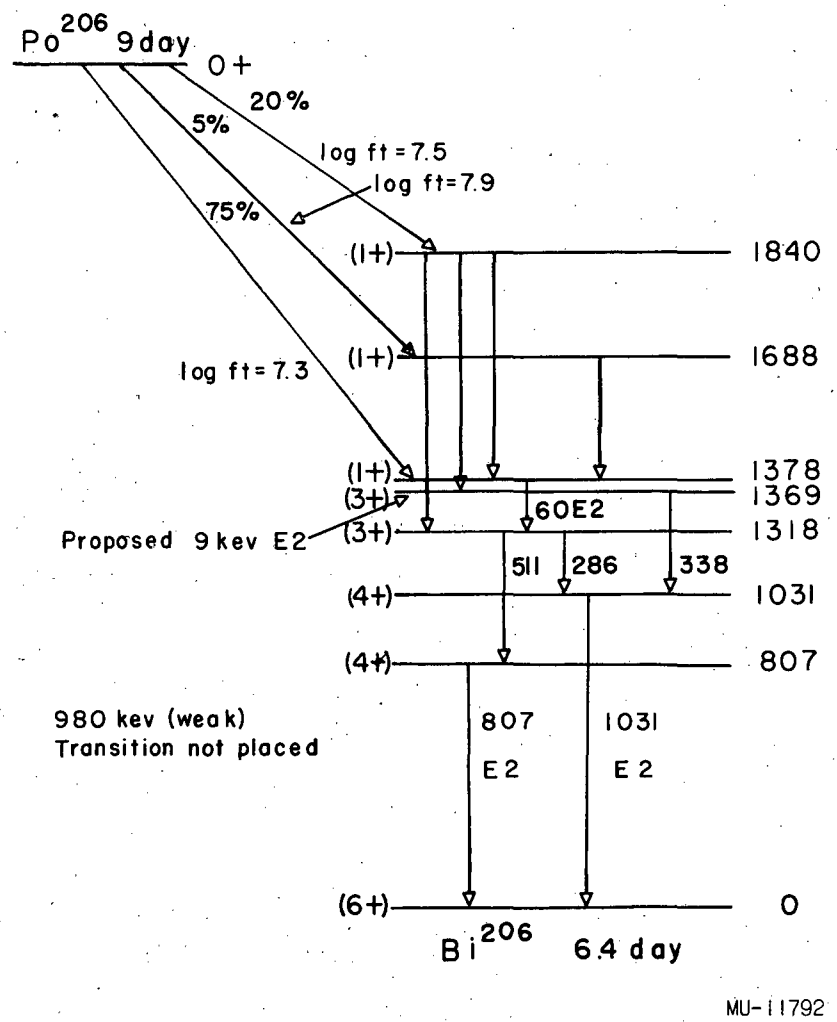

Fig. 11. Proposed electron-capture decay scheme for Po^{206}.

The ground-state spin of Po^{206} is zero with even parity by even-even nuclide systematics. The ground-state spin of Bi^{206} has been tentatively assigned 6 by Alburger and Pryce, with even parity by a detailed analysis of its decay to excited states of Pb^{206}.[5] In order to obtain electron capture to the higher excited states, the spin change must be either [$\Delta I = 0, \pm 1$, No] between the state and the Po^{206} ground state. Any spin change greater than this can be ruled out. A "second forbidden" process [$\Delta I = 2, \pm 3$ No] would require too long a half life to fit this decay.[29] A "first forbidden" process [$\Delta I = 0, \pm 1, \pm 2$, Yes] requires a parity change which is not plausible for this decay. This is because the transition types which allow parity changes were not observed in the experimental work. Since the spin change is either 0 or 1 between the Po^{206} ground state and the Bi^{206} excited state, this excited state has to depopulate to the ground state (6+) by a series of transitions to accomplish the spin change of either 5 or 6 if no spin changes larger than 2 are present. The decay scheme proposed is one possibility that agrees with the experimental data. The spin assignments are rather rigidly set if the ground-state spin and the multipolarities of the gamma rays are correct. One weakness appears in the population of the 1369-kev level. This state has been assigned a spin of 3+ and therefore it cannot receive any direct electron capture. It must get its population from 9 kev E2 transition from the 1378-kev level. This requires that a 9-kev E2 compete with the 60 kev transition, which is three times more intense. This is reasonable, but it is considered a weakness since no transition of this low energy has been observed.

Estimation of Electron-Capture Decay Energy of Polonium-206

The electron-capture decay for Po^{206} has been estimated by the proton, neutron binding-energy closed cycle. An explanation of this method was given in the discussion on Po^{207} in this dissertation, and a detailed explanation in an article by Glass, Thompson, and Seaborg, which constituted the original source.[27] The neutron and proton binding energies required for this case were estimated by extrapolating binding-energy curves. The binding energy for the last proton in Po^{206} was estimated to be 4.8 ± 0.3 Mev. The binding energy for the last neutron in Bi^{206} and Po^{207} were calculated to be 8.2 ± 0.3 Mev and 7.2 ± 0.3 Mev,

respectively. These binding energies give a value of 2.3 ± 0.6 Mev for the electron-capture decay energy of Po^{206}. With this estimated decay energy it is possible to determine log (ft) values for the electron-capture process to the various excited states of Bi^{206}. The log (ft) values calculated are 7.5 for the decay to the 1839-kev level, 7.9 to the 1688-kev level, and 7.3 to the 1377-kev level. These values are all high for what is usually considered significant. The log (ft) value when compared with the population going to the same state shows the expected relative value to the other two electron-capture decays. So the complete decay scheme put forth agrees quite reasonably with the experimental data and the other information derived from them.

It is very difficult to determine what configurations give rise to the various excited states that were observed. The ground state of Bi^{206} is an odd-odd nuclear type with an $h_{9/2}$ proton and an $f_{5/2}$ neutron hole in addition to a pair of $p_{1/2}^{-2}$ neutron holes. The odd proton and neutron will couple and give the spin of the ground state, which was considered to be a 6+ state by Pryce and Alburger.[5] The excited states can arise from the promotion of either the proton or the neutron or both and the subsequent coupling into different resultant spins. The number of levels that can be predicted in this manner is very great.

It is interesting to note the alpha decay of At^{210} when considering the excited levels of Bi^{206}. At^{210} decays to Bi^{206} by three approximately equally intense alpha groups. They populate excited states 82 and 164 kev above the ground state. In the study of the Po^{206} electron-capture decay no transitions of these energies were observed, and it must be assumed that they are not populated to a very great extent. The explanation must lie in the fact that the $h_{9/2}$ proton and $f_{9/2}$ neutron in the ground state can couple in several ways to yield states of the same configuration with different spin values which will be split by a small energy difference owing to interaction between particles. The alpha decay of At^{210} would be expected to populate all states of the same configuration when one state is populated if the energy difference is not too great. Alpha decay is essentially spin-independent, and the partial alpha half life for each group depends on the amount of decay energy available. For At^{210} the groups are very close together in

energy, so that equal abundance for the three groups is consistent with what is known concerning alpha decay. However, it is difficult to assume that these low-lying excited states are present and are not populated by Po^{206} decay, since favored transitions can be postulated for any spin that an $h_{9/2}$ and $f_{5/2}$ coupling can give.

This example of states that are present but not populated in Po^{206} decay points out the great complexity that is expected for Bi^{206} excited states. Each configuration should be a group of close-lying levels that arise from the coupling of the odd particles. These levels, when superimposed on the excited levels of the neutron pair, make the theoretical levels of Bi^{206} very complicated.

C. Astatine-209

The isotope At^{209} was first identified by Barton, Ghiorso, and Perlman, who reported that it decayed predominantly by electron capture.[9] They measured the alpha emission to electron capture branching ratio to be 0.05 and an alpha energy of 5.65 Mev. A preliminary study of the electron conversion lines given by Mihelich, Schardt, and Segrè yielded transitions of 83.8, 91.1, 195.0, 545, and 784 kev.[33] These electron lines were assigned to At^{209} on the basis of change in relative intensity of known At^{210} lines as the energy of the accelerated helium ions was varied to change the amount of At^{209} to At^{210} present in the bismuth target. This is the extent of the previously published information on At^{209} decay.

The study of this isotope was undertaken with the hope of completely elucidating the alpha and electron-capture decay schemes. It was first necessary to determine if any alpha fine structure was present, in order to determine if the reported gamma rays all belong to the electron-capture decay. Samples of At^{209} were made by bombarding bismuth metal with 40-Mev helium ions in the 60-in. cyclotron at the Crocker Radiation Laboratory. A line source was prepared by plating the astatine on a 10-mil silver wire. This source was then exposed in the alpha-particle spectrograph for 8 hr; a count of the alpha tracks in the emulsion from this run showed a peak, assignable to At^{209}, which had a height of 5600 tracks above background. The same sample was then exposed for an additional 14 hr and a peak height of 2000 tracks was obtained. This

decrease in intensity is consistent with a 5.5-hr half life, and made it certain that this peak could be definitely assigned to At^{209}. Since At^{210} was also produced in this bombardment, the three At^{210} groups at 5.519, 5.437, and 5.355 Mev (each peak about one-tenth that of the At^{209} peak height) and Po^{210} group at 5.299 Mev were also present. These groups were used as internal energy standards, which gave the At^{209} group an energy of 5.642 ± 0.005 Mev on each exposure. The experimental error arises from the uncertainty in exact energies of the standards and in locating the peaks accurately on a photographic plate. The spectrum observed on the second exposure with this sample is shown in Fig. 12.

The presence of the At^{210} and Po^{210} group obscures somewhat the search for low-intensity alpha groups of At^{209} decay. A limit of 2.5% abundance can be set down, however, to an energy of 600 kev below the main At^{209} group. This limit is not valid in the immediate vicinities of the At^{210} and Po^{210} groups; i.e., 5.53 to 5.50, 5.45 to 5.42, and 5.37 to 5.26 Mev. It does seem highly improbable, however, that any low-lying complex structure in large abundance exists in the At^{209} alpha decay. Hence we can conclude that all the transitions reported for At^{209} must come from the electron-capture decay.

Gamma-Ray Measurements on Scintillation Spectrometers

In order to measure the intensity of the gamma rays, pure At^{209} was prepared by the "milking" procedure based on a preliminary preparation and isolation of Ra^{213} as outlined in the section on experimental techniques. These samples yielded very excellent photon spectra on the scintillation spectrometer. A typical example of such a spectrum is shown in Fig. 13. The three peaks observed are due to 195-, 545-, and 784-kev gamma-rays. The intensities of the photopeaks when corrected for counting efficiency are 24, 66, and 100, respectively, on a relative scale of 100 for the 784-kev gamma ray. These intensities are good to at least ±20%, and are probably much better than this. Any other gamma rays in At^{209} decay above 100 kev in energy must be very weak.

Conversion-Electron Studies of Astatine-209

The conversion-electron lines of At^{209} were studied very carefully by several methods. The samples used for these runs were mixtures of At^{209}, At^{210}, and At^{211}, and were prepared by bombarding bismuth metal

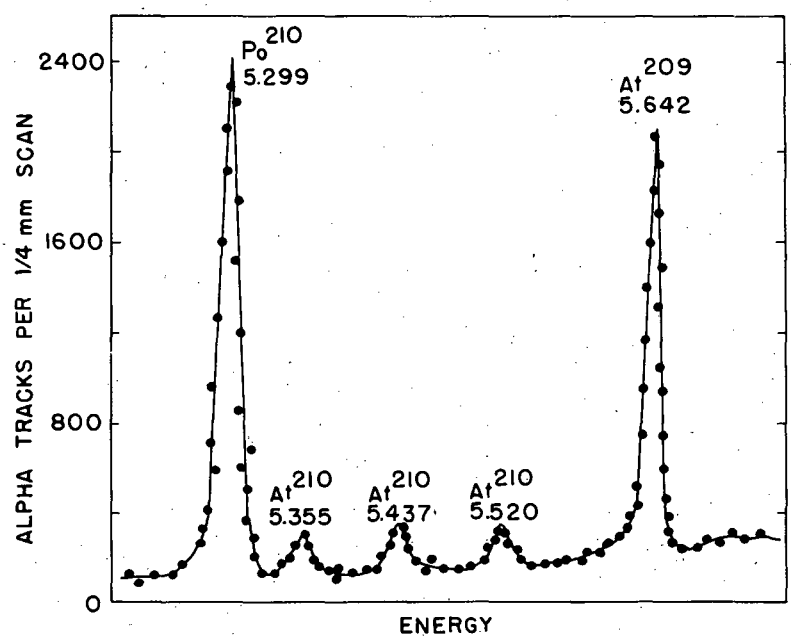

MU-10019

Fig. 12. Alpha spectrum of At^{209} and At^{210} as observed on the alpha-particle spectrograph.

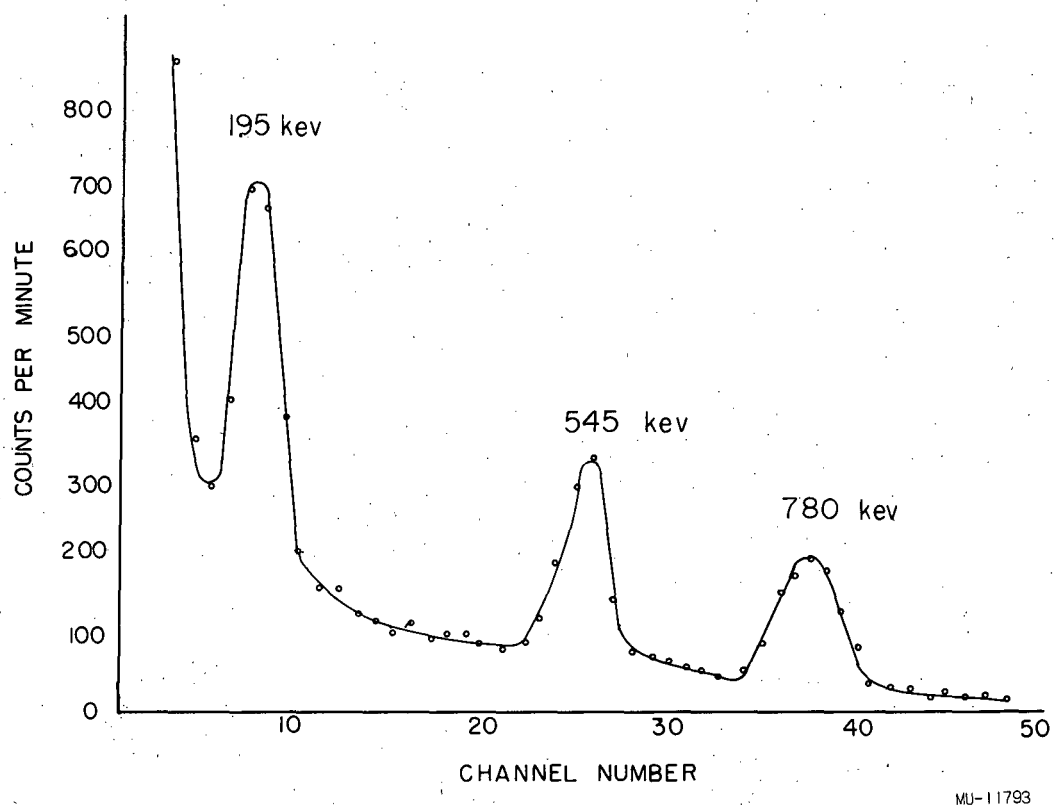

Fig. 13. Gamma-ray spectrum of At^{209} as observed on the scintillation spectrometer.

with helium ions. A mixture had to be used because this is the only way in which large quantities of At^{209} would be produced. Samples were run on the double-focusing beta-ray spectrometer at 0.3% resolution. At this high resolution the At^{209} conversion electrons can easily be separated from the numerous At^{210} lines. Table XIX gives a summary of the results obtained from the double-focusing beta spectrometer.

Table XIX

At^{209} conversion electron intensities from double-focusing spectrometer

Gamma energy (kev)	Gamma	Intensities K electrons	L electrons	K/L ratio
195	24	68	13.5	4.9 ± 0.5
545	66	11.5	3.0	3.8 ± 0.5
784	100	7.5	-	-

Samples of the mixed astatine isotopes were also exposed on several of the permanent-magnet spectrographs. From these runs exact energies and assignment of lines to the correct isotopes were obtained. In conjunction with R. W. Hoff, samples of pure At^{210} were run and compared with other samples, which ran as high as 50% At^{209}. By careful comparison of the intensities observed, the conversion electrons from At^{209} can be picked out. The lines that we assigned to At^{209} are shown in Table XX. The intensities given were visually estimated and are relative to the most intense line appearing on the plate. The gamma-ray energies observed were 90.8 ± 0.2 kev, 195.0 ± 0.4 kev, 544.5 ± 4.5 kev, and 780 ± 2.4 kev. The value of 780 ± 2.4 kev is just outside the experimental error of the previous measurement, which recorded the energy as 784 kev. The 83.8-kev transition that was reported by Mihelich, Schardt, and Segrè to belong to At^{209} was seen in our runs. We assign this transition to At^{210}, however, instead of to At^{209}. In Fig. 14, a photograph of two plates of exposures made on the permanent-magnet spectrograph covering the region of interest shows our reason for this assignment. The first exposure has a very high ratio of At^{210} to At^{209} activity, and the other plate has been exposed to the same amount of At^{210} activity but also an approximately equal amount of At^{209} activity. By comparing the intensity of the K conversion line of the 195-kev transition of At^{209} one can very clearly determine the difference between

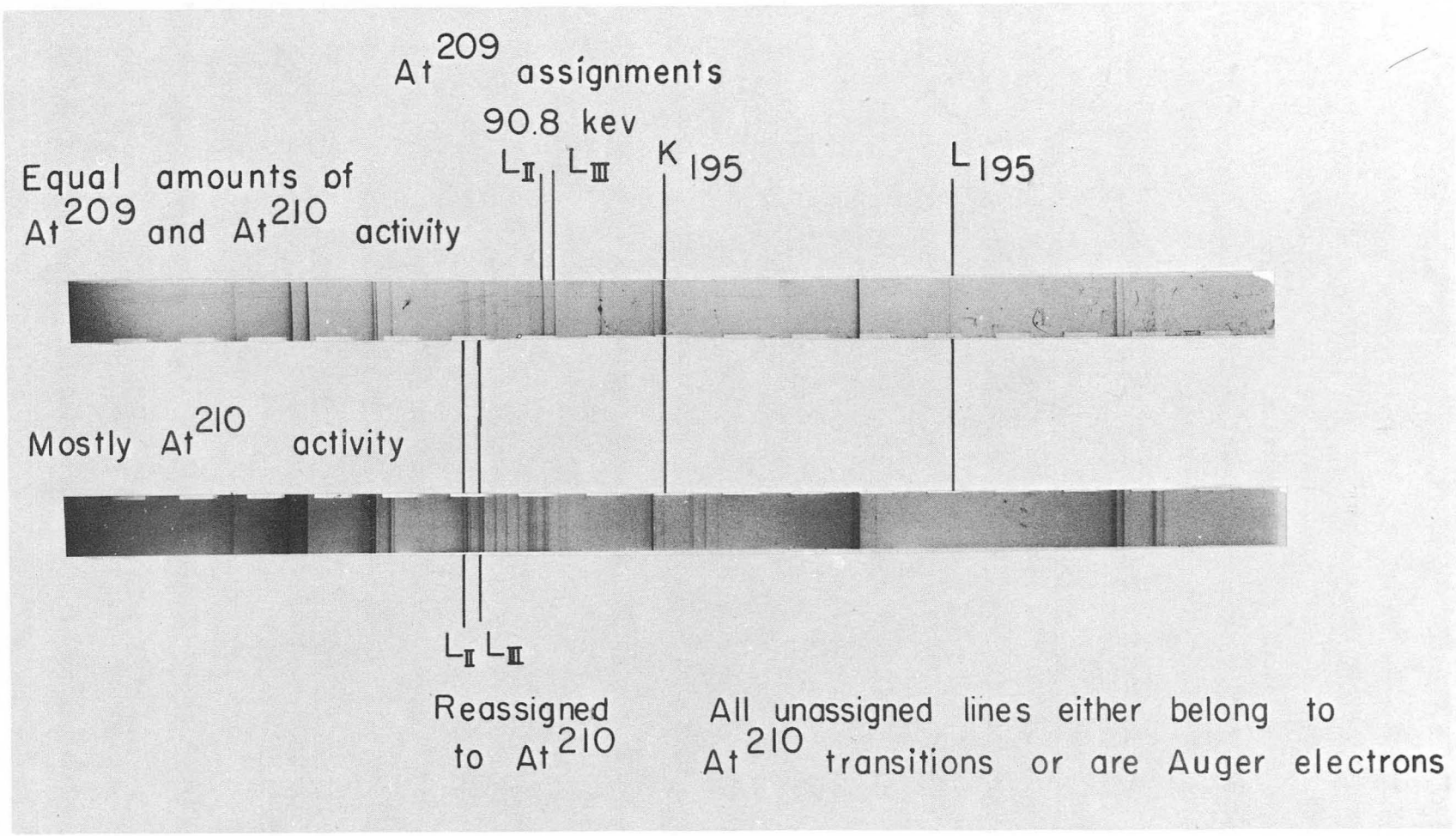

ZN-1526

Fig. 14. Photographic exposure of the At^{209} and At^{210} electron spectra from the 350-gauss permanent-magnet spectrograph.

the plates, in the amounts of activity. The intensities of the 83.8 kev conversion lines are about the same on both plates corresponding to the relative intensity between plates of the other known At^{210} conversion lines. The 90.8-kev transition can also be observed in the plate containing At^{209}. From these observations concerning the change in intensity of lines in the exposures of At^{209}, the 83.8-kev transition was assigned to the At^{210} decay.

Table XX

Summary of At^{209} conversion electrons observed in permanent-magnet spectrographs

Electron energy (kev)	Intensity (visual)	Conversion shell	Gamma ray energy (kev)
74.5	M	L_{II}	90.8
77.0	M	L_{III}	90.8
86.9	WM	M_{II}	90.7
87.5	W	M_{III}	90.7
90.1	W	N_{II}-N_{II}	90.8
90.7	VW	O_{II}-O_{III}	90.8
102.0	S	K	195.2
140.5	W	-	-
178.1	M	L_{II}	195.0
190.8	W	M_{I}	194.8
451.3	S	K	544.5
527.3	M	L_{I}	544.2
536.6	W	-	-
540.2	W	M_{I}	544.2
686.2	SM	K	779.4
695.8	W	-	-

Multipolarity Assignments

From the experimental work the transitions observed can be assigned to certain multipole orders. For the 90.8-kev gamma ray, the assignment is very easy and unambiguous because the conversion lines uniquely determine it to be an E2 transition. The conversion lines of the 195-kev gamma ray indicate that it is either an M1 or E1. The E1 possibility is eliminated by intensity considerations and the empirical

relation to Pb^{207} which has no low-lying odd-parity state. The K/L ratio favors M1, but the limits of error are large enough that the possibility of an E2 admixture cannot be ignored. If one assumes that the 195-kev gamma ray is an M1 transition, then by use of the theoretical conversion coefficients by Rose, the intensity of the K conversion electrons can be calculated from the photon intensity. By normalizing the other K conversion electrons to the value for the 195 kev transition, the ratio between the conversion electrons and the photon intensity yields the K conversion coefficients for the 545 and 780 kev transitions. In Table XXI these derived values have been calculated and are compared with the theoretical values for pure transition types. This indirect procedure is necessary because our electron intensities are not on an absolute basis.

Table XXI

Derived conversion coefficients for At^{209} transitions

Gamma energy (kev)	Multipolarity Assignment	Intensity K electrons	Intensity Gamma	K-conversion coefficients Derived	K-conversion coefficients Theoretical
195.0	M1	43	24	-	1.8
545	M1	8	66	$1.2 \pm 0.5 \times 10^{-1}$	1.5×10^{-1}
-	E2	-	-	-	2.3×10^{-2}
780	M1	5	100	$5.0 \pm 0.5 \times 10^{-2}$	5.4×10^{-2}
-	-	-	-	-	1.1×10^{-2}

The 780-kev transition agrees within the experimental error for an M1 assignment. The 545-kev transition falls within the experimental error for an M1, but the low K/L ratio given previously (K/L = 3.8 ± 0.8) lies between that expected for a pure E2 (K/L = 3.0) and a pure M1 (K/L = 5.0). The K-conversion coefficient indicates that the transition is essentially M1 in character with only a small amount of E2 admixture. These considerations give the following multipole order assignments which are consistent with the data: 90.8, E2; 195, M1 (+ E2); and 780, M1.

Gamma-Gamma-Ray Coincidence Measurements and Decay Scheme

With this information and some gamma-gamma-ray coincidence measurements, a tentative decay scheme can be constructed. Such a decay scheme is shown in Fig. 15. The spins and parities given are discussed

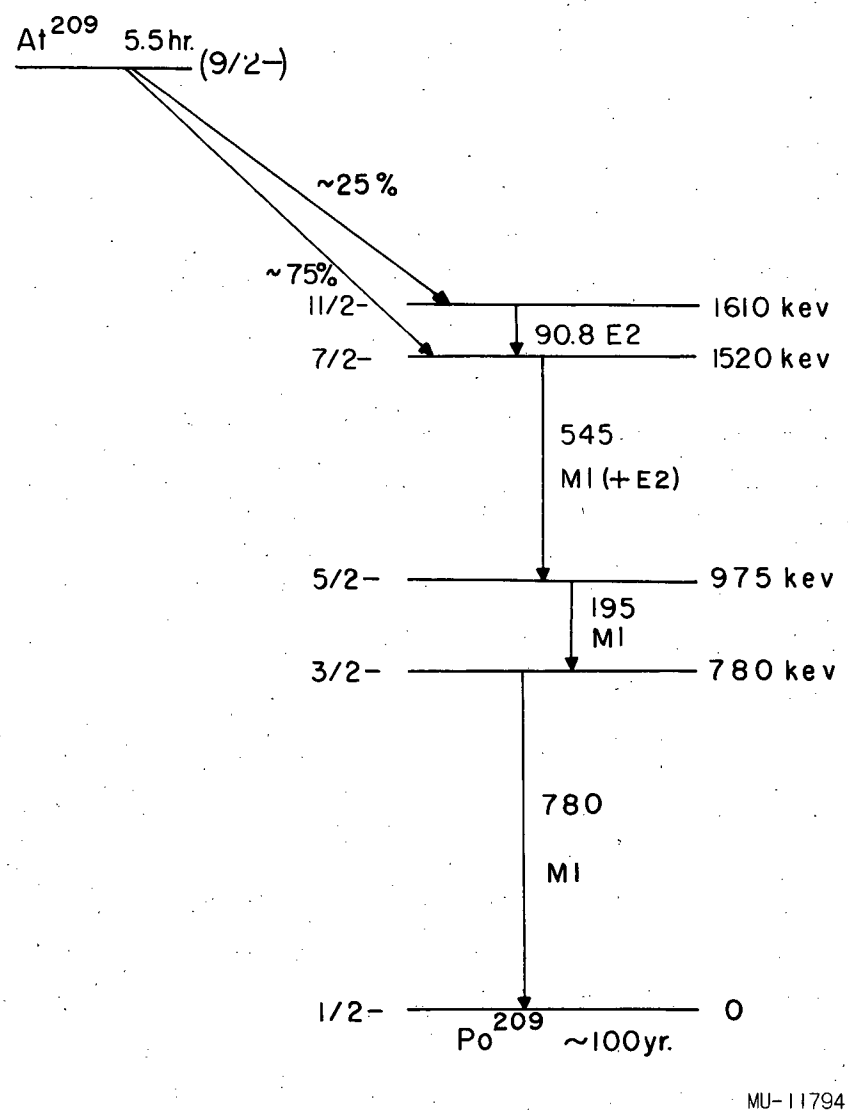

Fig. 15. Proposed electron-capture decay scheme for At^{209}.

later. Gamma—gamma-ray coincidence measurements were made on pure At^{209}, which had been isolated from Ra^{213}. Coincidence measurements using the 780-kev photon as the gate have shown that the 545- and 195-kev photon are in coincidence with it. Similar measurements on the 545-kev photon showed both the 195- and 780-kev gamma rays to be in coincidence with it. The only unambiguous way of placing these three transitions so that they are in agreement with the coincidence measurements is in a triple cascade. The order was determined by the total intensity of the transitions. The total intensities are given in the following table.

Table XXII

Total transition intensities for At^{209}

Gamma energy	Transition intensity
90.8	23
195.0	76
545.0	76
780.0	105

These were calculated by summing the photon and electron intensities from Table XIX. These intensities are good to within ± 20%. The 780-kev transition was put at the bottom because it is the most intense, but the order of the 195.0- and 545-kev transition cannot be definitely stated. It is possible within the experimental error that the 195-, 545-, and 780-kev transitions are all of equal intensity. If this is the case, the greatest amount of the electron capture goes to a level at 1520 kev and cascades down to the ground state. The placement of the 90.8-kev E2 transition is only tentative, and is discussed more thoroughly later. Approximately 20% of the decay, however, passes through this transition, so that its placement in the complete decay scheme is very important.

The spin assignment of 1/2 for the ground state of Po^{209} is the result of a recent experimental measurement.[34] In Pb^{207} the ground-state spin has been determined to be 1/2, and this must arise from a $p_{1/2}$ neutron vacancy in the double closed shell.[35,47] Pb^{207} and Po^{209} differ only by two protons, which should be paired off to give no effect on the ground-state spin. By analogy the ground state of Po^{209} must also arise

from this same $p_{1/2}$ vacancy, since both isotopes have the same number of neutrons. The excited states of Po^{209} should then look somewhat like those in Pb^{207} except that they will probably lie at lower energies, since the isotope is further removed from the double closed shells. The experimental levels in Pb^{207} are a $p_{1/2}$ ground state, a $f_{5/2}$ state at 570 kev, a $p_{3/2}$ state at 870 kev, an $i_{13/2}$ state at 1.6 Mev and a $f_{7/2}$ state at 2.35 Mev.[3] The first excited level in Po^{209} appears at 780-kev, and is comparable with the $p_{3/2}$ state in the Pb^{207} levels. A 3/2- spin and parity assignment to this level also agrees with all the experimental data concerning Po^{209} levels. It allows the 780-kev transition to be M1, and such a low spin rules out the possibility of much direct electron capture populating it. The other two levels at 975- and 1520-kev have no corresponding states in the level sequence of Pb^{207}. A level at 1.61 Mev does appear in Pb^{207} with a spin of 13/2 and + parity.[3] This can be ruled out as being the same as the 1520-kev level in Po^{209}, since the high spin would cause a very long half life for the depopulation of the state, which is contrary to the experimental data for the 1520-kev level. The two remaining levels cannot be assigned spins and parities by a comparison to Pb^{207} levels.

The ground-state spin of At^{209} is 9/2, from simple shell-model theory.[2] At^{209} ground state consists of a neutron pair, a proton pair, and an odd proton beyond the closed shell. The odd proton, most likely, lies in the $h_{9/2}$ state and since this orbit started filling with Bi^{209}, it needs 10 protons to be completely filled. If the ground state of At^{209} is taken as 9/2-, the spins of the 975- and 1520-kev levels can be inferred from the intensity data. The two transitions have the same intensity, so that all the population must go to the 1520-kev level. A spin and parity of 7/2- can be assigned to this level, and a 5/2- assignment can be made for the 975-kev level. The electron capture probably goes by an "allowed" process that has the beta-selection rule of [$\Delta I = 0, \pm 1$, No].[29] This would account for the electron capture's going to a 7/2- state and not to a 5/2- state. The remaining electron capture, which does through the 90.8-kev transition, is still not placed in the decay scheme. The best place for this transition appears to be on top of the 1520-kev level. With a spin assignment of 7/2 for the 1520-kev

level, the new level at 1610 kev can have either a 3/2 or 11/2 spin and agree with an E2 multipolarity assignment of the 90.8-kev transition. The 3/2 assignment can be ruled out on the basis that the transitions to the 1/2, 3/2, and 5/2 levels are not observed. This leaves an assignment of 11/2 for the 1610-kev level. This makes the electron capture process "allowed," by beta-selection rules, to both the 11/2 and 7/2 levels, and electron capture to both levels should be expected. From consideration of the intensity of the transitions, it appears that 20% of the electron capture goes to the 11/2 level and the remaining 80% to the 7/2 level.

The decay scheme for At^{209} presented agrees quite favorably with all the experimental data. However, the excited-level structure deduced for Po^{209} differs greatly from what is expected from a comparison with the excited states in Po^{210}. The excited levels in Po^{210} arise from a $(h_{9/2})^2$ configuration. The experimental data of Mihelich, Schardt, and Segrè show that the 2 + and 4 + states agree quite closely with the theoretical calculations, but they report no 6 + state.[33] A further study here shows that the 6 + state does appear at approximately 1500 kev.[43] The difference between Po^{209} and the level structure observed in Po^{210} is that in Po^{209} a neutron hole must be coupled to the proton configuration, which results in half-integer spins. One possible set of levels that agrees with the observed levels in Po^{209} can be easily established. The ground state of Po^{209} must be from a $(h_{9/2})^2_{J=0}\,(p_{1/2})^{-1}_{J=1/2}$ configuration, which can couple to give only a resultant 1/2 spin. The first and second excited states can be considered as arising from the $(h_{9/2})^2_{J=2}\,(p_{1/2})^{-1}_{J=1/2}$ configuration. This configuration, due to interaction between the particles, would be split into two levels -- one with a 3/2 spin and the other with a 5/2 spin. The third and fourth excited levels could be a doublet due to the $(h_{9/2})^2_{J=4}\,(p_{1/2})^{-1}_{J=1/2}$ configuration, which would give a 7/2 and a 9/2 state. Here the lower spin state (11/2) of the $(h_{9/2})^2_{J=6}\,(p_{1/2})^{-1}_{J=1/2}$ state would have to fall below the 9/2 state in order to explain the order in the experimental levels. This does not seem to be too great a discrepancy, since the $(h_{9/2})^2_{J=4}$ and the $(h_{9/2})^2_{J=6}$ state are separated by only 41 kev in Po^{210} levels. In this manner the order of the excited states may be

outlined if it is assumed that the excitation energy goes into the pair of protons and leaves the neutron in the $p_{1/2}$ state.

The bad feature of this method of predicting the excited states mainly comes from the assumption that had to be made. It seems that the neutron hole $(p_{1/2})^{-1}$ would be excited to the $(f_{5/2})^{-1}$ state before the $(h_{9/2})^2_{J=2}$ state would be formed, since the former requires 570 kev in Pb^{207} while the proton pair requires 1100 kev to be excited in Po^{210}. This same excitation of the neutron hole $(p_{1/2} \longrightarrow f_{5/2})$ should also be seen as the first excited state in the strict single-particle model. The failure of this $(f_{5/2})^{-1}$ state to appear near the expected energy in either model tends to make the assumption concerning excitation of the proton pair before the neutron hole more feasible.

If both types of configurations are excited (i.e., single-particle levels superimposed on the different nondegenerate levels of the proton pair), the number of levels expected in the decay scheme would be very great. As one example the $(h_{9/2})^2_{J=2}\,(f_{5/2})^2_{J=5/2}$ configuration would give rise to 1/2, 3/2, 5/2, 7/2, and 9/2 states, which would be split into different energy levels by particle interaction. As one continues through the possibilities that lie rather close to this group in energy, it soon becomes apparent that the level scheme becomes quite complex. Since so many states of the same spin would appear within a 1-Mev range, it is hard to state why some are seen and others are not. The simple level structure found experimentally for Po^{209} indicates, I believe, that one of the two types of excitation is dominant over the other. If the single-particle excitation is dominant, then the levels are explained by showing that the order of filling these levels has changed. If the excitation of the paired protons is dominant, then the neutron hole must remain a $(p_{1/2})^{-1}_{J=1/2}$ state. If one of these two models is not correct, then it becomes very difficult to explain the extreme simplicity of the level structure when such a complex structure is predicted.

The two things that stand out from this study of At^{209} decay are that the sequence of levels in Po^{209} is completely different from what is expected from a comparison with Pb^{207}, and that the decay scheme is so simple. A quantitative, theoretical consideration of the interaction between a neutron and a proton pair would be very interesting, and might help explain the decay scheme of At^{209}.

D. Astatine-208

The isotope At^{208} was found by Hyde, Ghiorso, and Seaborg in a study of the decay scheme of Fr^{212}, which shows branching decay to At^{208} and Fr^{212}. The At^{208} daughter isotope was shown to have a 1.7-hr half life.[10] At^{208} emits alpha particles with an energy of 5.65 Mev, but the principal decay is by orbital electron capture to 2.9-yr Po^{208}. The branching ratio was estimated to be 180 ± 20 by comparing the initial alpha-counting rate of a pure sample of At^{208} with the final alpha-counting rate due to the Po^{208} daughter.

At about the same time, Barton and Perlman found indirect evidence for At^{208} that indicated that this isotope had a half life of 6.3 hr.[9] These authors prepared astatine isotopes by bombarding bismuth with high-energy protons. The astatine fraction from such bombardments contained a complex mixture of astatine isotopes with similar half lives, and it was impossible to learn anything about At^{208} by a direct examination of the astatine fraction. However, by removing polonium daughter activities at timed intervals and and measuring the Po^{208} alpha activity, it was possible to deduce a half life of 6.3 hr for At^{208}. These experiments by Barton and Perlman were completed before the work of Hyde et al. had been done.[10] The discrepancy in the two half-life values is explainable in terms of isomerism, but it seemed desirable first to confirm the experimental findings.

The assignment of the 1.7-hr At^{208} can be considered definite because of the well-established genetic relationship of Fr^{212}, Em^{212}, and At^{208} to the well-known 2.9-yr Po^{208}. The properties of the 1.7-hr daughter At^{208} are unambiguous so far as reported, because pure samples of the activity could be "milked" from Fr^{212}. It seemed desirable, then, to repeat the experiments by Barton and Perlman to determine whether the 6.3-hr half life could be reproduced and if, in addition, evidence could be found for the 1.7-hr form of At^{208} in bismuth targets.

The experiment was carried out under conditions similar to Barton's "milking" experiments. The astatine was produced by bombarding bismuth metal in the internal beam of the 184-in. cyclotron with 100- to 120-Mev alpha particles. All the astatine isotopes from 206 through 211 are formed. These isotopes and their polonium daughters are shown in Table XXIII.

Table XXIII

Astatine isotopes and their polonium daughters

Astatine isotopes in solvent phase giving rise to polonium daughters.		Polonium daughters stripped into $HCL-HNO_3$ phase.		
			$T_{1/2}$	E_α
At^{211}	$\xrightarrow{EC}$	Po^{211}	=0.5 sec	
At^{210}	$\xrightarrow{EC}$	Po^{210}	138 days	5.30
At^{209}	$\xrightarrow{EC}$	Po^{209}	100 yr	4.86
At^{208}	$\xrightarrow{EC}$	Po^{208}	2.9 yr	5.10
At^{207}	$\xrightarrow{EC}$	Po^{207}	no α	
At^{206}	$\xrightarrow{EC}$	Po^{206}	9 day	5.21

The chemical purification of the target and the chemistry used in the "milking" experiment are as follows. The bismuth target was dissolved in concentrated hydrochloric acid, and the solution was evaporated to dryness after excess hydrochloric acid had been added. Excess hydrochloric acid was again added and the solution taken down to dryness to remove all the nitrate ion. The residue was then taken up in 6 M hydrochloric acid, from which the astatine was extracted into a diisopropyl ether layer. The organic layer was washed several times with 6 M hydrochloric acid and then diluted with tributyl phosphate until it was 20% tributyl phosphate solution. It was then washed with a 2M nitric acid and 4M hydrochloric acid solution. These solutions were immediately analyzed for a short-lived activity (astatine) to determine if any was removed from the organic fraction. No short-lived activity was found in any sample; therefore, it was certain that the polonium activity present represented only the decay of the parent during a certain time interval. The polonium isotopes present and their decay properties are given in Table XXIII. Portions of each polonium sample were analyzed in the alpha-pulse analyzer to determine the ratio of Po^{210} to Po^{208} alpha activity. In addition to these two activities, the alpha group of Po^{206}, which is the daughter of At^{206} decay, was observed.

In milking experiments the amount of activity of the daughter plotted versus time gives directly the half life of the parent. However, this requires that the chemical separation be quantitative. In this ex-

periment a much better method, which depends on At^{210} as an internal standard for the chemical yield, can be utilized. The half life of At^{210} is well known, so that Po^{210} activity can be arbitrarily put on an 8.3-hr half-life line. Then from the ratio of Po^{208} to Po^{210} activity in each milking fraction, the correct amount of Po^{208} activity can be determined. From these Po^{208} points the half life of At^{208} can be directly determined. The same procedure can be used to determine the At^{206} half life from the ratios of Po^{206} to Po^{210}. The results of such an experiment are shown in Fig. 16. The curve shows a complex decay curve, which can be resolved into a 1.6 ± 0.2-hr and a 6.2 ± 0.3-hr half life. Also, to further verify the accuracy of the experiment, the half life of At^{206} was determined to be 2.9 ± 0.4 hr. This is within the experimental error of the only other previous determination, 2.6 hr. These results indicate very strongly that both half lives are correct and that there must be an isomeric state present in At^{208}. It cannot be stated whether the 1.7-hr or the 6.2-hr isomer constitutes the ground state. Further studies on the 6.2-hr isomer must be deferred until some better method for its preparation is devised. The heavy-ion linear accelerator that is being built at this laboratory may be very useful in making At^{208} with only small amounts of At^{209} and At^{210} present.

A study of the alpha and electron-capture decay of At^{208} has been carried out as completely as possible with the small amount of pure At^{208} activity that can be produced. Only samples that were prepared by milking the At^{208} from Fr^{212} gave any significant results. Samples prepared in this manner rule out any possibility of observing any radiations of the isomeric transition, since only the 1.7-hr half life is found as the daughter of Fr^{212} alpha decay. In all the other present methods of preparation of large quantities of At^{208}, all the isotopes from At^{206} through At^{211} are produced, and the large number of gamma raidations present completely mask At^{208} gamma rays. The gamma-ray spectrum of At^{208} as observed on the scintillation spectrometer is shown in Fig. 17. The energies of the gamma rays are 660 ± 20 kev and 175 ± 10 kev; the other peak at 75 kev is assigned to the K x-rays of polonium. When corrected for counting efficiency, the 610-kev photon is approximately 4 times as intense as the 175-kev gamma ray. Gamma—gamma-ray coincidence measurements show that the two gamma rays are in cascade. The coincidence

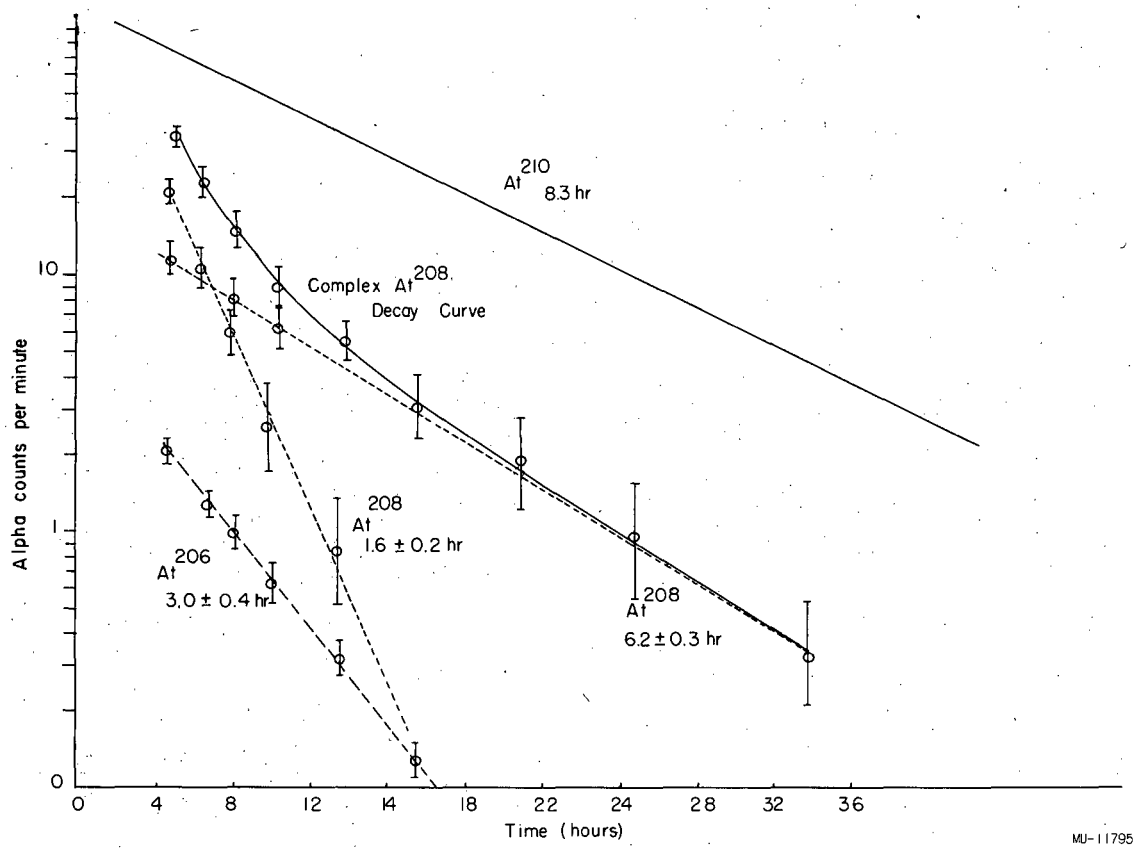

Fig. 16. Decay curves for At^{208} and At^{206} from "milking" polonium daughters.

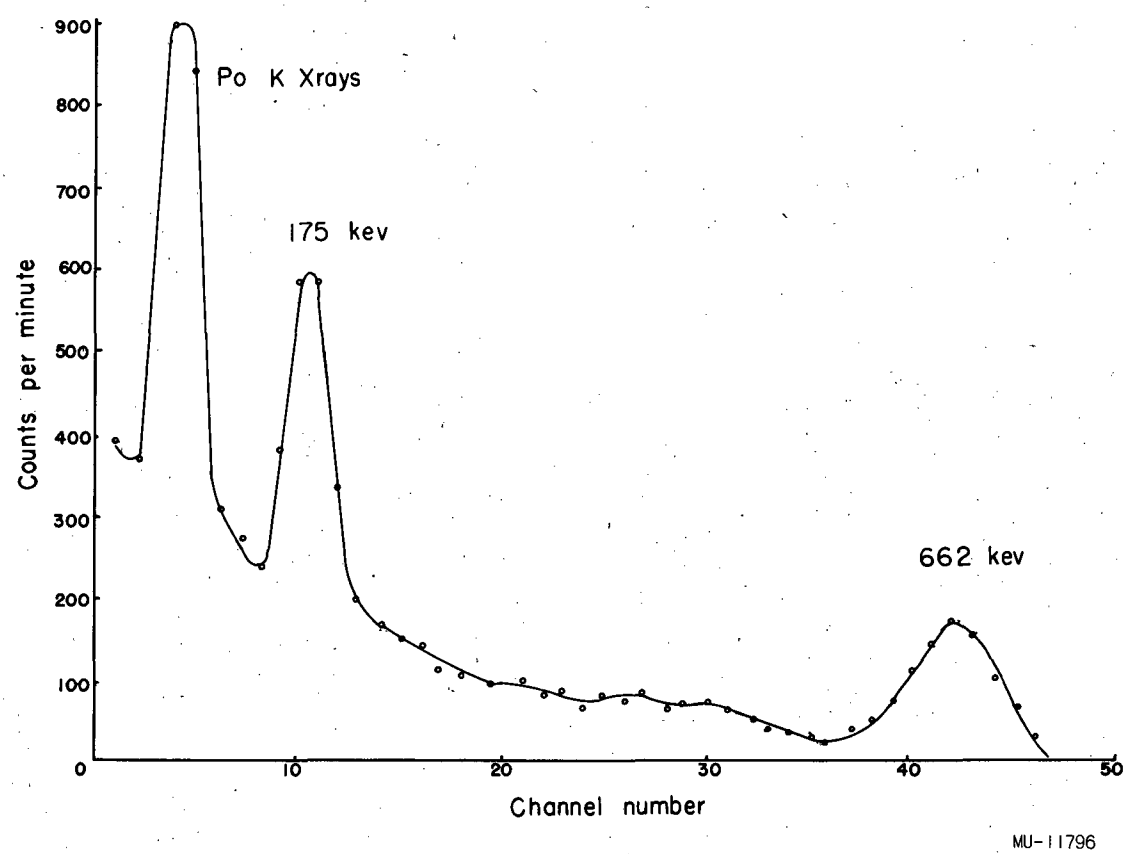

Fig. 17. Gamma-ray spectrum of At^{208} as observed on the scintillation spectrometer.

measurements also show a weak 250 ± 15-kev gamma ray in coincidence with the 660-kev gamma ray. This gamma ray was too weak to be observed in the straight gamma-ray spectrum as seen on the scintillation spectrometer. The above radiations are all that were observed in the electron-capture decay, and they all decayed with a 1.7-hr half life.

The alpha decay of At^{208} was investigated by alpha-gamma coincidence measurements. It was shown that there was a gamma-ray of 120 ± 10 kev in coincidence with some of the alpha particles. The intensity of the gamma ray was determined to be 0.03 ± 0.03% of the total alpha decay. Hence the lower-energy alpha group could not be seen in ion-chamber measurements. A calculation of the alpha population going to this level depends on the multipole order of the transition, which is not known. One would expect either an E2 or M1; so, assuming these two possibilities, the population will be either ~0.2% (E2) or ~1% (M1). In either case the population of this excited state is quite small, and a limit of 10^{-3}% can be set for any other gamma transitions in coincidence with alpha particles.

A tentative decay scheme for At^{208}, using the above experimental data, is shown in Fig. 18. The daughter nucleus of the electron capture is Po^{208}, which is an even-even nucleus. The excited levels of this nuclear type have been quite extensively studied, and a definite pattern of levels has been observed. The ground-state spins of all even-even nuclei have been found to have zero spin and even parity. The first excited state has been shown to be a 2 + state and the second excited state either a 4 + or 2 + state. The energy separation between the ground and first excited states and between the first and second excited states depends very strongly on the nearness of the particular isotope to a closed shell. The spacing becomes progressively larger with a nearer approach to a closed shell, and in the immediate vicinity of a closed shell the separation becomes quite large for the ground to first excited state. The levels of Po^{208} would be expected to show this type of level pattern, since it is an even-even nucleus and the energy separations would be rather large, as the isotope is very near a closed shell (two protons from the 82-proton shell and two neutrons from the 126-neutron shell). It is partly on this empirical relationship that the spin and parity assignments have been made.

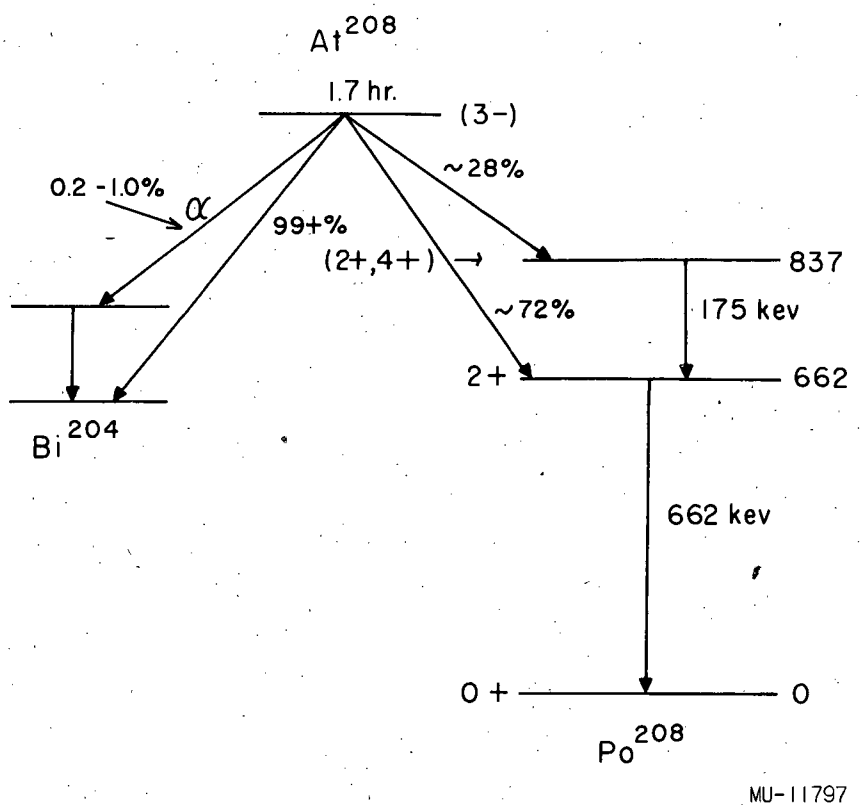

Fig. 18. Tentative electron-capture decay scheme for At^{208}.

In addition to the general case of even-even nuclei for assigning the first two excited states, one may reasonably expect the pattern of excited states in Po^{208} to be very similar to that in Po^{210}, which has been carefully determined. Po^{210} lies two protons above the 82-proton closed shell and has a closed shell of neutrons. Since both isotopes are even-even, the same levels should appear in Po^{208} as in Po^{210}, but at a smaller energy separation between ground and first excited state, since Po^{208} is further removed from the closed shells. Mihelich, Schardt, and Segrè have published a very complete study of the energy levels in Po^{210}. By angular correlation measurements in addition to complete characterization of the transitions, they assigned spins and parities of 2 + and 4 + to the first and second excited states. The first excited state (2 +) is at 1185 kev and the second (4 +) state at 1431 kev in Po^{210}. Therefore, if the 662- and 837-kev levels in Po^{208} are assigned 2 + and 4 + spins and parities, respectively, they show the expected energy lowering. Thus these states in At^{208} decay are assigned on the basis of even-even nuclei systematics and by comparison with Po^{210} excited states.

On the basis of the above spin assignments, the two observed gamma rays must be E2 transitions. Assuming this, and using the ratio of photon intensities, we can calculate the total intensity for each transition. With the assumption that there is no electron capture directly to the ground state of Po^{208}, the amount of electron capture proceeding to each level can be determined as ~72% to the 2 + state and ~28% to the 4 + state. From this the ground-state spin of At^{208} can be estimated. Since At^{208} captures directly to a 2 + and a 4 + level and has a short half life, the process must be "allowed" and obey the [$\Delta I = 0, \pm 1$, No] beta-selection rule.[29] This requires that the spin and parity of the ground state of At^{208} be 3 +. At^{208} is an odd-odd isotope, with the odd particles an $h_{9/2}$ proton and an $f_{5/2}$ neutron, from strict shell-model considerations. The 3 + spin assignment agrees with Nordheim's rule of ground-state spins for odd-odd nuclei, which predicts that the coupling of an $h_{9/2}$ proton and an $f_{5/2}$ neutron hole can given any spin from 2 + to 7 +.[37] However, it disagrees with a theorum by Kurath that the lowest state of a configuration of one proton in a level j and one neutron in a level j' is 1, with $I = j + j' - 1$, which is 6 + for the

At^{208} nucleus.[38] This spin would require an [$\Delta I = \pm 2$, No] type of beta decay to the 4 + state and a much higher spin change for the capture to a 2 + state. Such large spin changes would require a long half life, and can be ruled out of this electron-capture decay.

E. Emanation-211

Em^{211} was first identified by Momyer and Hyde in the bombardment of thorium foils with 340-Mev protons.[8] This isotope has a 16 ± 1-hr half life and decays by electron capture and alpha emission; the branching ratio of electron capture to alpha emission is 2.8 ± 0.3. The mass assignment was made by observing the growth of At^{211} and Po^{211} alpha groups from the electron-capture decay. Momyer, Asaro, and Hyde investigated the alpha spectrum on the alpha-particle spectrograph and observed two alpha groups of 5.847 and 5.778 Mev, with abundances of 35% and 65%, respectively.[42] Gamma rays of 65 ± 10, 150 ± 30, 400 ± 30, and 600 ± 50 kev were assigned to Em^{211}.[8] This is all the published information concerning Em^{211}.

Alpha-Decay Study

The alpha decay was studied again to determine if there were any additional alpha groups. This was first done by alpha particle—gamma ray coincidence measurements. In addition to the 69-kev gamma ray between the ground and first excitation state, two additional gamma rays were observed at 169 and 234 kev. Each gamma ray had an intensity of approximately 6.5% of the 69-kev peak. Fig. 19 shows the spectrum observed. The small peak just before the 69-kev peak is an escape peak, which is caused by an iodine K x-ray escaping from the sodium iodide crystal. The two higher-energy gamma rays observed may arise from a single additional level and be de-exciting to the ground and first excited state, or they may arise from two additional excited levels populated by low-intensity alpha groups. This can be most easily determined by a direct observation of the alpha group or groups.

Large samples of Em^{211} were prepared by the glow discharge technique on 10-mil platinum wire and run on the alpha-particle magnetic spectrograph. The region below 5.778 Mev was carefully scanned for alpha groups that could give rise to the two observed gamma rays. A peak was observed at 5.615 ± 0.005 kev, and careful scanning of the plate showed

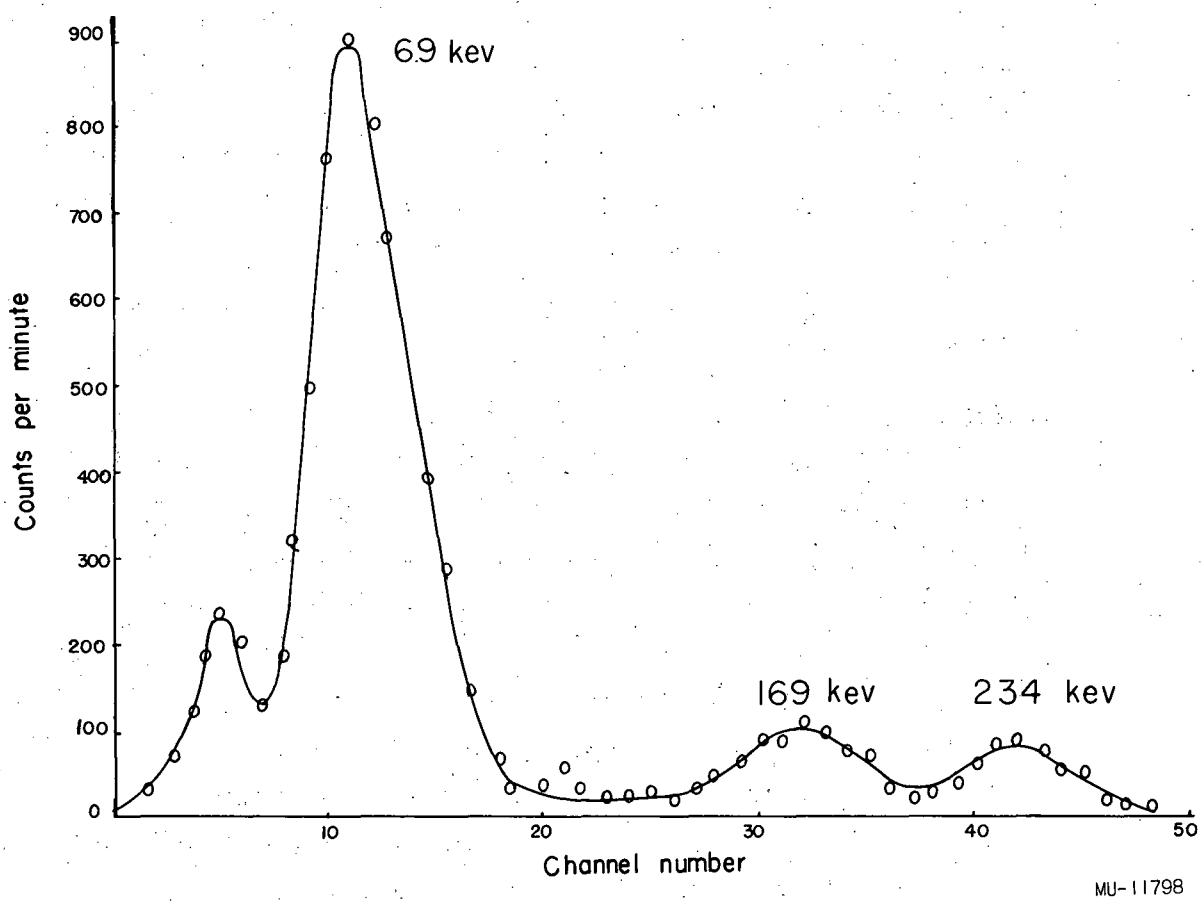

Fig. 19. Gamma rays in coincidence with alpha particles of Em^{211}.

no other alpha groups between 5.778 Mev and an energy 350 kev lower. An alpha group at 5.615 Mev may depopulate to the ground and first excited state, and the transitions expected agree with the observed gamma rays. Including this group, the Em^{211} alpha decay has alpha groups of the following energies and intensities: 5.847 ± 0.005 Mev, 33.5%; 5.778 ± 0.005 Mev, 64.5%; and 5.615 ± 0.005 Mev, 2%.

The conversion electrons of the 69-kev transition have been observed in a permanent-magnet spectrograph exposure. The conversion lines observed were L_{II}, L_{III}, M_{II}, M_{III}, N_{II}, and O_{II} (they are recorded in Table XXVI). This pattern of lines uniquely determines the transition to be an E2 of 68.7 ± 0.1 kev. No conversion lines were seen corresponding to the less intense transitions, therefore nothing can be said concerning their multipole order. The alpha spectrum observed on the alpha-particle spectrograph, and the alpha-decay scheme, are shown in Fig. 20.

Gamma-Ray Study

The electron-capture decay has been studied as completely as possible with the instruments available. The gamma rays observed on the 50-channel scintillation spectrometer are shown in Fig. 21 and recorded along with their intensities in Table XXIV. Additional runs were made in order to investigate the high-energy and low-energy regions of the photon spectrum. In the high-energy region one gamma ray at 1.8 Mev was observed. In the low-energy region a 32-kev transition was observed on the scintillation spectrometer and in a proportional counter. Because of low abundance due to high conversion and the high Compton background, the intensity data on the lower-energy radiations are not included in the table. These data disagree with the previously reported gamma rays by Momyer, and no explanation of the discrepancy has been discovered.

Table XXIV

Gamma-ray intensities observed on the scintillation spectrometer

Gamma-ray energy (kev)	Intensity (arbitrary)
32 ± 2	-
220 ± 10	-
320 ± 10	-
345 ± 15	39 ± 8
675 ± 15	100 ± 20
870 ± 20	24 ± 5
950 ± 20	29 ± 6
1140 ± 20	31 ± 6
1300 ± 20	52 ± 10
1800 ± 25	~0.8

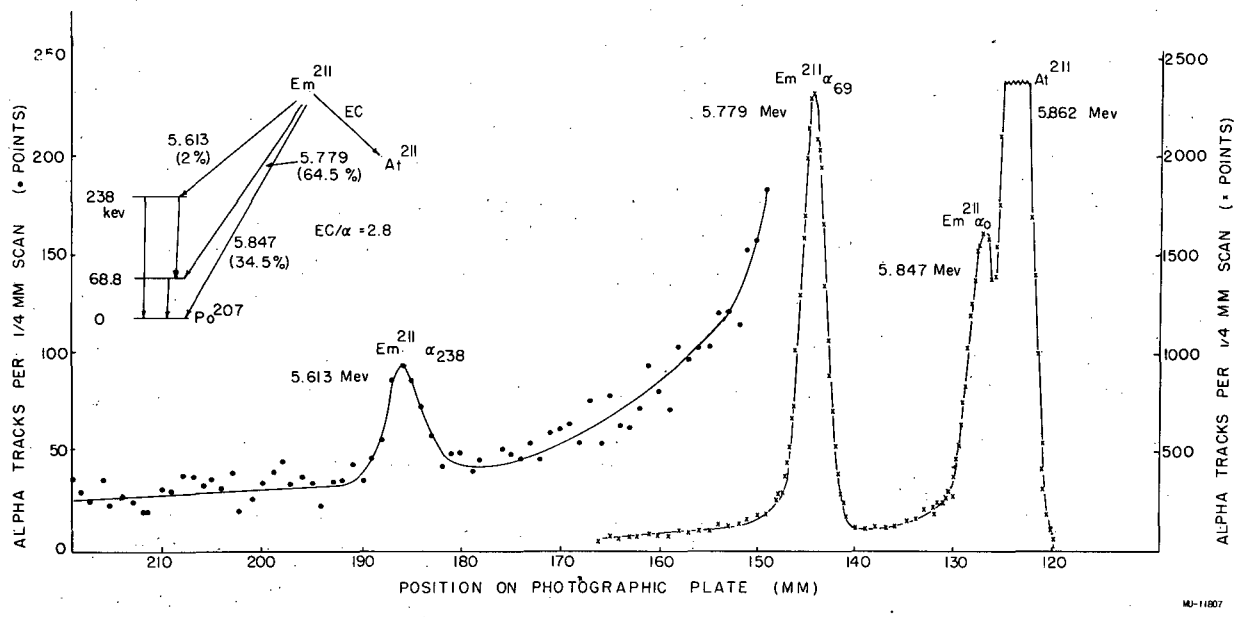

Fig. 20. Alpha spectrum from alpha-particle spectrograph, and alpha-decay scheme for Em^{211}.

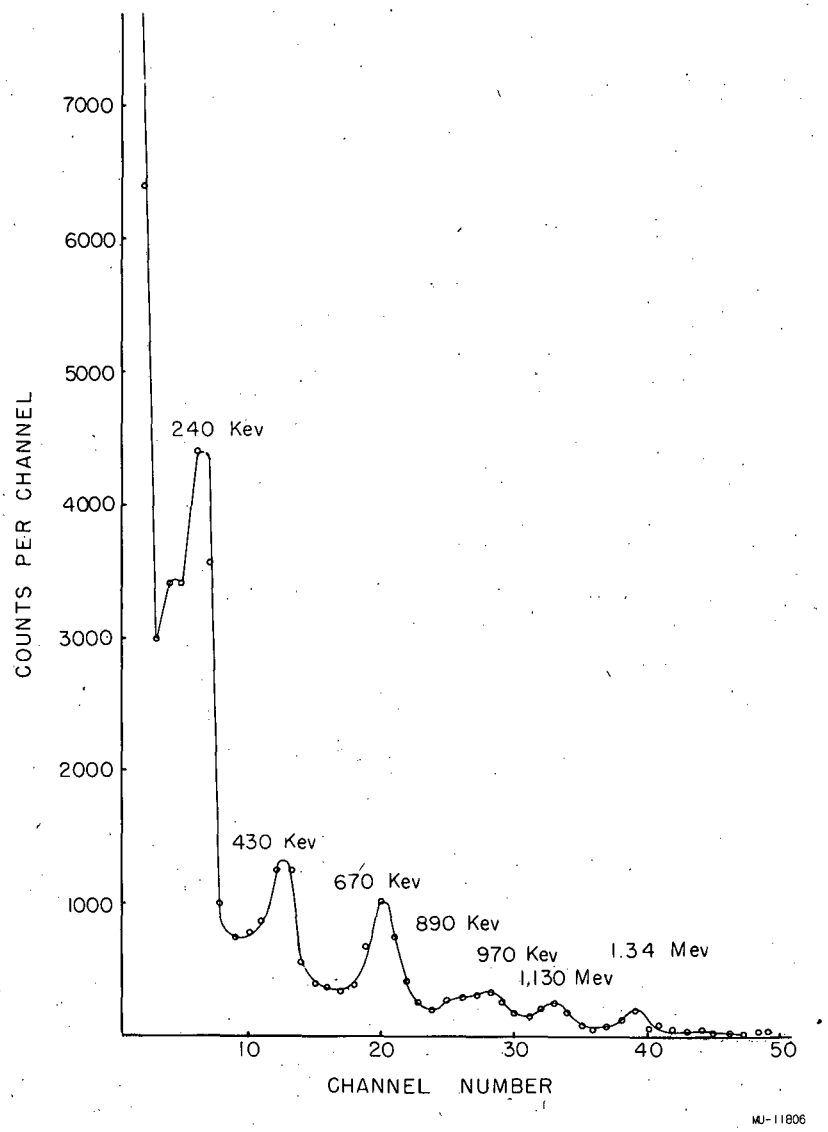

Fig. 21. Gamma-ray spectrum of Em^{211} as observed on the scintillation spectrometer.

Coincidence Studies

Coincidence measurements were run by using the prominent peaks in the gamma-ray spectrum as gates. These results are somewhat ambiguous, owing to the background of Compton-scattered radiation under the peaks below 1.0 Mev. This scattered radiation gates the coincidence circuits to count gamma rays in coincidence with it. Then, the gamma rays that are in coincidence with the scattered background radiation are counted in addition to those in coincidence with the photon being used as a gate. All the gamma rays in the spectrum are actually observed, but their intensities change as the gating photon is changed. Comparing the difference between the intensities of the various peaks as the gating photon was changed permitted a reasonable estimation of the true coincidences for each gamma ray. The results are summarized in Table XXV. This table shows only the coincidences measured, and some results that are not readily interpretable have been omitted. The observation of a 670-kev gamma ray in coincidence with itself is of special interest in constructing the decay scheme, as is shown later. The coincidence data does not clearly indicate whether there are two transitions of nearly the same energy or whether the coincidence is due to the Compton background effect.

Table XXV

Gamma—gamma ray coincidence studies on Em^{211}

Gating Photon (kev)	Gamma Rays in Coincidence (kev)
435	230, 670, 1140, 1360
670	430, 670, 960, 1140, 1360
865 - 946	670, 865, 946
1140	232, 445, 670
1360	445, 670

Conversion Electrons of Emanation-211

The internal conversion electrons in the range 20 to 250 kev were observed on the permanent-magnet spectrographs. Table XXVI lists the conversion electrons seen, together with their intensities and conversion shell assignments. The intensities are relative to the total L conversion of the 168.6-kev transition. This was done so that these intensities can be related through this peak to the rest of the conversion

electrons, which were observed in the other variable field spectrometers. The 68.7-kev E2 transition has been already assigned to the alpha decay. The other two transitions, 168.6-kev E2 and 113.9 kev, are both in the electron-capture decay. The 168.6-kev transition is too intense to be assigned as the transition from the second to the first excited state (167 kev energy difference) in the alpha decay. Also the excellent agreement achieved by using astatine conversion edges cannot be obtained with polonium conversion edges. These two facts were the basis of assigning the 168.6-kev transition to the electron-capture decay.

Table XXVI

Internal conversion electrons of Em^{211} from permanent-magnet spectrograph exposures

Electron energy (kev)	Assignment	Photon energy (kev)	Relative intensity
46.4	-	-	~ 45
52.5	Po L_{II}	68.7	120
54.9	Po L_{III}	68.7	110
64.8	Po M_{II}	68.6	33
65.5	Po M_{III}	68.7	34
67.8	Po N_{II}	68.7	17
68.6	Po O_{II}	68.7	< 10
73.2	At K	168.9	44
151.1	At L_{I}	168.6	< 10
151.9	At L_{II}	168.6	34
154.4	At L_{III}	168.6	33
164.4	At M_{II} M_{III}	168.5	< 10
93.4	At L_{I}	113.9	< 19
59-62	K-LL Auger	-	< 10
75-78	K-LX Auger	-	< 10

It would have been highly desirable, at the same time as the above exposures were made on permanent-magnet spectrographs, to make exposures to cover also electrons of higher energy, but unfortunately the high-field magnets were not in operation. Consequently, the conversion electron lines above 200 kev could not be investigated on the permanent magnets. Samples of Em^{211} could be prepared only large enough for examination on the high-transmission low-resolution magnetic-lens spectro-

meter. The conversion electron spectrum obtained in one run is shown in Figs. 22 a, b, and c. The spectrum was followed through two half lives in order to verify the assignment to Em^{211} decay. A summary of the electron lines and their intensities is given in Table XXVII. The intensities are relative to the L conversion peak of the 168.6-kev transition, and this forms the basis for the over-all approximate intensity relationship between this and the permanent-magnet exposures. The energy determinations on this instrument are good only to ± 3% and the intensities to ± 20%.

Table XXVII

Internal conversion electrons of Em^{211} from magnetic lens spectrometer

Electron energy (kev)	Assignment at edges	Gamma-ray energy (kev)	Relative intensity
155	L	170	70
200	K	296	48
217	L	232	10
256	-	-	6
168	K	264	33
249	L	264	7
237	K	333	47
318	L	333	7.5
349	K	445	31
433	L	445	17
584	K	680	100
665	L	680	29.5
767	K	863	7
852	L	867	10
	K	948	-
931	L	946	2
1035	K	1131	4
1118	L	1131	1
1278	K	1374	1
1359	L	1374	~0.1

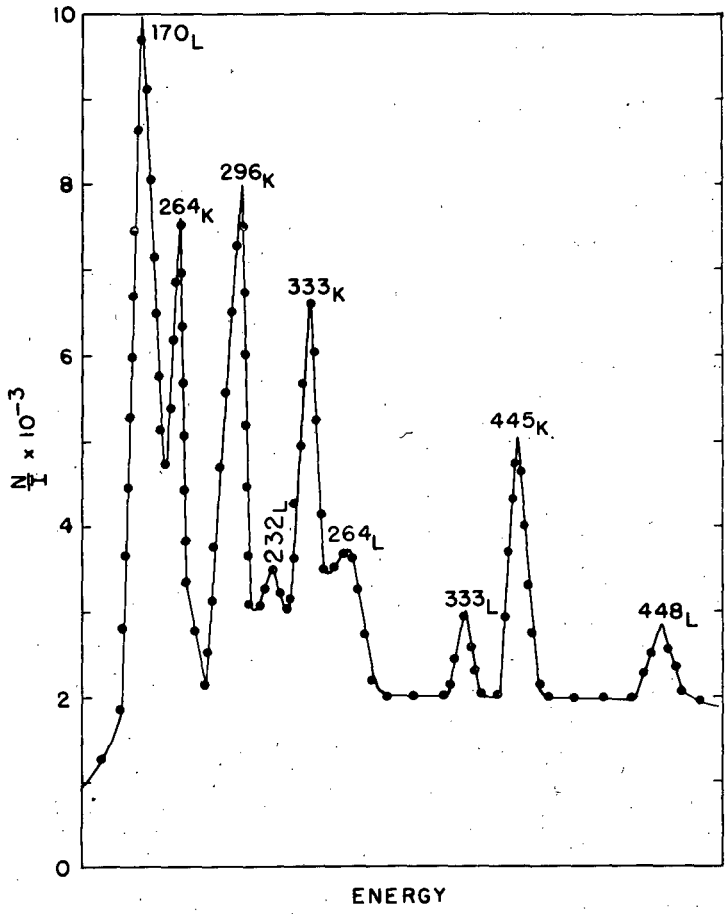

MU-10013

Fig. 22a. Electron spectrum of Em^{211} as observed on the magnetic-lens spectrometer--80- to 450-kev region.

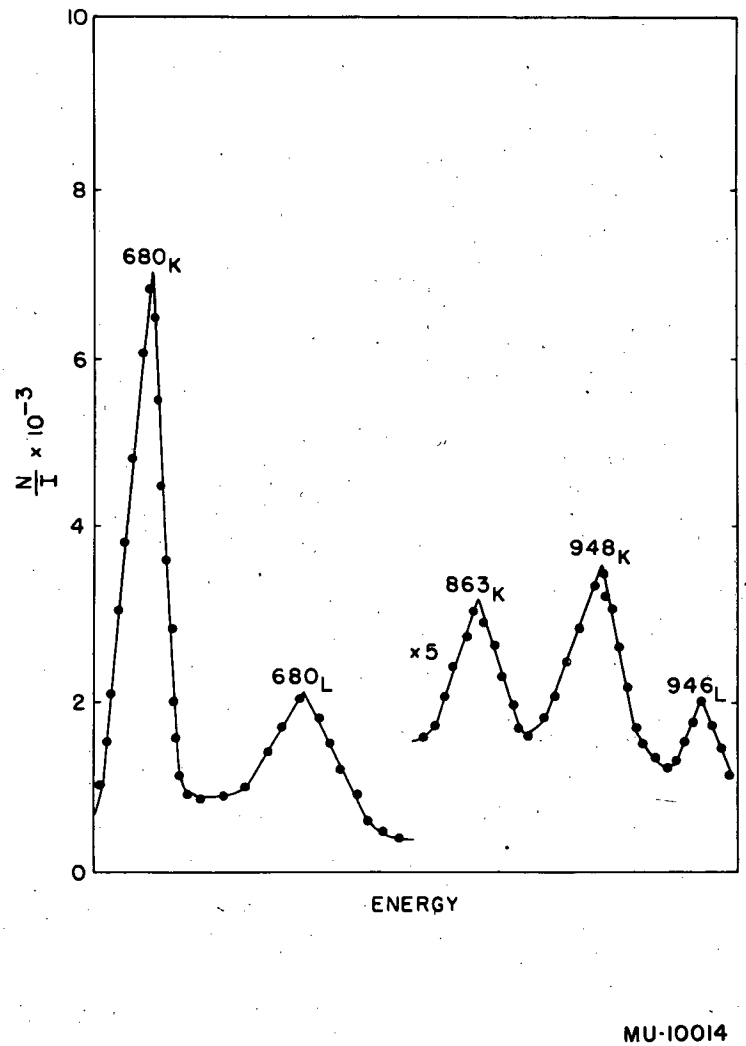

Fig. 22b. Electron spectrum of Em^{211} as observed on the magnetic-lens spectrometer --500- to 950-region.

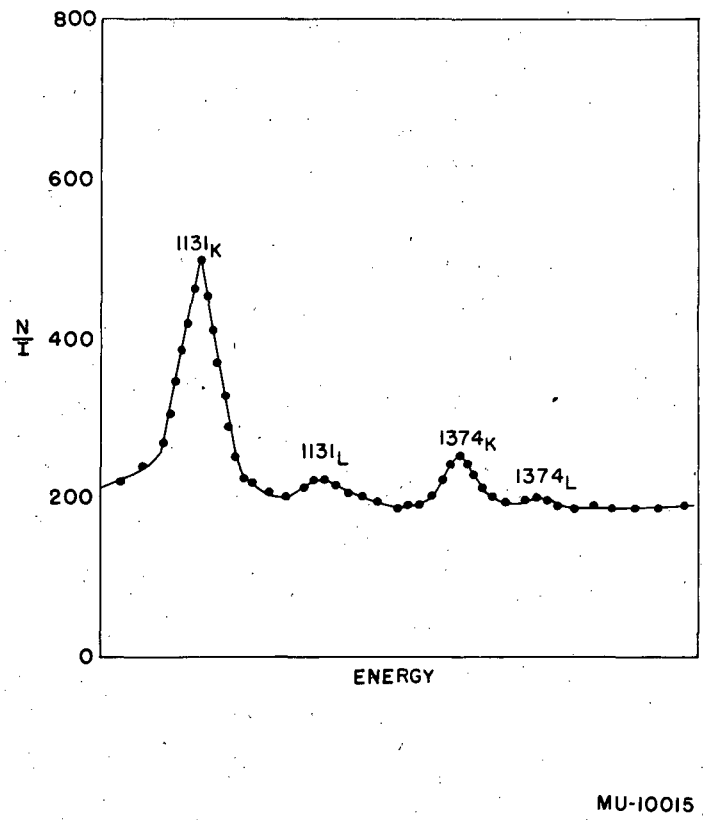

Fig. 22c. Electron spectrum of Em^{211} as observed on the magnetic lens spectrometer -- 950- to 1400-kev region.

Multipolarity Assignments

From the data given, experimental K/L ratios can be calculated for several of the transitions. These experimental ratios are listed in Table XXVIII along with the theoretical K/L ratios of the more reasonable possible assignments. The last column contains the most reasonable assignments as determined by comparison with the theoretical and experimental K/L ratios by Pryce and Alburger.[5] The 169-kev gamma ray is undoubtedly an E2 transition, because of the characteristic pattern of the L-shell conversion electrons observed on the permanent-magnet spectrograph. Assignment of the other gamma radiations cannot be made unambiguously. The K/L ratios suggest that the 445- and 680-kev radiations are also E2 transitions, and the other gamma rays are either M1 or M1 + E2 admixtures. From the relative intensities of the conversion coefficients for transitions of various multipole orders the theoretical intensities of the gamma rays can be calculated and compared with experimental values. Because only relative intensities are known, and intensity ratios must be used, only those gamma rays whose intensities are listed in Table XXIV can be compared. The only seemingly consistent results obtained by this method are these: if the 445-kev gamma ray is assumed to be an E2 transition (a probable assignment on the basis of K/L ratios), then the 865- and 1131-kev transitions are E2 also, and the 946-kev transition is an M1 (+ E2) admixture. The 680-kev gamma transition is presumably an M2 if only one gamma ray of that energy is present. In the decay scheme to be presented, however, there are two separate differences between excited levels of 680 kev, and -- since the coincidence data indicate the 680-kev gamma may be in coincidence with itself -- it is entirely possible that there are two gamma rays of approximately the same energy. This would make the assignment of a multipole order to the 680-kev gamma ray impossible until the electron lines are resolved. An alternate assignment is possible if one assumes that only one 680-kev transition is present and that the coincidence with itself arises from the high Compton background gating the coincidence counter. Then if the 680-kev gamma ray is assumed to be pure M1, the 865-, 946-, and 445-kev radiations are all M1 (+ E2) transitions. This, however, is rather unsatisfactory, as it would require a much higher K/L ratio for the 445-kev transition than is measured. All the other possible

assignments, i.e., the ones of higher multipole order, were ruled out by delayed-coincidence measurements. Lifetimes for all the gamma rays observed in the gamma-ray spectrum have been shown to be less than 5×10^{-9} second. The M2 assignment for the 680-kev gamma ray cannot be ruled out by these measurements, since the half life for an M2 of this energy is 6.7×10^{-12} second according to Weisskopf's single particle formula. This formula should be valid this near a closed shell, where many of the transitions are believed to be single-particle changes. The present data do not uniquely determine the multipole order of the various transitions.

Table XXVIII

K/L conversion electron ratios

Gamma energy (kev)	K/L (Exp.)	Theoretical E1	E2	E2	M1	M2	M3	Tentative Assignment
169	0.6	5.2	0.44	0.08	5.7	2.4	-	
264	5.0	5.9	1.1	0.3	5.6	3.5	1.9	M1/M1 (+E2) or E1
333	6.3	5.9	1.65	0.5	5.7	3.8	2.4	M1 or M1 (+ E2)
445	1.9	5.4	2.24	1.0	5.4	3.9	2.7	E2
680	3.5	5.6	3.5	2.1	4.9	4.2	3.4	E2, M2
863	~5	5.3	4.4	2.9	5.0	4.6	3.9	E2, M1
946	~5	5.2	4.6	3.0	5.8	4.6	4.3	E2, M1
1131	3.6	6.5	4.6	3.5	5.8	5.2	4.6	E2
1374	~7	~6.8	~6.5	-	6.4	-	-	E2

Decay Scheme

In attempting to present a decay scheme for Em^{211} for the electron-capture branching decay, it would be well to point out that the following sums of transition energies are very nearly the same:

$$1820 + 0 = 1820$$
$$1374 + 445 = 1819$$
$$1131 + 680 = 1811$$
$$865 + 946 = 1811$$

These all agree within the limits of experimental error, and coincidence measurements have been shown between appropriate gamma rays to substantiate this summing. Also, coincidences have been determined between these gamma rays and the intense 680-kev radiation. A tentative decay

scheme consistent with these data is shown in Fig. 23. The order of the 865- and the 946-kev transitions may be reversed, since they are of approximately the same intensity. The total intensity for each transition arrived at by summing the electron and photon intensities is consistent with the assumption that approximately 75% of the electron-capture events lead to the 2488-kev level.

The ground-state spin of Em^{211} is most probably 1/2, with negative parity. This is because it falls in the 125-neutron group with four coupled protons beyond the 82-proton closed shell. The spin would be that of the 125th neutron, which has been measured as 1/2 in both Po^{209} and Pb^{207}.[34,47] The large amount of electron-capture decay that proceeds to the 2.490-Mev level in At^{211} is expected, since not much would go to the ground and first excited states which probably have 9/2 and 7/2 or 5/2 spins. The number of transitions depopulating this high energy level suggests that there are many levels with similar spins lower in the level structure. A more complete description of the excited states of At^{211} will have to wait until additional experimental data are available.

Electron-Capture Decay Energy

The total electron-capture decay energy of Em^{211} can only be estimated by use of neutron-binding energy cycles. The cycle used to calculate this decay energy utilizes the neutron- and proton-binding energies of Em^{212} and At^{211}. The proton-binding energy of Em^{212} and the neutron-binding energy of At^{211} have been calculated through their use in other cycles. The other two binding energies required must be estimated from binding-energy systematics. Based on the data compiled by Glass et al.,[27] the values used in the calculations are:

Neutron-binding energies

$At^{210-211}$, 7.72 Mev (calculated);

$Em^{211-212}$, 7.9 ± 0.5 Mev (estimated).

Proton-binding energies:

At^{211} - Em^{212}, 4.63 Mev (calculated);

At^{210} - Em^{211}, 4.22 ± 0.3 Mev (estimated).

The estimated electron-capture decay energy available for Em^{211}, on the basis of these data, is 2.6 ± 0.3 Mev. This is very close to the total

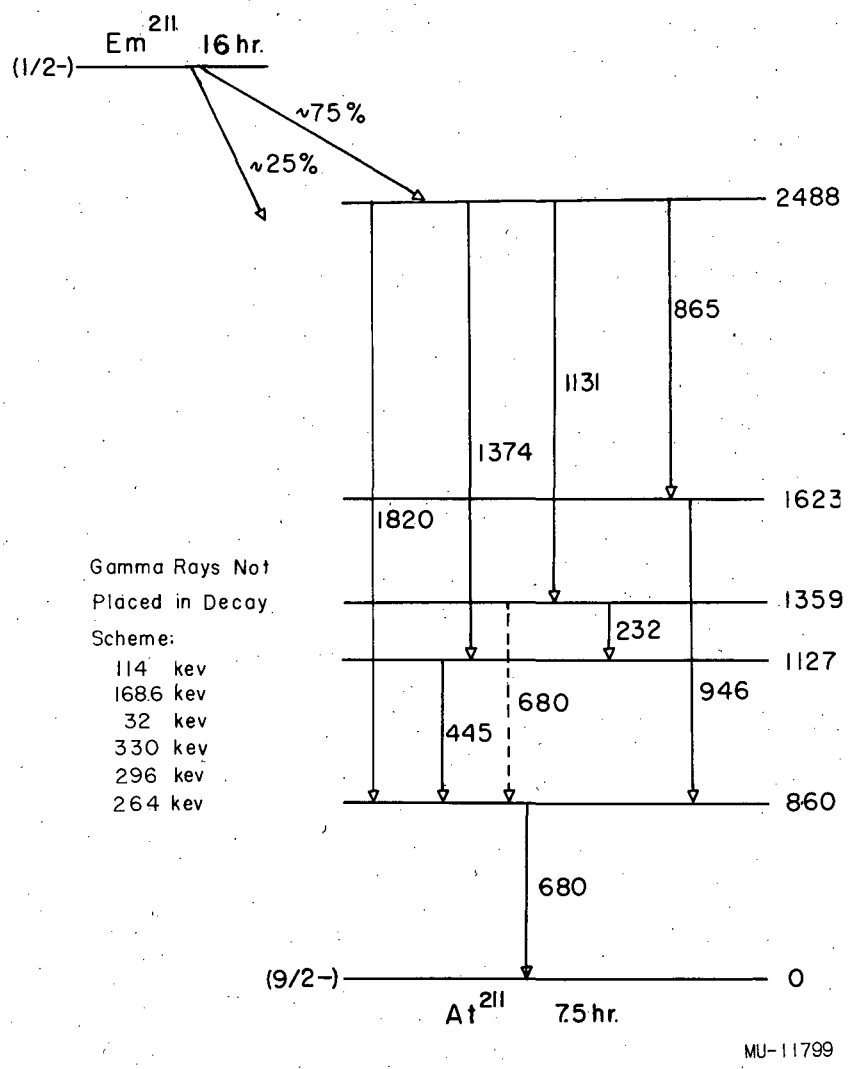

Fig. 23. Proposed electron-capture decay scheme for Em^{211}.

decay energy of 2.5 Mev required in the tentative decay scheme. The main conclusion from the rough estimate of decay energy is that the tentative decay scheme is not unreasonable from the standpoint of total decay energy.

Summary

In discussing the decay scheme of Em^{211} with the single-particle model in mind, one would expect the excited states of At^{211} to come from the promotion of the odd proton. Two of the protons beyond the closed shell of 82 protons would be paired off to give zero angular momentum, and the third proton should give the excited states starting with $h_{9/2}$. The neutrons cannot be excited very easily, since the 126-neutron closed shell makes the configuration for this isotope very stable. The great number of levels that must be present to explain the numerous transitions are closely spaced and very difficult to fit into a single proton-excitation scheme. If the ground-state is considered to have a 9/2-spin and parity, the first excited state may be either 7/2- or 5/2-, depending on the order of filling of the proton orbits beyond the 82-proton closed shell. This first excited state can be considered the excitation of the odd proton, but this is the only tentative assignment that can be made.

The numerous levels of At^{211} above 700 kev may be explained qualitatively by considering the coupling of the proton pair in different energy states with the odd proton. The type of interaction has previously been discussed for both Bi^{207} and Po^{209} excited levels. For At^{211} the ground state would consist of the $(h_{9/2})^2_{J=0}$, $(h_{9/2})^1_{J=9/2}$ configuration, which can give only 9/2 as the spin of the state. The first group of excited states may arise from a $(h_{9/2})^2_{J=2}$ energy state for the paired protons, coupled with either an $(h_{9/2})^1$ or $(f_{7/2})^1$ state for the odd proton. This would give a great number of half-integral spins from 13/2 through 1/2 for the configuration, depending on the state taken for the odd proton. Interaction between the particles would split the various spin states into levels with different energies. In this manner the great number of levels in At^{211} required to explain the transitions, which are too numerous for the single-particle model, may be explained. It is of interest to note that the energy required to

raise the proton pair to J = 2 state (i.e., ~ 1000 kev) is approximately the same as that required to excite the $h_{9/2}$ proton to a $f_{7/2}$ state. This suggests strongly that the $(h_{9/2})^2_{J=2}$ state should be used in some manner to explain the levels of At^{211}.

Further investigations of the levels of At^{211}, by both experimental and theoretical methods, will be of great interest in determining if this qualitative method of establishing the level scheme can be used to explain the observed levels.

Part II

IV. INTRODUCTION

Since the very early days of the study of natural radioactivity the question of the interrelationship of alpha-particle energies, half lives, and neutron and proton numbers has engaged the attention of those interested in systematization of the empirical facts so that clues to their basic meaning would be more readily predicted. Such correlations have in recent years come to be known as "alpha systematics". One of the chief generalizations concerning the relationship of the alpha disintegration energy and the mass number of the isotope of a particular element stated that the disintegration energy decreased in a nearly linear fashion with increasing mass number. This generalization holds quite well for most of the heavy elements, as can be seen by inspection of Fig. 24. However, in those elements having alpha-emitting isotopes coviering the region immediately above and below the neutron number 126, this relationship breaks down and a very sharp discontinuity of about 4 Mev occurs in the alpha-disintegration energy. The points for astatine, polonium, and emanation isotopes in Fig. 24 indicate this discontinuity most dramatically. The break is quite understandable in terms of the Mayer[1] and the Haxel, Jensen, and Suess[2] single-particle model of the nucleus, and is related to the closed shell at 126 neutrons, as is discussed more fully by Perlman, Ghiorso, and Seaborg.[39] The last reference also cites considerable past and recent literature bearing on the general subject of alpha systematics. Recent developments in alpha radioactivity (up to mid - 1954) are reviewed by Asaro and Perlman.[40]

Momyer and Hyde discussed the influence of the 126-neutron shell on the alpha-decay properties of several emanation, francium, and

radium isotopes.[8] Their work extended the curve of alpha-disintegration energy versus mass number to the neutron-deficient side of the 126-neutron shell. Their article included a summary of the results of the work to be reported here, and these data are included in Fig. 24. It was the chief purpose of this study to further extend the curve by a new method of production for neutron-deficient emanation isotopes.

The emanation isotopes were produced by bombarding gold foil with +6 nitrogen ions. The nuclear reaction that took place to form Em^{208} was:

$$_{79}Au^{197}_{118} + {}_{7}N^{14}_{7} \longrightarrow {}_{86}Em^{208}_{122} + {}_{0}n^{1}_{1}.$$

Additional neutrons were emitted from the compound nucleus, in many cases, and subsequently Em^{207}, Em^{206}, and Em^{204} were formed. These isotopes were identified by half lives, alpha-particle energies, and genetic relationships. Information concerning the half life of At^{207} and the branching ratio of Po^{202} was also obtained by watching these activities grow into a purified emanation sample. The advantage in using nitrogen ions to form the emanation isotopes is that no isotope heavier than Em^{208} is formed. This allows the study of the neutron-deficient isotopes of emanation without any interference from Em^{209}, Em^{210}, Em^{211}, Em^{212}, or Em^{221}. Previously the method of production -- i.e., spallation of thorium with 340-Mev protons -- formed <u>all</u> emanation isotopes, which made the study of the short-lived ones very difficult.

V. EXPERIMENTAL

The emanation isotopes were produced by bombarding gold (mass number 197) with nitrogen ions, which were accelerated in the 60-in. cyclotron of Crocker Radiation Laboratory.[48] Only the +6 species of nitrogen ions were accelerated to high enough energies to cause nuclear reactions in gold. The +6 nitrogen ion is not produced in the primary ionization source for the beam particles, but it is formed during the acceleration. Nitrogen ions with a + 2 charge are introduced into the cyclotron from the primary ionization source, and these undergo a preliminary harmonic acceleration. During this initial acceleration some of the + 2 ions are stripped of additional electrons, and ions with all possible charges are formed. The design parameters of the cyclotron

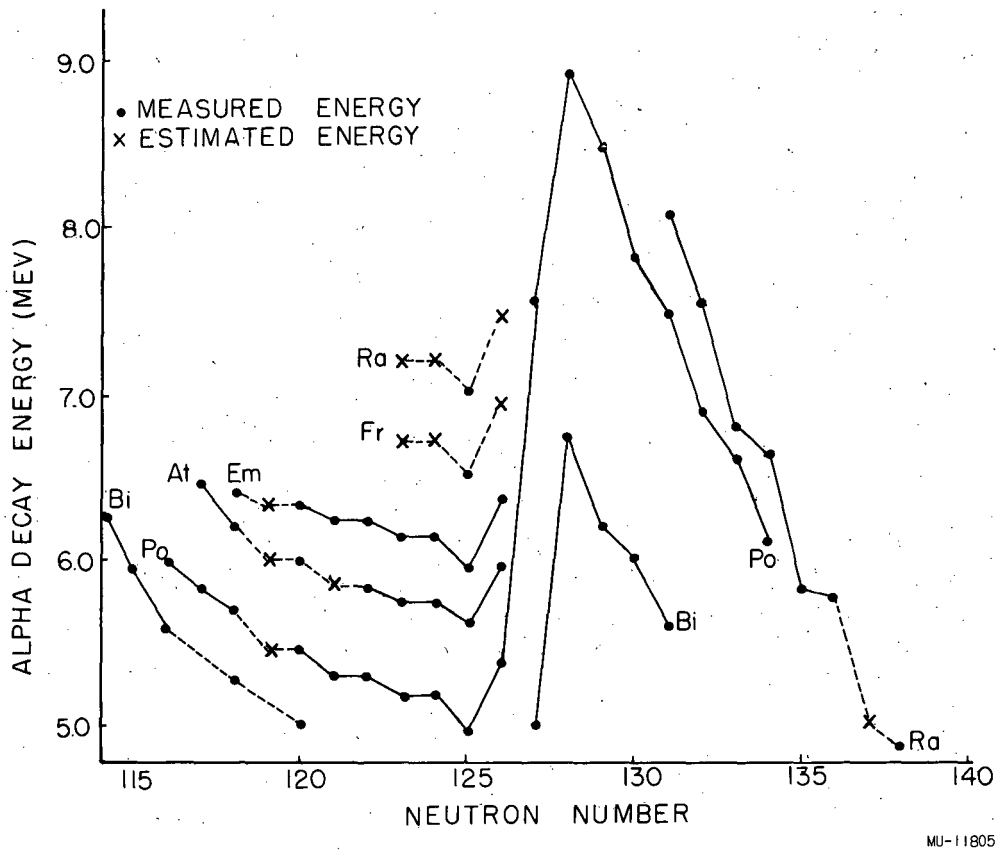

Fig. 24. Plot of alpha disintegration energy versus mass number of the alpha-emitting isotopes.

allow only the + 2 and + 6 ions to be accelerated; the remainder are deflected from the acceleration orbit. The beam achieved in this manner is a mixture of + 2 and + 6 nitrogen with a continuous variation up to a maximum of approximately 140 Mev for the + 6 ions. The gold target is mounted so that it intercepts this entire beam at the outer edge of the cyclotron dees.

Two different target assemblies were used for bombardment of the gold foil. In the first experiments a 5-mil gold foil was placed on a holder in front of the beam. However, this was unsatisfactory because the gold was heated to such a high temperature by the beam that a water-cooled target was needed to reduce the loss of emanation. The gold foil was then placed on a semicircular water-cooled probe. This probe allowed the target to intercept the same beam but still be cooled on the back by a stream of water under pressure. This cooling is required because of the high intensity of + 2 nitrogen ions, which are not energetic enough to cause nuclear reactions but are completely stopped by the gold foil. The target assembly was designed so that it could be dismantled rapidly in order to study products of short half life.

The emanation was extracted from the gold foil by amalgamating the gold with mercury. The gold foil, after bombardment, was placed in a pool of mercury in a vacuum system. The system was pumped down to 10^{-4} mm Hg, then was heated with an induction heater for several minutes. As the gold dissolved in the mercury, the emanation was freed and subsequently collected in a trap in the vacuum system at liquid nitrogen temperature. The sample was then mounted on aluminum foil by the glow-discharge technique.(*) Briefly, this technique is as follows: the emanation is introduced, at between 100 and 1000 microns pressure, into a special chamber, which has two electrodes. A potential of several hundred volts is placed across the electrodes; this ionizes and accelerates the emanation into the metal lattice of the negative electrode. A detailed description of the glow-discharge technique is given by Momyer and Hyde.[8] The separation, purification, and mounting of an

* The name for the process is derived from the bluish-purple glow that accompanies this ionization.

emanation sample was carried out in a very short period of time. Samples were ready to be counted between 15 and 20 minutes after the end of the bombardment.

The emanation samples prepared in this manner consisted of a mixture of Em^{208}, Em^{207}, Em^{206}, and Em^{204} alpha activities. After a period of time the electron-capture and alpha-decay daughters grew in. Table XXIX is a summary of the information deduced from this research on these isotopes. This work constitutes the first determination of the properties of these isotopes except for some data on Em^{208} obtained by Momyer and Hyde, and information obtained independently and at the same time on the emanation isotopes by nitrogen bombardments by Burcham.[41] The genetic relationships of the emanation isotopes that were demonstrated by this work are given in Fig. 25.

Table XXIX

Summary of experimental data from this work

Isotope	Half life (min)	Alpha-particle energy (Mev)	Branching
Em^{208}	21 ± 3	6.14 ± 0.05	-
Em^{207}	10 ± 2	6.12 ± 0.05	4% α, 96% EC
Em^{206}	6.2 ± 0.5	6.25 ± 0.05	65% α, 35% EC
Em^{204}	3 ± 1	6.28 ± 0.05	-
At^{207}	107 ± 5	5.75 ± 0.05	-
Po^{202}	51 ± 3	5.60 ± 0.05	2% α, 98% EC

VI. RESULTS

Let us now review the experimental data from which these properties were deduced. It will be noted from Fig. 25 that the alpha-particle energies for these emanation isotopes fall in the range from 6.2 to 6.4 Mev. Hence for careful study of the decay of these alpha activities, the alpha pulse-height analyzer was set to expand the 6.2-to-6.5-Mev range over the entire 48 channels. The alpha spectrum thus observed in one bombardment is shown in Fig. 26. This spectrum shows the two main peaks at 6.12 and 6.25 Mev, and also small shoulders on these peaks at 6.14 and 6.28 Mev, all of which were identified as alpha

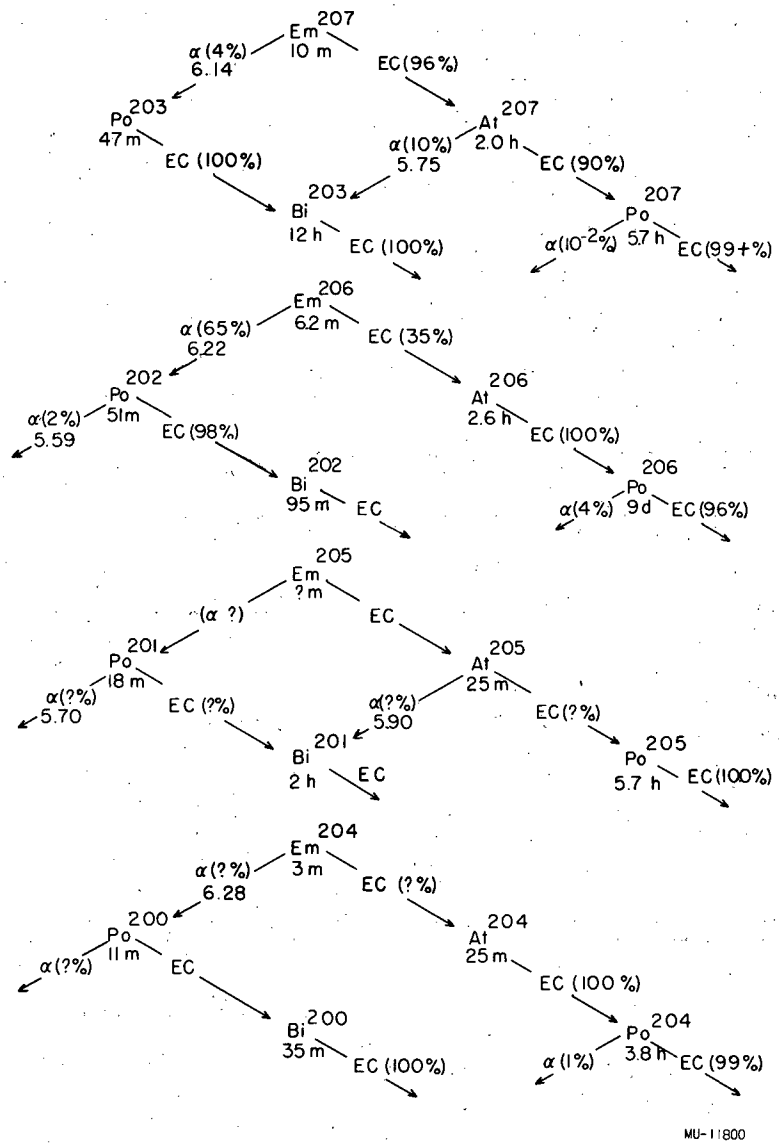

Fig. 25. General genetic relationships of some emanation isotopes.

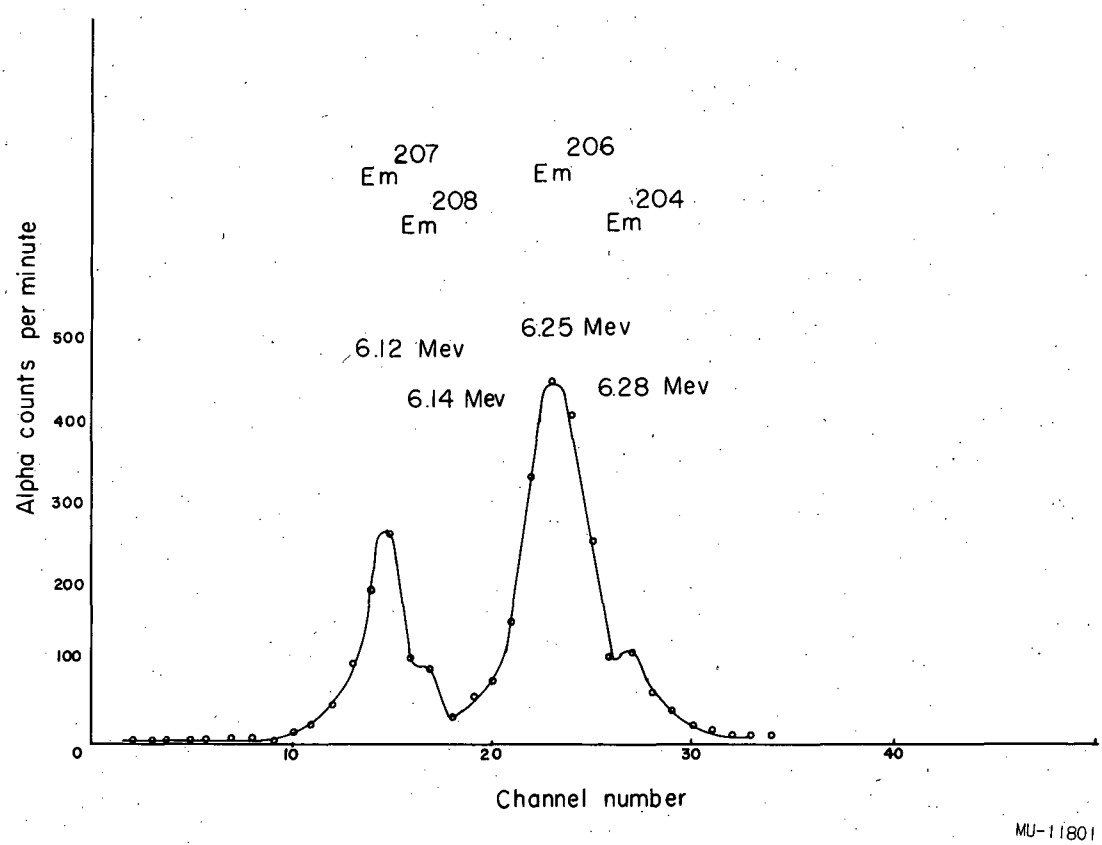

Fig. 26. Alpha spectrum of the emanation as observed on the alpha-pulse analyzer.

decay of emanation isotopes. The decay of these peaks was followed, and the decay of the 6.12-Mev peak was resolved into 21- and 11-minute components. The 6.25-Mev peak and its 6.28-Mev shoulder were resolved into 6.2-minute and 3-minute half lives. The assignment of these half lives to certain emanation isotopes, as shown in Table XXIX is justified in detail in later sections.

The alpha energy of the astatine and polonium activities covered a much wider energy range. In separate runs the alpha pulse-height analyzer was set to cover a larger energy range, so that the growth and decay of the alpha peaks due to the daughter isotopes could be followed and correlated with the decay of the emanation alpha peaks. In Fig. 27 the alpha spectrum of the emanation and daughter activities that were observed is shown. This alpha-pulse analysis was made 1 hour after the sample had been prepared. Much better statistics were obtained on Po^{208} and Po^{206} by counting the sample for the long periods of time several days after the short activities had decayed away.

Mass Assignment of Emanation-208

Em^{208} has previously been observed by Momyer and Hyde.[8] They assigned to it a 23-minute half life, and based their mass assignment on the growth and identification of Po^{204} and Po^{208} in an emanation fraction. Momyer, Asaro, and Hyde measured the alpha-particle energy in the alpha-particle spectrograph, and found it to be 6.138 ± 0.005 Mev.[42] In this experimental work on alpha peak at 6.14 ± 0.05 Mev was observed with a 21±3-minute half life. On the basis of the agreement between half lives and alpha-particle energy, this peak was assigned to Em^{208}.

Mass Assignment of Emanation-207

The alpha group at 6.12 Mev was observed to decay with a 10-minute half life. This activity was assigned to Em^{207} by observing the growth of At^{207}. Figure 28 shows the growth curve of At^{207} that was observed in one run. The two isotopes were related by calculating the time after purification that the maximum amount of At^{207} activity had grown in. This maximum time depends on the half lives of both the parent and daughter activities, and is determined experimentally from the At^{207} growth curve. By comparing the time of maximum At^{207} activity

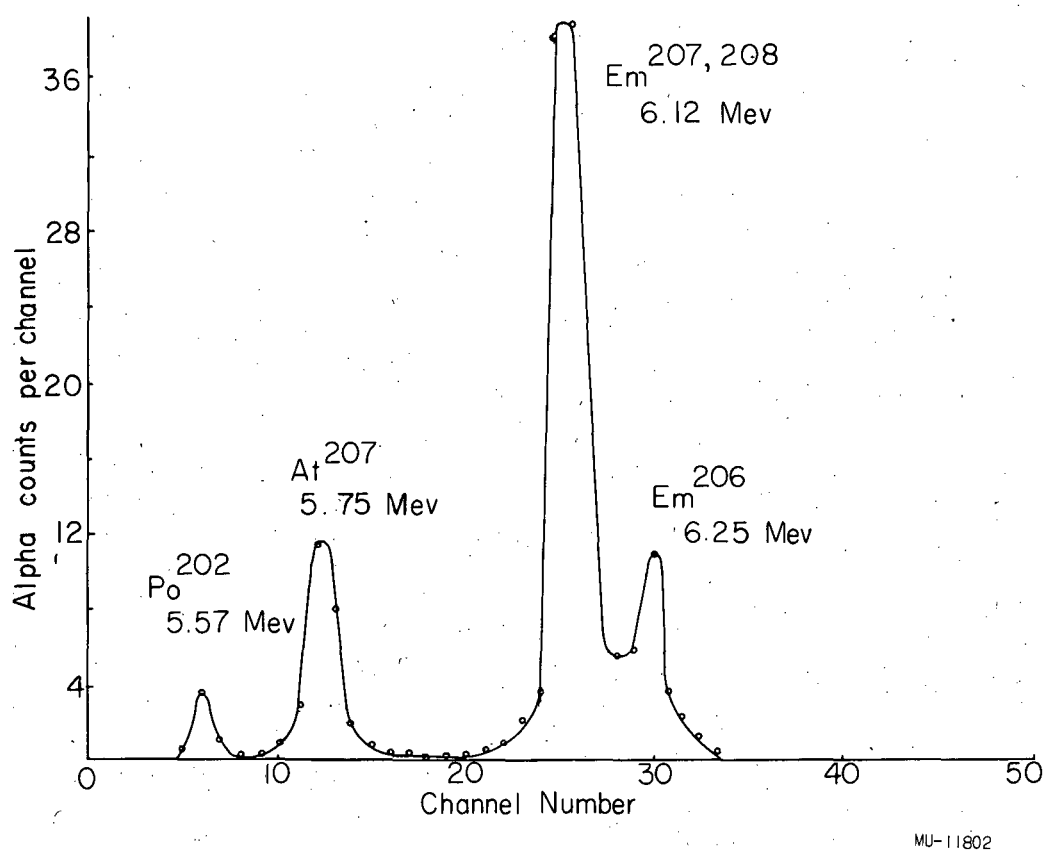

Fig. 27. Alpha spectrum of the polonium and astatine daughter activities of the emanation isotopes as observed in the alpha-pulse analyzer.

calculated using each possible half life for the parent and the experimental value, one can establish the correct parent-daughter relationship. The equation that represents this relationship is

$$t_m = \frac{1}{\lambda_B - \lambda_A} \ln \frac{\lambda_B}{\lambda_A} ,$$

where λ_B is the characteristic decay constant for the daughter activity, λ_A the decay constant for the parent activity, and "t_m" the time at maximum activity of the daughter. Using the measured half life of 10 minutes for Em^{207} and 107 minutes for At^{207}, one calculates the time at maximum activity to be 40 minutes. This corresponds to the experimental value of 39 ± 4 minutes that was taken from the growth curve in Fig. 28. The two dotted growth curves shown in Fig. 28 represent calculated curves based on the assumption that the half life of the parent is 8 minutes or 13 minutes. These two curves aid in showing that the 10-minute half life for the parent gives the best agreement.

The branching ratio for Em^{207} can be calculated from the alpha decay of Em^{207} and the alpha decay of At^{207}. The At^{207} is the product of the electron-capture decay of Em^{207}, and its alpha activity gives a measure of the amount of electron capture Em^{207} undergoes. The alpha branching of At^{207} has previously been measured as approximately 10%. Taking the At^{207} alpha activity at any known time, one can easily calculate the number of atoms of Em^{207} that are required to give rise to this At^{207} activity. By comparing this number with the number of atoms of Em^{207} required to give the alpha disintigration rate, one can determine the amount of alpha and electron-capture decay of Em^{207}. The average of two experiments gave a value of 4% alpha and 96% electron-capture decay for Em^{207}. These values are based on a 10% alpha branching for At^{207}, and should be recalculated when a better value for At^{207} is available.

Emanation-206 - Mass Assignment and Branching Ratio

The assignment of the 6.2 minute half life and the 6.25 ± 0.05-Mev alpha group to Em^{206} was achieved by observing the growth of the alpha daughter, Po^{202}. The nuclear properties of Po^{202} have previously been reported by Karraker and Templeton.[23] The growth curve for Po^{202}

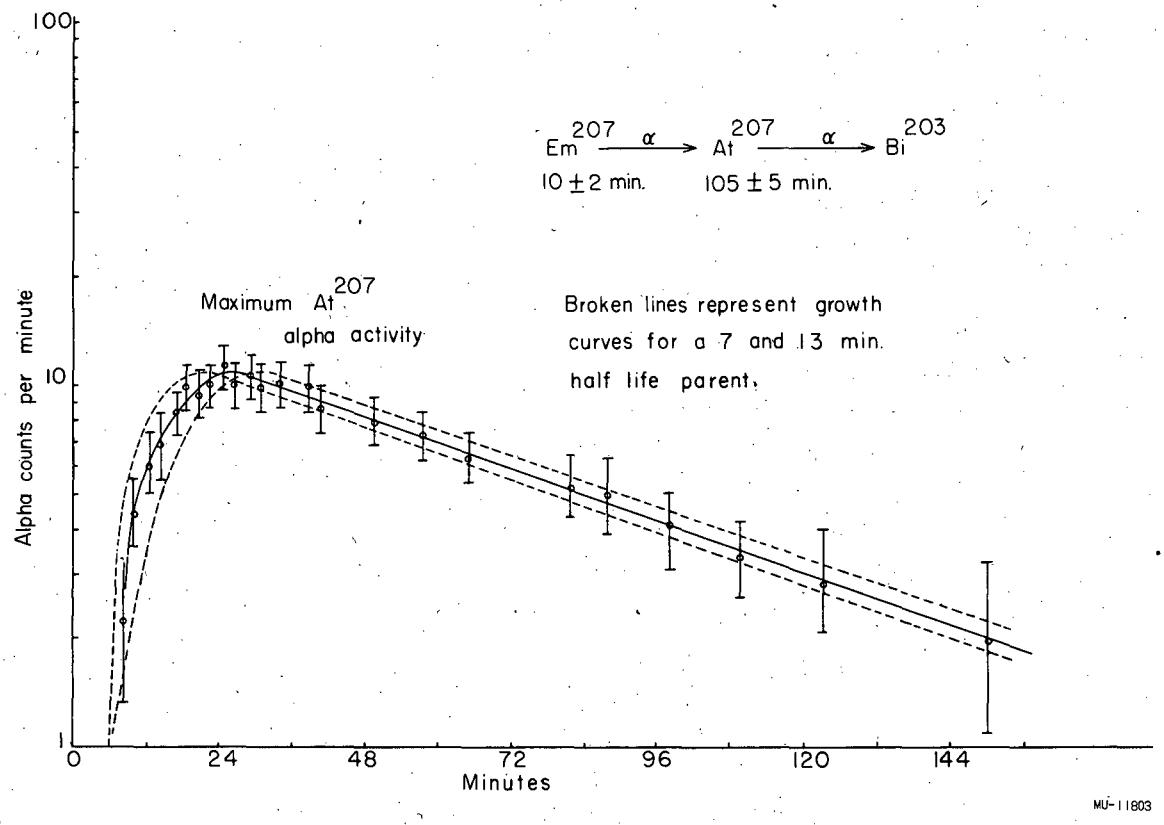

Fig. 28. Growth and decay curve for At^{207}.

alpha activity that was observed in one experiment is shown in Fig. 29. The time of maximum Po^{202} activity was calculated with 6.2 minutes for the Em^{206} half life and 52 minutes as the Po^{202} half life. This calculated "t_m" value of 19.5 minutes agrees with the experimental value from the Po^{202} growth curve in Fig. 29. (The dotted growth curves show what the curve would look like with 4 minutes or 10 minutes used as the half life of the parent of Po^{202}.) The growth of At^{206} could not be observed for further checking of the mass assignment because of the low alpha branching of At^{206}.

The alpha electron-capture branching ratio for Em^{206} was determined by comparing the Em^{206} alpha activity with the Po^{206} alpha activity. Po^{206} is the electron-capture product of At^{206}, which is the electron-capture daughter of Em^{206}. This decay chain is illustrated in Fig. 25. Since no alpha branching of At^{206} has been determined, it may be considered very small. The Po^{206} activity, when corrected for its electron-capture branching, gives a measure of the amount of electron capture of Em^{206}. The number of atoms of Em^{206} required to produce a certain number of Po^{206} counts can be determined and compared with the number of Em^{206} atoms giving rise to the alpha disintegration rate. A comparison of these two values yields a branching of 65% alpha and 35% electron-capture.

Branching Ratio for Polonium-202

The branching ratio of Po^{202} can be determined from these experimental data. The Po^{202} is produced only as the daughter of the alpha decay of Em^{206}. From the alpha disintegration rate of Em^{206}, the number of atoms of Po^{202} at any time can be calculated. The observed alpha disintegration rate of Po^{202} can then be used to determine the number of atoms undergoing alpha decay. This fractional part of the Po^{202} atom gives the branching ratio. A value of 2% alpha and 98% electron capture was determined in this manner.

Emanation-204 Mass Assignment

The assignment of the 3-minute 6.28-Mev alpha group to Em^{204} is only tentative. The properties of the daughter activities are shown in Fig. 25. It is not possible to observe the growth of Po^{200}, because the activity will have completely grown in by the time the first alpha-

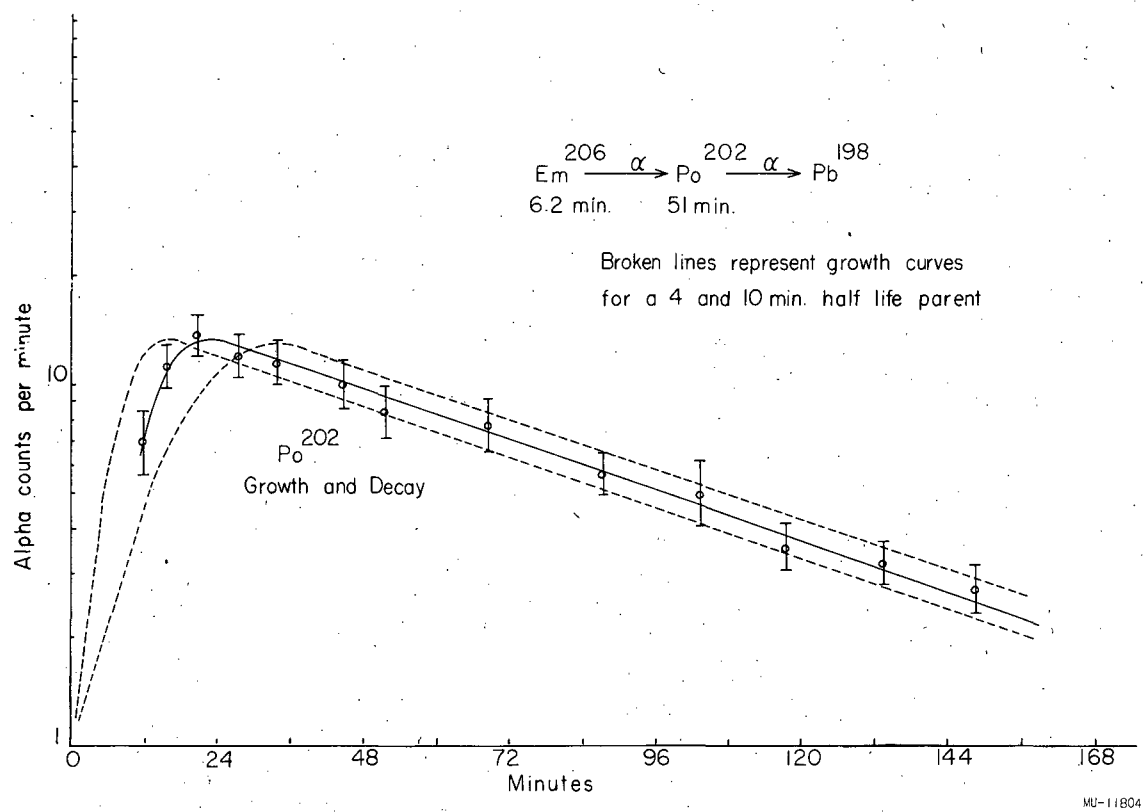

Fig. 29. Growth and decay curve for Po^{202}.

pulse analysis is made. The At^{204} has no alpha branching, and Po^{204} has only 1% alpha branching. The amount of Em^{204} probably undergoing electron capture is so small that the alpha branching of Po^{204} would not be detected. The mass assignment of the activity is made by using alpha systematics. If one compares the branching ratios for the odd-mass emanation isotopes -- i.e., Em^{207} and Em^{209} -- the amount of alpha branching is observed to be getting smaller as the mass number decreases. For the even-mass isotopes of emanation the alpha branching is observed to be getting larger as the mass number decreases. Therefore, by comparing Em^{205} with the alpha branching of Em^{207} and Em^{209}, one concludes that Em^{205} should have very low alpha branching, (less than 1%). Em^{204} would be expected, from the trend in the even-mass isotopes, to have a very high alpha branching. With this as a basis for assignment, the 3-minute alpha half life was assigned to Em^{204}.

Additional evidence for the assignment comes from a close inspection of the plot of alpha-disintegration energy versus mass number in Fig. 24. The graph shows a very pronounced dependence on the odd neutron for emanation, astatine, and polonium isotopes below 126 neutrons. The alpha energy for the odd-neutron isotopes is lower than the previous even-neutron isotopes, and about equal to the next higher even-neutron isotope of the same element. This effect is quite pronounced for all isotopes between 119 and 126 neutrons -- a region where mass assignments are quite certain. With this used as a criterion for the emanation isotopes, the assignment of the 6.28-Mev alpha group to Em^{204} is in agreement with the trend. If the alpha group belonged to Em^{205} it would be expected to have an alpha energy of 6.22 Mev. Therefore, on the basis of alpha-energy systematics and alpha-branching considerations, the 3-minute 6.28-Mev alpha group is assigned to Em^{204}.

VII. DISCUSSION

The results of these experiments were summarized in Table XXVII. In addition to the results previously discussed, the half life for At^{207} that was measured in several experiments is reported. This value of 107 ± 5 minutes is shorter than the previous measured half life by approximately 10%. At about the same time these experiments were being

carried out, a similar investigation was under way at the University of Birmingham, England by Prof. W. E. Burcham.[42] His work has already been published, and the agreement between the two works is quite excellent. The only differences occur in the branching ratio for Em^{207} and in that he did not observe the 3-minute Em^{204} or the 21-minute Em^{208}.

This information on the emanation isotopes extends the alpha systematics in the region before the 126-neutron shell. It also extends the odd-isotope effect in the alpha disintegration energies that was previously discussed to one more isotope (Em^{207}). From the short half life found for these isotopes it may be summarized that any lower-mass isotopes of emanation will be even shorter-lived and very difficult to detect.

ACKNOWLEDGMENTS

Most of the work described in this theses could not have been done without the advice, cooperation, and the support given the author by the entire staff of the Chemistry Department of the University of California Radiation Laboratory. The author would particularly like to acknowledge the help and guidance given by Dr. Earl K. Hyde throughout the complete study. The many helpful discussions with Drs. Glenn T. Seaborg, David H. Templeton, John Rasmussen, Frank Asaro, Frank Stephens, Isadore Perlman, Peter Gray, Richard Glass, and Mr. Arnold Fritsch have been appreciated.

The author appreciated the aid given by Drs. Jack Hollander and Warren G. Smith in carrying out the permanent magnet spectrograph studies, Father Frederick Canavan, Jose Juliano, and Charles Gallagher in the beta-ray spectrometer studies, John P. Hummel in the alpha particle spectrograph measurements, and Drs. Donald Strominger and Frank Stephens for the numerous coincidence measurements.

The cooperation of James Vale, Lloyd Hauser, William Jones, the late G. Bernard Rossi and the crews of the 184-in and 60-in cyclotrons is greatfully acknowledged. Finally I would like to express my appreciation to the Health Chemistry group who have made it possible to carry out this work with a minimum of radiation hazard.

This work was preformed under the auspices of the U. S. Atomic Energy Commission.

REFERENCES

1. M. G. Mayer, Phys. Rev. 75, 1969 (1949).
2. Haxel, Jensen, and Suess, Z. Physik 128, 295 (1950).
3. J. R. Prescott, Proc. Phys. Soc. (London) 67, 540 (1954).
4. M. H. L. Pryce, Proc. Phys. Soc. (London) A65, 773 (1952).
5. D. E. Alburger and M. H. L. Pryce, Phys. Rev. 95, 1482 (1954).
6. W. W. True, Phys. Rev. 101, 1342 (1956).
7. A. R. Fritsch, "The Energy Levels of Neutron-Deficient Lead Isotopes" UCRL-3452, June 1956.
8. Momyer and Hyde, J. Inorg. Nucl. Chem. 1, 274 (1955).
9. Barton, Ghiorso, and Perlman, Phys. Rev. 82, 13 (1951).
10. Hyde, Ghiorso, and Seaborg, Phys. Rev. 77, 765 (1950).
11. E. K. Hyde, J. Am. Chem. Soc. 74, 4181 (1952).
12. L. H. Treiman and M. W. Treiman, "Purification of Polonium by the Glass Wool Adsorption of Colloidal Polonium Hydroxide" LA-1403, May 1952.
13. P. R. Gray, private communication.
14. F. L. Reynolds, Rev. Sci. Instr. 22, 749 (1951).
15. Ghiorso, Jaffey, Robinson, and Weissbourd, National Nuclear Energy Series. Plutonium Project Record, The Transuranium Elements, Research Projects, Vol. 14B, McGraw-Hill, New York, 1949, 1226.
16. A. Ghiorso and A. E. Larsh, to be published.
17. M. I. Kalkstein and J. M. Hollander, "A Survey of Counting Efficiencies for a $1\frac{1}{2}$-inch diameter by 1-inch high Sodium Iodide Crystal" UCRL-2964, October 1954.
18. F. S. Stephens, Jr., "Decay Schemes and Nuclear Spectroscopic States in the Heavy-Element Region" UCRL-2970, June 1955.
19. K. Siegbahn, "Beta and Gamma Ray Spectroscopy, Interscience, New York, 1955, Chap. 7.
20. G. D. O'Kelley, "The Spectrometric Determination of Some Beta Particles and Conversion Electron Energies" UCRL-1243, May 1951.
21. G. D. O'Kelley and J. L. Olsen, "A Ring-focused Long Lens Magnetic Lens Beta-Ray Spectrometer" MTA-38, May 1954.
22. Templeton, Howland, and Perlman, Phys. Rev. 72, 758 (1947).
23. Karraker, Ghiorso, and Templeton, Phys. Rev. 83, 390 (1951).

24. P. R. Gray, "Electron Capture and the Auger Effect in the Heaviest Elements" UCRL-3104, August 1956.
25. Rose, Goertzel, and Perry, "K-shell Internal Conversion Coefficients"; Revised Tables. ORNL-1023, June 1951.
26. Prestwood, Smith, Browne, and Hoffman, Phys. Rev. 98, 1324 (1955).
27. Glass, Thompson, and Seaborg, J. Inorg. Nucl. Chem. 1, 3 (1955).
28. R. M. Kiehn and C. Goodman, Phys. Rev. 95, 989 (1954).
29. G. Gamow and E. Teller, Phys. Rev. 49, 895 (1936).
30. E. K. Kelly, "Excitation Functions of Bismuth" UCRL-1044, December 1950.
31. Rosenblum, Percey, Valadares, and Guillot, private communication, October 1952.
32. F. S. Stephens, Jr., private communication.
33. Mihelich, Schardt, and Segrè, Phys. Rev. 95, 1508 (1954).
34. K. L. Vander Sluis and P. M. Griffin, J. Opt. Soc. Am. 45, 1087 (1955).
35. D. E. Alburger and A. W. Sunyar, Phys. Rev. 99, 695 (1955).
36. D. Strominger, "A Study of Isomers in the Millimicrosecond Region" UCRL-3374, May 1956.
37. L. W. Nordheim, Revs. Modern Phys. 23, 322 (1951).
38. D. Kurath, Phys. Rev. 87, 528 (1952).
39. Perlman, Ghiorso, and Seaborg, Phys. Rev. 77, 26 (1950).
40. F. Asaro and I. Perlman, Ann. Rev. Nucl. Sci. 4, 157 (1954).
41. W. E. Burcham, Proc. Phys. Soc. (London) A67, 555 (1954).
42. Momyer, Asaro, and Hyde, J. Inorg. Nucl. Chem. 1, 267 (1955).
43. J. M. Hollander and R. W. Hoff, private communication.
44. Thompson, Ghiorso, and Seaborg, Phys. Rev. 80, 781 (1950).
45. Hill, Church, and Mihelich, Rev. Sci. Instr. 23, 523 (1952).
46. W. G. Smith, "Conversion Electron Spectra of Some Heavy Elements" UCRL-2974, June 1955.
47. J. E. Mack, Rev. Mod. Phys. 22, 64 (1950).
48. Rossi, Jones, Hollander, and Hamilton, Phys. Rev. 93, 256 (1954).